CEP BRINGS YOU...

The Best of Equipment Series

Contents

CEP BRINGS YOU...

The Best of Equipment Series

Pump Sizing: Bridging the Gap Between Theory and Practice

Seán Moran
Expertise Ltd.

This article explains some of the core concepts behind pump sizing.

When I left university, I found that I needed additional information to turn my theoretical knowledge of fluid mechanics into the practical knowledge required to specify a pump. Judging by the questions I see asked nearly every week on LinkedIn and elsewhere, I believe this is a problem shared by many engineers early in their careers. This article gives practical insight on how to specify a pump.

Pump types

Pumps can be used to move fluids, which flow from regions of high pressure to regions of low pressure, by increasing the pressure of the fluid. Before you purchase a pump, you must specify the type of pump and make sure it is capable of delivering a given flowrate at a given pressure.

There are two main pump types: rotodynamic and positive-displacement. In a rotodynamic pump, a rotating impeller imparts energy to the fluid. The most common type of rotodynamic pump is the centrifugal pump (Figure 1). The amount of liquid that passes through the pump is inversely proportional to the pressure at the pump outlet. In other words, the outlet flowrate of a rotodynamic pump varies nonlinearly with pressure.

In a positive-displacement (PD) pump, a discrete amount of fluid is trapped, forced through the pump, and discharged. A gear pump is an example of a PD pump (Figure 2). This pumping principle produces a pulsating flow, rather than a smooth flow. Its output flow tends to vary little with respect to the pressure at the pump outlet, because the moving displacement mechanism pushes the slug of liquid out at a constant rate.

Most process pumps are rotodynamic pumps, so you need to know the required outlet pressure to specify the pump that will provide the required flow. Alhough certain system head parameters are calculated the same way whether the driving force for flow is a pump or gravity, this article mainly addresses sizing concerns for rotodynamic pumps.

Pump sizing

Pump sizing involves matching the flow and pressure rating of a pump with the flowrate and pressure required for the process. The mass flowrate of the system is established on the process flow diagram by the mass balance. Achieving this mass flowrate requires a pump that can generate a pressure high enough to overcome the hydraulic resistance of the system of pipes, valves, and so on that the liquid must travel through. This hydraulic resistance is known as the system head.

In other words, the system head is the amount of pressure required to achieve a given flowrate in the system downstream of the pump. The system head is not a fixed quantity — the faster the liquid flows, the higher the system head becomes (for reasons to be discussed later). However, a curve, known as the system curve, can be drawn to show

the relationship between flow and hydraulic resistance for a given system.

Pump sizing, then, is the specification of the required outlet pressure of a rotodynamic pump (whose output flow varies nonlinearly with pressure) with a given system head (which varies nonlinearly with flow).

Understanding system head

The system head depends on properties of the system the pump is connected to — these include the static head and the dynamic head of the system.

The static head is created by any vertical columns of liquid attached to the pump and any pressurized systems attached to the pump outlet. The static head exists under static conditions, with the pump switched off, and does not change based on flow. The height of fluid above the pump's centerline can be determined from the plant layout drawing.

The dynamic head varies dynamically with flowrate (and also with the degree of opening of valves). The dynamic head represents the inefficiency of the system — losses of energy as a result of friction within pipes and fittings and changes of direction. This ineffiency increases with the square of the average velocity of the fluid.

Dynamic head can be further split into two parts. The frictional loss as the liquid moves along lengths of straight pipe is called the straight-run headloss, and the loss as a result of fluid passing through pipe fittings such as bends, valves, and so on is called the fittings headloss.

Fully characterizing a hydraulic system is incredibly complex. Remember that in order to specify a pump, you only need to characterize the system well enough to choose a pump that will perform the job in question. How exact you need to be depends on where in the design process you are. If you are at the conceptual stage, you may be able to avoid specifying the pump at all, but experience suggests that you should use rules of thumb to specify certain parameters (such as superficial velocity) to prevent difficulties later. I also recommend designing the process so that it does not have two-phase flow. Two-phase flow is difficult to predict, and should be avoided in your design if at all possible — head losses can be one thousand times those for single-phase flow. Installing knock-out drums in the system and arranging pipework so that gases are not entrained in liquids can help mitigate two-phase flow.

Superficial velocity is the same as average velocity and is the volumetric flowrate (in m^3/sec, for example) divided by the pipe's internal cross-sectional area (*e.g.,* in m^2). A very quick way to start the hydraulic calculations is to use the following superficial velocities:

- pumped water-like fluids: <1.5 m/sec
- gravity-fed water-like fluids: <1 m/sec
- water-like fluids with settleable solids: >1, <1.5 m/sec
- air-like gases: 20 m/sec

Keeping the system within these acceptable ranges of superficial velocities, and avoiding two-phase flow, will typically produce sensible headlosses for the pipe lengths usually found in process plants.

Determining frictional losses through fittings

Dynamic, or friction, head is equal to the sum of the straight-run headloss and the fittings headloss.

The fittings headloss is calculated by what is known as the *k*-value method. Each type of valve, bend, and tee has

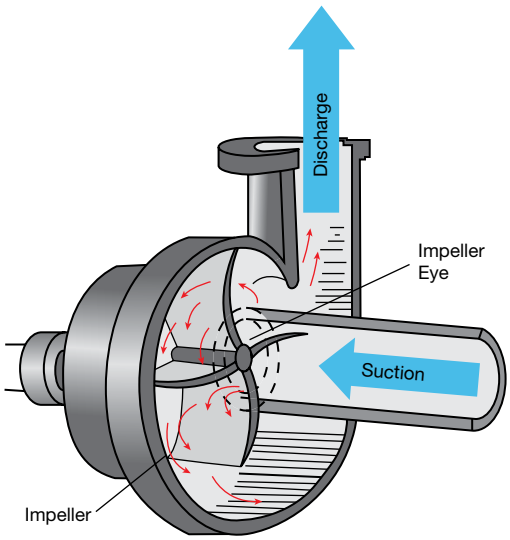

▲ **Figure 1.** In a centrifugal pump, a rotating impeller imparts energy to the liquid moving through the pump.

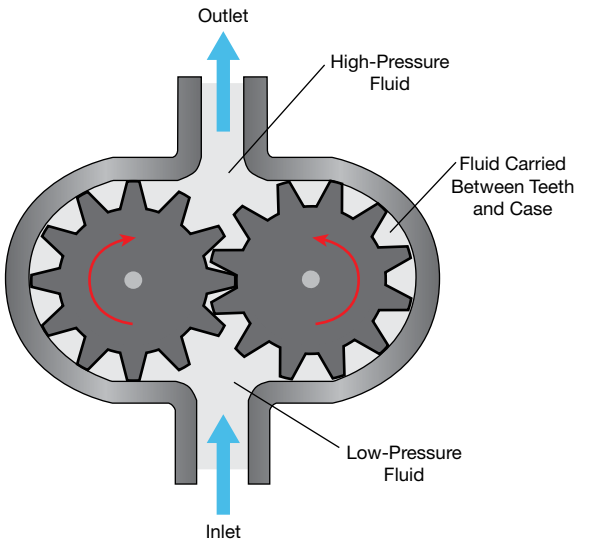

▲ **Figure 2.** A gear pump is a type of positive-displacement pump in which a discrete volume of fluid is trapped and then discharged.

a characteristic resistance coefficient, or k value, which can be found in Perry's Handbook *(1)* and other sources (Table 1) *(2)*.

To use this method, count the number of valves on the piping and instrumentation diagram (P&ID), and the fittings, bends, and tees on the plant layout drawing for the relevant suction or delivery line. Multiply the number of each type of fitting by the corresponding k value, and add the k values for the various types of fittings to get the total k value. Use the total k value to calculate the headloss due to fittings:

$$h_f = \frac{kv^2}{2g} \qquad (1)$$

where h_f is the fittings headloss in meters water gauge (mwg), k is the total k value, v is the superficial velocity (m/sec), and g is the acceleration due to gravity (9.81 m/sec^2).

Calculating straight-run headloss

At a more-advanced stage of design, you might want to know a pump's physical size to try out on a plant layout drawing. An easy way to determine the straight-run headloss — the most difficult part of a headloss calculation — is to use a nomogram such as Figure 3 or a table. Pipe manufacturers (and others) produce tables and nomograms that can be used to quickly look up headloss due to friction for liquids.

To use the nomogram, use a ruler to draw a straight line through any pair of known quantities to determine unknown quantities. For example, for a 25-mm nominal-bore pipe with a flow velocity of 1 m/sec, the straight-run headloss is about 6 m per 100 m of pipe. So the headloss through 10 m of this pipe is around 0.6 mwg.

At an early design stage, you often need to calculate the straight-run headloss multiple times. Rather than referring to a table or nomogram numerous times, it can be quicker to set up an Excel spreadsheet and use a formula to calculate the Darcy friction factor and headloss.

Table 1. Each type of pipe fitting has a resistance coefficient, or *k* value, that can be used to calculate the fittings headloss for the pump system *(2)*.

Fitting Type	*k* Value
Short-radius bends, for every 22.5 deg. allow	0.2
Long-radius bends, for every 22.5 deg. allow	0.1
Open isolation valve	0.4
Open control valve	10.8
Tee (flow from side branch)	1.2
Tee (flow straight-through)	0.1
Swing check non-return valve	1
Sharp entry	0.5

Chemical engineering students are usually taught to find the Darcy friction factor using a Moody diagram, which is a summary of a large number of empirical experiments. You can use curve-fitting equations and software such as Excel to approximate the Moody diagram's output.

Don't confuse the Darcy friction factor with the Fanning friction factor — the Darcy friction factor is by definition four times the Fanning friction factor. If you do decide to use a Moody diagram to find the friction factor, be aware of which friction factor is on the y-axis.

I prefer the Colebrook-White approximation to calculate the Darcy friction factor. Although it is an approximation, it

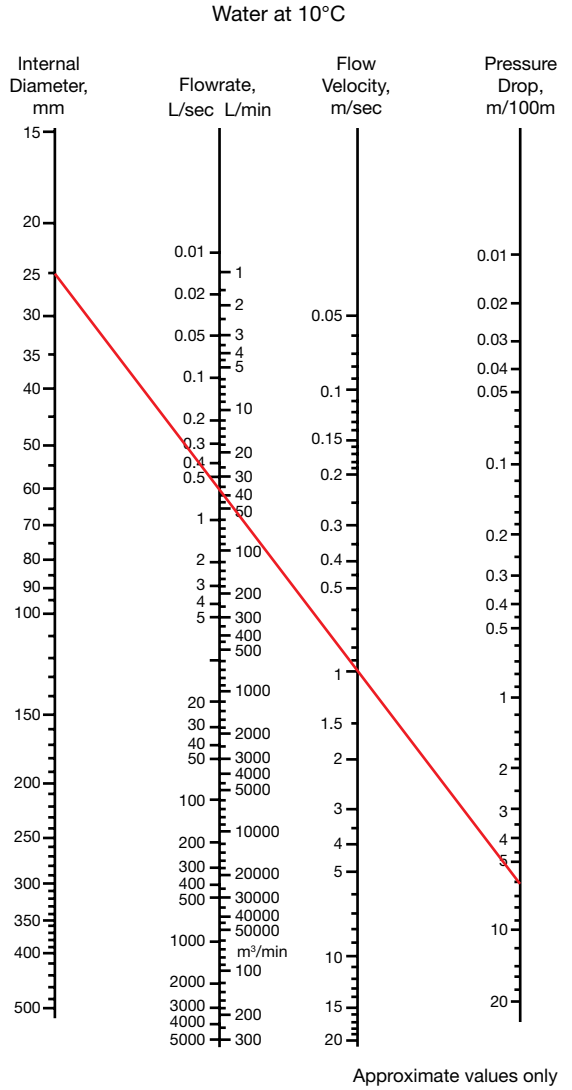

▲ **Figure 3.** A piping nomogram, available from pipe manufacturers, can be used to estimate the straight-run headloss for a pump system. In the example shown by the red line, a 25-mm pipe with a flow velocity of 1 m/sec has a straight-run headloss of about 6 m per 100 m of pipe. Copyright image reproduced courtesy of Durapipe SuperFLO ABS technical data.

might be closer to the true experimental value than what the average person can read from a Moody diagram.

The Colebrook-White approximation can be used to estimate the Darcy friction factor (f_D) from Reynolds numbers greater than 4,000:

$$\frac{1}{\sqrt{f_D}} = -2\log\left(\frac{\varepsilon}{3.7D_h} + \frac{2.51}{Re\sqrt{f_D}}\right) \quad (2)$$

where D_h is the hydraulic diameter of the pipe, ε is the surface roughness of the pipe, and Re is the Reynolds number:

$$Re = \frac{\rho v D}{\mu} \quad (3)$$

where ρ is the density of the fluid, D is the pipe internal diameter, and μ is the fluid dynamic viscosity.

The Colebrook-White approximation can be used iteratively to solve for the Darcy friction factor. The Goal Seek function in Excel does this quickly and easily.

The Darcy-Weisbach equation states that for a pipe of uniform diameter, the pressure loss due to viscous effects (Δp) is proportional to length (L) and can be characterized by:

$$\frac{\Delta p}{L} = f_D \frac{\rho v^2}{2D} \quad (4)$$

This iterative approach allows you to calculate straight-run headloss to the degree of accuracy required for virtually any practical application.

I recently came across a paper *(3)* that suggested there are other equations that provide more accurate results through curve-fitting than the Colebrook-White approximation. If you are producing your own spreadsheet for this purpose, I suggest you look into the Zigrang and Sylvester *(4)* or Haaland equations *(5)* (Table 2). These equations also apply for Reynolds numbers greater than 4,000.

Adding together the static head, the fittings headloss, and the straight-run headloss will give you the total head the pump needs to generate to overcome resistance and deliver the specified flowrate to the system.

Suction head and net positive suction head

Even at an early stage, I also recommend determining the pump's required net positive suction head and calculating the net positive suction head (NPSH), as they can affect much more than pump specification. The pump's required net positive suction head takes into consideration the liquid's vapor pressure to avoid cavitation in the pump.

I recommend creating an Excel spreadsheet that uses the Antoine equation to estimate the vapor pressure of the liquid at the pump inlet and then calculate the NPSH at that vapor pressure.

The Antoine equation may be expressed as:

$$\log P_v = A - \frac{B}{C+T} \quad (5)$$

where P_v is vapor pressure of the liquid at the pump inlet, T is temperature, and A, B, and C are coefficients that can be obtained from the NIST database (http://webbook.nist.gov) among other places. Table 3 shows an example for water.

The net positive suction head is:

$$NPSH = \frac{P_o}{\rho g} + h_o - h_{Sf} - \frac{P_v}{\rho g} \quad (6)$$

where P_o is the absolute pressure at the suction reservoir, h_o is the reservoir liquid level relative to the pump centerline, and h_{Sf} is the headloss due to friction on the suction side of the pump.

Note that NPSH is calculated differently for centrifugal and positive-displacement pumps, and that it varies with pump speed for positive-displacement pumps rather than with pressure as for centrifugal pumps. Equation 6 should only be used with centrifugal pumps.

Table 2. These alternative curve-fitting equations can be used in lieu of the Colebrook-White equation to determine the Darcy friction factor.

Equation	Range	Source
$f_D = \left(-2\log\left[\frac{\varepsilon}{3.7} - \frac{5.02}{Re}\log\left\{\varepsilon - \frac{5.02}{Re}\log\left(\frac{\varepsilon}{3.7} + \frac{13}{Re}\right)\right\}\right]\right)^{-2}$	ε = 0.00004–0.05	*(4)*
$f_D = \left(-1.8\log\left[\left(\frac{\varepsilon}{3.7}\right)^{1.11} + \frac{6.9}{Re}\right]\right)^{-2}$	ε = 0.000001–0.05	*(5)*

Table 3. Vapor pressure for water at 30°C, calculated using the Antoine equation.

Material	*A*	*B*	*C*	T, °C	T, K	P_v, bar	P_v, Pa
Water	5.40221	1,838.675	–31.737	30	303.15	0.042438	4,243.81

Article continues on next page

Determining pump power

After the system head has been calculated, it can be used to calculate an approximate pump power rating for a centrifugal pump:

$$P = \frac{Q\rho g H}{3.6\times10^{6}\eta} \qquad (7)$$

where P is the pump power (kW), Q is the flowrate (m^3/hr), H is the total pump head (m of fluid), and η is the pump efficiency (if you do not know the efficiency, use $\eta = 0.7$).

The pump manufacturer provides the precise power ratings and motor size for the pump, but the electrical engineers need an approximate value of this (and pump location) early in the design process to allow them to size the power cables. You should err on the side of caution in this rating calculation (the electrical engineers will be much happier if you come back later to ask for a lower power rating than a higher one).

In certain stages of design development, the preliminary drawings are modified to match likely hydraulic conditions across the design envelope. This may require you to do many approximate hydraulic calculations before the design has settled into a plausible form.

After you have performed the hydraulic calculations, the pump and possibly the pipe sizes might need to be changed, as might the minimum and maximum operating pressures at certain points in the system. As the system design becomes more refined, there might even be a requirement to change from one pump type to another.

Hydraulic networks

The previous sections describe how to calculate the headloss through a single line, but what about the common situation where the process has branched lines, manifolds, and so on? When each branch handles a flow proportional to its headloss, and its headloss is proportional to the flow passing through it, producing an accurate model can become complex very quickly.

My approach to this is to first simplify and then improve the design as much as possible with a few rules of thumb:

- Avoid manifold arrangements that provide a straight-through path from the feed line to a branch. Entry perpendicular to branch direction is preferred.
- Size manifolds such that the superficial velocity never exceeds 1 m/sec at the highest anticipated flowrate.
- Specify progressively smaller manifold diameters to accommodate lower flows to downstream branches.
- Include a small hydraulic restriction in the branch so the branch headloss is 10–100 times the headloss across the manifold.
- Design-in passive flow equalization throughout the piping system wherever possible by making branches hydraulically equivalent.

Perform headloss calculations for each section of the simplified plant design at expected flows to find the flow path with the highest headloss. Use the highest-headloss path to determine the required pump duty — calculate the pump duty at both the average flow with working flow equalization, and at full flow through a single branch. Usually these do not differ much, and the more rigorous answer lies between them. Only if the two results of this approach are very different will I do a more rigorous (and time-consuming) analysis.

If such a rigorous analysis is needed, I create an Excel spreadsheet based on the Hardy Cross method — a method for determining the flow in a pipe network when the flows within the network are unknown but the inputs and outputs are known — and solve for individual pipe flows. Excel's Solver function can be used to find the change in flow that gives zero loop headloss. In the unlikely event that you have to do this, an explanation of how to carry out the method can be found in Ref. 6. There are many computer programs available to do these calculations.

Pump curves

A pump curve is a plot of outlet pressure as a function of flow and is characteristic of a certain pump. The most frequent use of pump curves is in the selection of centrifugal pumps, as the flowrate of these pumps varies dramatically with system pressure. Pump curves are used far less frequently for positive-displacement pumps. A basic pump curve plots the relationship between head and flow for a pump (Figure 4).

On a typical pump curve, flowrate (Q) is on the horizontal axis and head (H) is on the vertical axis. The pump curve shows the measured relationship between these variables, so

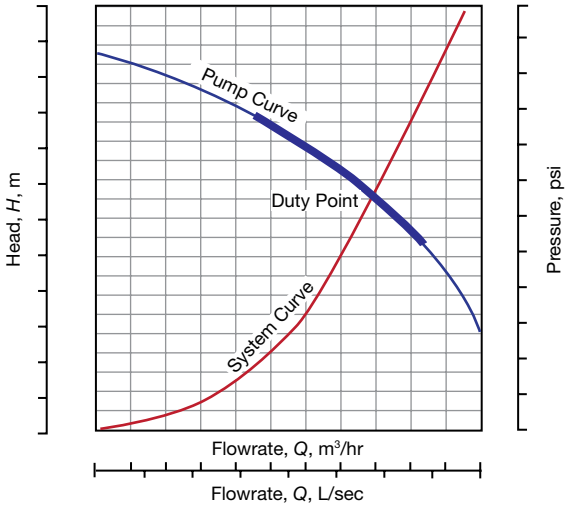

▲ **Figure 4.** A basic pump curve plots pressure (or head) as a function of flowrate.

it is sometimes called a *Q/H* curve. The intersection of this curve with the vertical axis corresponds to the closed valve head of the pump. These curves are generated by the pump manufacturer under shop test conditions and ideally represent average values for a representative sample of pumps.

A plot of the system head over a range of flowrates, from zero to some value above the maximum required flow, is called the system curve. To generate a system curve, complete the system head calculations for a range of expected process flowrates. System head can be plotted on the same axes as the pump curve. The point at which the system curve and the pump curve intersect is the operating point, or duty point, of the pump.

Remember that a system curve applies to a range of flows at a given system configuration. Throttling a valve in the system will produce a different system curve. If flow through the system will be controlled by opening and closing valves, you need to generate a set of curves that represent expected operating conditions, with a corresponding set of duty points.

It is common to have efficiency, power, and NPSH plotted on the same graph (Figure 5). Each of these variables requires its own vertical axis. To obtain the pump efficiency at the duty point, draw a line vertically from the duty point to the efficiency curve, and then draw a horizontal line from there to the vertical axis that corresponds to efficiency. Similarly, to obtain the motor power requirement, draw a line down from the duty point to the motor duty curve.

More sophisticated curves may include nested curves representing the flow/head relationship at different supply frequencies (*i.e.,* the AC electrical supply's frequency in Hz) or rotational speeds, with different impellers, or for different fluid densities. Curves for larger impellers or faster rotation lie above curves for smaller impellers or slower rotation, and curves for lower-density fluids lie above curves for higher-density fluids. A more-advanced pump curve might also incorporate impeller diameters and NPSH. Figure 6 depicts pump curves for four different impellers, ranging from 222 mm to 260 mm. Corresponding power curves for each impeller are shown on the bottom of the figure. The dashed lines in Figure 6 are efficiency curves.

These curves can start to look a bit confusing, but the important point to keep in mind is that, just as in the simpler examples, flowrate is always on a common horizontal axis, and the corresponding value on any curve is vertically above or below the duty point.

These more-advanced curves usually incorporate efficiency curves, and these curves define a region of highest efficiency. At the center of this region is the best efficiency point (BEP).

Choose a pump that has an acceptable efficiency across the range of expected operating conditions. Note that we are not necessarily concerned with the entire design envelope —

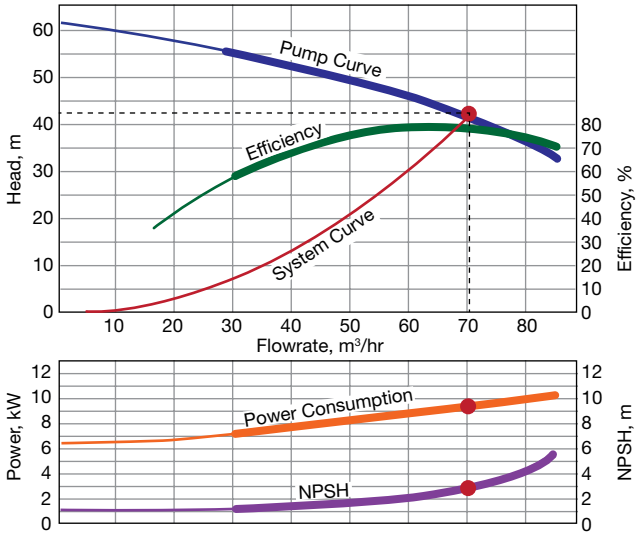

▲ **Figure 5.** Efficiency, power, and net positive suction head can also be plotted on a pump curve. Original image courtesy of Grundfos.

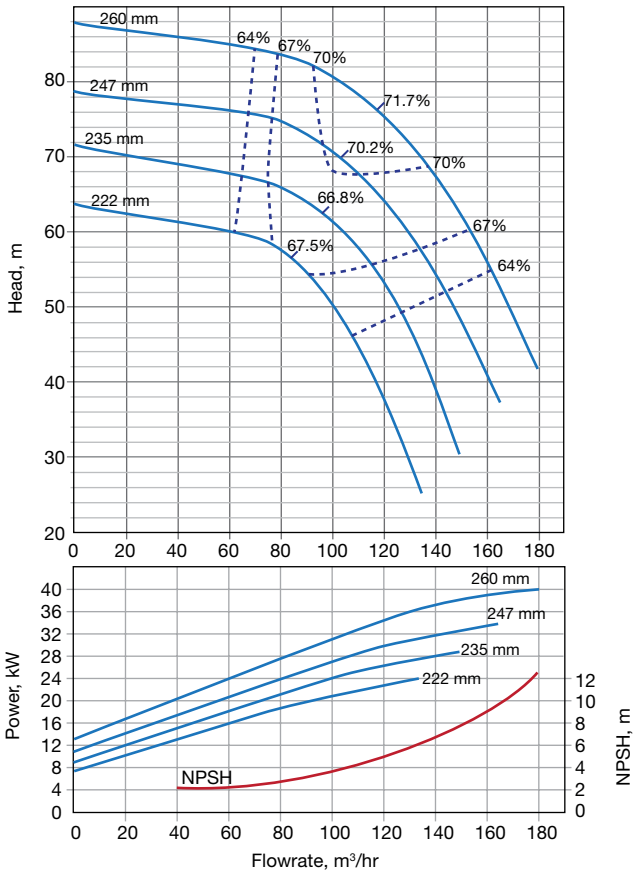

▲ **Figure 6.** A complex pump curve integrates efficiency, NPSH, and impeller diameters on one diagram. Copyright image reproduced courtesy of Grundfos.

it is not crucial to have high efficiency across all conceivable conditions, just the normal operating range.

The optimal pump for your application will have a BEP close to the duty point. If the duty point is far to the right of a pump curve, well away from the BEP, it is not the right pump for the job.

Even with the most cooperative pump supplier, sometimes the curves that you need to make a pump selection may not be available. This is commonly the case if you want to use an inverter to control pump output based on speed.

However, you can often generate acceptable pump curves using the curves you have and the following approximate pump affinity relationships:

$$\frac{Flowrate_2}{Flowrate_1} = \frac{Impeller\ Diameter_2}{Impeller\ Diameter_1} = \frac{Pump\ Speed_2}{Pump\ Speed_1} \quad (8)$$

$$\frac{Dynamic\ Head_2}{Dynamic\ Head_1} = \left(\frac{Impeller\ Diameter_2}{Impeller\ Diameter_1}\right)^2 = \left(\frac{Pump\ Speed_2}{Pump\ Speed_1}\right)^2 \quad (9)$$

$$\frac{Power\ Rating_2}{Power\ Rating_1} = \left(\frac{Impeller\ Diameter_2}{Impeller\ Diameter_1}\right)^3 = \left(\frac{Pump\ Speed_2}{Pump\ Speed_1}\right)^3 \quad (10)$$

$$\frac{NPSH_2}{NPSH_1} = \left(\frac{Impeller\ Diameter_2}{Impeller\ Diameter_1}\right)^x = \left(\frac{Pump\ Speed_2}{Pump\ Speed_1}\right)^y \quad (11)$$

where the subscript 1 designates an initial condition on a known pump curve and subscript 2 is some new condition.

The NPSH relationship in Eq. 11 is more of an approximation than the others. The value of x lies in the range of –2.5 to +1.5, and y in the range of +1.5 to +2.5.

Closing thoughts

These are the basics of pump selection. A final word of advice: If you don't understand what is presented here, or need to know more, I suggest that you talk to a pump supplier in private. Think twice before you post on social media to ask for advice on the basics of pump selection — the advice you receive may not be correct, and your post may reflect badly on you and your employer. CEP

SEÁN MORAN has had 25 years of experience in process plant design, troubleshooting, and commissioning. He was an associate professor and Coordinator of Design Teaching at the Univ. of Nottingham for four years, and is presently a visiting professor at the Univ. of Chester. He has written three books on process plant design for the Institution of Chemical Engineers. His professional practice now centers on acting as an expert witness in commercial disputes regarding process plant design issues, although he still has cause to put on a hardhat from time to time. He holds a master's degree in biochemical engineering from Univ. College London.

Literature Cited

1. **Perry, R. H., and Green, D. W.,** "Perry's Chemical Engineers' Handbook," 8th Ed., McGraw-Hill, New York, NY, p. 6-18 (2007).
2. **Moran, S.,** "An Applied Guide to Process and Plant Design," Butterworth-Heinemann Oxford, U.K. (2015).
3. **Genić, S., *et al.,*** "A Review of Explicit Approximations of Colebrook's Equation," *FME Transactions,* **39**, pp. 67–71 (June 2011).
4. **Zigrang, D. J., and N. D. Sylvester,** "Explicit Approximations to the Solution of Colebrook's Friction Factor Equation," *AIChE Journal,* **28** (3), pp. 514–515 (May 1982).
5. **Haaland, S. E.,** "Simple and Explicit Formulas for the Friction Factor in Turbulent Flow," *Journal of Fluids Engineering,* **105** (1), pp. 89–90 (1983).
6. **Huddleston, D., *et al.,*** "A Spreadsheet Replacement for Hardy-Cross Piping System Analysis in Undergraduate Hydraulics," *Critical Transitions in Water and Environmental Resources Management*, pp. 1–8 (2004).

Nomenclature

A, B, C	= Antoine coefficients
D	= pipe internal diameter
D_h	= hydraulic diameter of the pipe
f_D	= Darcy friction factor
g	= acceleration due to gravity (9.81 m/sec^2)
H	= total system head
h_f	= headloss due to fittings in meters water gauge (mwg)
h_o	= reservoir liquid level relative to the pump centerline
h_{Sf}	= headloss due to friction on the suction side of the pump
k	= resistance coefficient of valves, fittings, bends, tees, etc.
L	= length of pipe
$NPSH$	= net positive suction head
P	= power (kW)
P_v	= vapor pressure of the liquid at the pump inlet
P_o	= absolute pressure at the suction reservoir
Q	= flowrate
Re	= Reynolds number
T	= temperature
v	= superficial velocity

Greek letters

Δp	= pressure loss due to viscous effects
ε	= surface roughness of the pipe
η	= pump efficiency
μ	= fluid dynamic viscosity (kg/(m-sec))
ρ	= density of fluid (kg/m^3)

Consider Moving to Fixed Valves

Scott Hebert
Neil Sandford
Koch-Glitsch, LP

CPI companies are switching to fixed valves despite a slight loss in operational flexibility. Fixed valves offer better reliability, fouling resistance, and more robust valve designs.

Distillation is an essential separation technology for a wide range of applications in the chemical process industries (CPI). Of critical importance to the separation are the mass-transfer devices on distillation trays that create intimate mixing of the liquid and vapor.

The most common types of mass-transfer devices for conventional cross-flow trays (Figure 1) are moving valves and fixed valves. Although moving valves provide operational flexibility, many CPI companies have started selecting fixed valves. They are willing to accept the loss of some operational flexibility to gain benefits provided by fixed valves, including better reliability, fouling resistance, and more robust valve designs that can better withstand operational upsets.

This article discusses moving valves and fixed valves, explains their advantages and disadvantages, and offers guidance on selecting the appropriate valves for distillation trays. The article also includes several examples that illustrate the benefits of fixed valves.

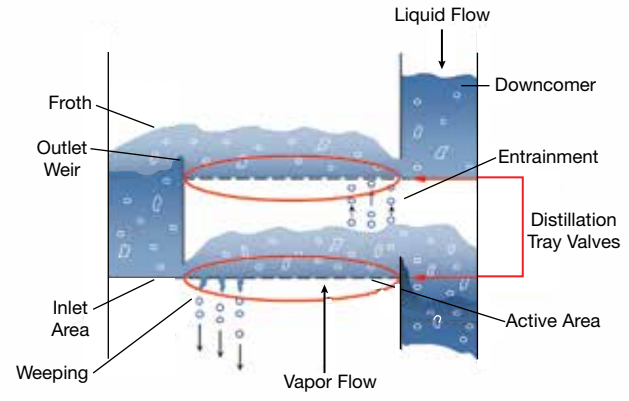

▲ **Figure 1.** In a conventional cross-flow distillation tray, liquid moves down as vapor moves up.

Bubble-cap trays and sieve trays

Before discussing fixed and moving valves, it is important to first discuss two non-valve tray designs — bubble-cap trays (Figure 2) and sieve trays (Figure 3) — that were used in the early days of industrial distillation. These provide a reference point against which to compare other designs.

Bubble-cap trays have been in use since the early 1800s *(1)*. The bubble-cap tray contains holes with a riser on each hole covered by a cap. Vapor passes through the riser as

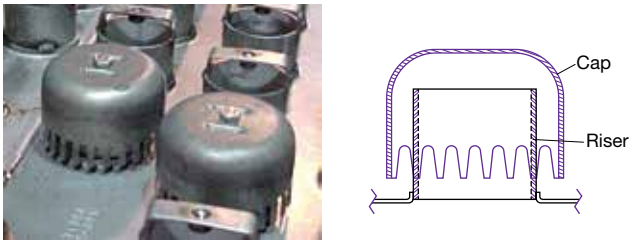

▲ **Figure 2.** A bubble-cap tray has risers on each hole with caps covering the risers.

▲ **Figure 3.** Sieve trays have round holes punched or drilled into the tray.

it moves upward and is forced downward by the cap, and then it moves back up as it bubbles through the liquid on the tray. Bubble-cap trays require extensive labor and more materials to produce than extruded fixed valves, and therefore are significantly more expensive (by a factor of 2–3). Although very common in older plants, bubble-cap trays have fallen out of favor for general distillation use due to their high cost.

Bubble-cap trays do have advantages and are appropriate for some low-liquid-rate niche applications, as well as applications with widely varying vapor loads. If designed and installed properly, bubble-cap trays do not weep. If weeping occurs on a bubble-cap tray, it is the result of improper design or incorrect installation. A well-sealed bubble-cap tray can have almost infinite vapor turndown (ignoring tray activity, which is discussed later).

Sieve trays, which contain round holes cut or punched through the tray deck, were developed around the same time as bubble-cap trays. In contrast to bubble-cap trays, sieve trays are relatively easy to produce, as production involves simply creating round holes in the tray deck. While sieve trays are inexpensive to produce, they generally do not perform as well — in terms of capacity, flexibility, and fouling resistance — as other mass-transfer devices.

Sieve trays begin to experience entrainment at lower vapor flowrates than fixed-valve or moving-valve trays. Unlike on a valve tray, where vapor is deflected horizontally as it exits a fixed or moving valve, vapor exiting the holes of a sieve tray moves vertically. The vertically directed vapor creates higher froth heights, increasing the potential for entrainment.

This vapor deflection increases the vapor velocity on the tray deck around fixed or moving valves, which helps prevent zones of stagnation where solids can deposit, polymerization can begin, or corrosion can occur. Thus, valve trays offer more fouling resistance than small-hole sieve trays.

Valves

Although bubble-cap and sieve trays are sufficient for certain applications, valve trays have become the most common mass-transfer devices in the CPI. The vapor deflection helps induce more intimate vapor-liquid contacting than is experienced on sieve trays, and valve trays are less expensive than bubble-cap trays.

The valves can be fixed or moving. Fixed valves are permanently open, while moving valves are lifted open by the vapor flowing up through the tray holes.

Moving valves

After its introduction in the early 1950s, the modern moving-valve tray (Figure 4) became a standard for distillation in the chemical industry. Its chief advantage is that its variable vertical movement accommodates a wide operating range. The range of a valve's movement is determined by either the length of the valve legs that protrude through the tray deck orifice (Figure 5, left and right images), or by a cage assembly (Figure 5, center) that restricts vertical movement.

To take advantage of the moving valve's wide operating range, an operator can simply turn up or turn down the vapor flowrate within a certain operating window. Moving valves can generally achieve a nominal turndown (*i.e.*, the ratio of the maximum vapor flowrate to the minimum vapor flowrate) of 4:1.

Turndown ratio is primarily a function of available pressure drop. As the vapor flowrate decreases, so does the pressure drop across the tray. When the tray pressure drop becomes too low, the tray begins to weep, which causes the efficiency of the column to decline. On a moving-valve tray, however, some of the valves begin to close when the vapor flowrate decreases, reducing the effective open area of the tray and limiting the tendency to weep.

Another factor affecting turndown for moving-valve trays is tray activity. As the vapor flowrate decreases, so does the number of valves on the tray actively bubbling vapor. This is particularly important for multipass trays, which typically require a higher vapor flowrate to ensure that all passes are actively bubbling vapor. Tray efficiency declines sharply if one pass becomes inactive. The more flow passes a tray has, the more difficult it is to ensure complete activity on that tray.

One way to improve the turndown performance of moving-valve trays is to install the valves in rows of alternating metal thickness (*e.g.*, alternate 14-gauge and 16-gauge). Using valves of slightly different weights gives the designer control over which valves close first as the vapor flowrate decreases. This design can extend the operating range beyond the 4:1 turndown mentioned previously. Turndown ratios of 10:1 are possible with properly designed moving valves, provided the available pressure drop and tray spacing are reasonable and the system is nonfoaming.

While the standard moveable valves provide a high hydraulic turndown ratio and are more efficient than sieve trays, they also have disadvantages:

• Because they typically have more surface area available

▲ **Figure 4.** A moving-valve tray has valves that move up and down.

▲ **Figure 5.** Moving valves come in several shapes and sizes, including round valves with legs that protrude through the tray orifice (left), caged assemblies (center), and rectangular valves (right).

for the deposition of contaminants, moving valves are more prone to fouling than fixed valves. This is a serious concern for towers operating in severe environments that have a much higher potential for particulate deposition caused by dirt and debris, various forms of corrosion (*e.g.*, from acids), dewpoint salt formation, and, in some cases, polymerization.

• As moving valves open and close, the valve legs can contact the edges of the orifice, which can cause erosion and increase corrosion.

• Fouling or polymer deposition can cause moving valves to stick to the tray deck. To eliminate sticking, most valves are equipped with dimples that prevent complete contact between the valve cap and the tray deck. However, the small escape area provided by the presence of dimples can increase liquid weeping at low vapor flowrates.

• If subjected to an unexpected process upset, moving valves can pop free from their orifices, leaving behind *de facto* sieve holes, which have lower capacity and efficiency than valves.

• Moving valves are more expensive than conventional fixed valves, because more labor and material are required to manufacture them. A general rule of thumb is that moving valves are 10–15% more expensive than conventional fixed valves.

• If trays with moving valves are operated at excessively low vapor flowrates (very high turndown), like fixed valves, they will also experience reduced tray efficiency.

Fixed valves

The simplest fixed valves (Figure 6) are formed from the same piece of metal as the tray deck. Large metal-punching (or stamping) machines impart a tremendous amount of force on a relatively small area of metal sheet to extrude the valve from the tray deck. During this process, the metal is actually stretched from its initial state.

Fixed-valve trays made in this way have no moving parts and are rugged and durable. Thus, they do not suffer from the sticking, popping, and erosion and corrosion associated with moving valves. And, the relatively large opening between the valve and the deck makes extruded fixed valves resistant to fouling. Fixed valves can be manufactured with different heights, and, if necessary, can be made with a higher net rise (Figure 7) to provide more resistance to fouling.

In addition, the hydraulic capacity is inversely proportional to the size of the valve opening — the smaller the opening, the higher the capacity. And, the lower the net rise, the less entrainment that can be expected. Smaller-opening and lower-net-rise extruded fixed-valve trays are often used in heavily loaded tower sections, such as direct-contact heat-transfer pump-around zones.

Another benefit of extruded fixed valves is their ability to withstand process upsets. Due to their durable construction, the mechanical reliability of fixed valves makes them good choices for towers that require an uplift rating to guard against damage. Uplift refers to the forces that the metal internals in a distillation tower are subject to during upset conditions. It can occur, for example, when water is introduced into hot oil and the water rapidly expands as it transforms into steam, when a circulating pump stops working, or when the level of the bottoms liquid becomes so high that it covers reboiler vapor returns.

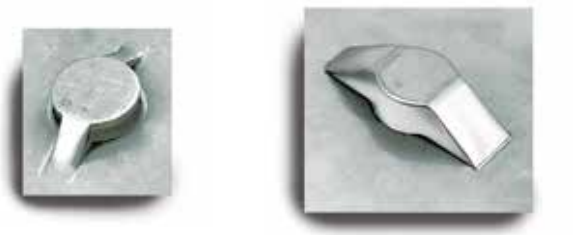

▲ **Figure 6.** The simplest fixed valve is an extruded hole and cover with small-diameter (left) or large-diameter (right) orifices.

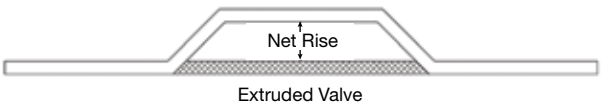

▲ **Figure 7.** The net rise of a fixed valve is the vertical distance from the tray deck to the underside of the valve apex.

Enhanced-fixed-valve designs

As they processed thicker metals and/or metals that could not tolerate as much stretching, mass-transfer equipment suppliers realized that the net rise improvements they could achieve became limited.

One way to address the limitations is a fixed-valve tray that combines large orifices in the deck with separate cover pieces that overhang the openings (Figure 8). The large orifice is similar in size to moving-valve orifices and larger than conventional, high-performance, fixed-valve orifices. The cover pieces have a unique tapered shape that, in effect, pushes the liquid flowing across the tray and prevents the formation of stagnant liquid on the tray deck. This feature also suppresses weeping, since the orifice is well-protected from the momentum of the liquid crossing the tray deck. And, the cover redirects the vapor horizontally from the valve cover, which promotes an even and low froth height, promotes vapor-liquid contacting, and suppresses jet flooding. This unique valve-tray design has excellent fouling resistance and is far superior to moving valves and conventional extruded fixed valves. Unlike extruded fixed valves, the tapered orifice covers cannot be fabricated by extrusion and must be assembled separately.

Mechanical testing showed that this valve construction is very durable and not prone to the problem of dislodging that sometimes occurs with traditional moving valves; in most situations, the tray structure would fail long before the valves could be dislodged. Hence, like trays with extruded fixed valves, the enhanced-fixed-valve tray construction is reliably durable.

Computational fluid dynamics (CFD) modeling was used to compare the predicted vapor flow from an enhanced fixed valve to the vapor flow from a conventional extruded fixed valve (Figure 9). The vapor flow from the enhanced fixed valve is more horizontal than that of the conventional fixed valve; this more horizontal vapor profile enhances mass transfer and aids in preventing fouling material from settling on the tray or around the orifices.

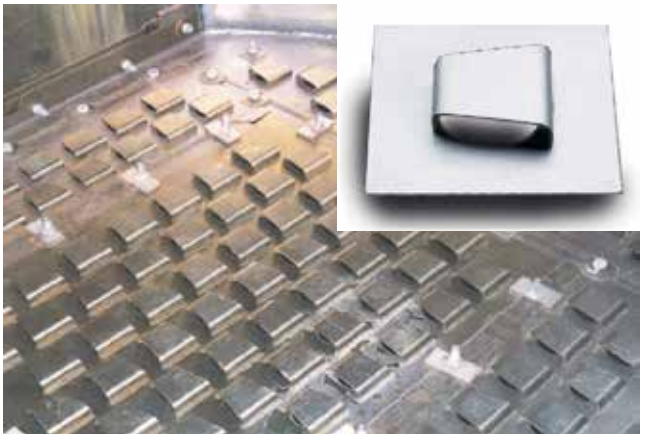

▲ **Figure 8.** An enhanced fixed valve consists of a large orifice in the deck combined with a separate cover piece that overlaps the orifice.

The CFD results show that the enhanced fixed valve eliminates the vertical component of the vapor distribution from a conventional extruded fixed valve. As noted previously, smaller valves tend to have higher capacity, and lower-net-rise valves tend to have less entrainment. The enhanced valve stands out because even though it is a larger valve, it achieves high performance, with a capacity approaching that of a smaller traditional fixed valve. Additional advancements to the enhanced fixed valve have focused on improving vapor-liquid mixing on the tray deck, which reduces liquid entrainment and thus increases tray separation efficiency and capacity.

Enhanced fixed valves are slightly more expensive than extruded fixed valves because their construction process requires the fabrication of the separate cover piece. Their cost is comparable to that of traditional moving valves; however, the benefits of enhanced-valve trays typically justify the incremental cost.

Valve selection

Whether considering distillation tray valves for a new tower or for a revamp, ask these two important questions:

1. Do I need a large operating range for my process?
2. Do I have a severely fouling process?

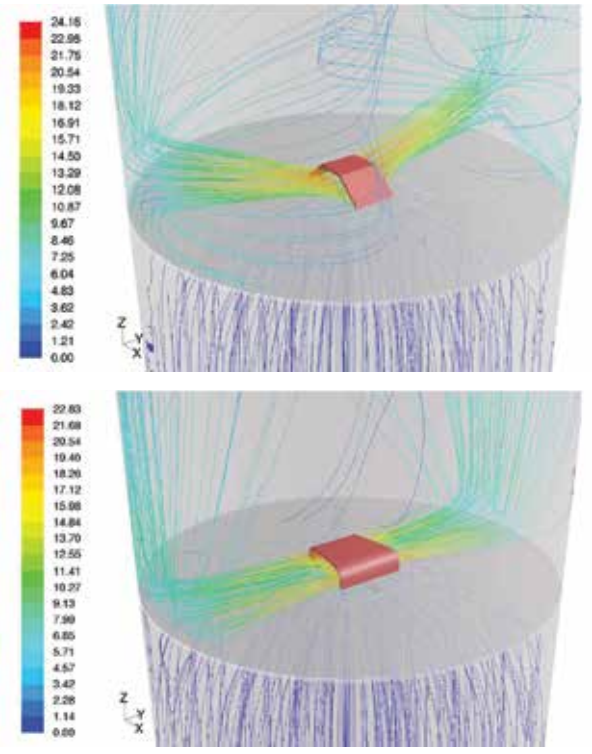

▲ **Figure 9.** CFD modeling compares the vapor flow through a conventional extruded fixed valve (top) and an enhanced fixed valve (bottom).

Article continues on next page

Operating range. In the petroleum refining industry, when profit margins are strong, companies tend to run operating units at full capacity (or beyond design rates, if possible), and not much variance in the hydraulic capacity of the trays is needed. While it may be desirable to run some units at minimum rates during periods of low economic margins or during maintenance on related units, very few units in refineries likely operate at less than 50% of their maximum rate. Changes in market conditions and unique product inventory-management considerations might make it necessary for chemical plants to operate units at rates less than design capacity, but it is unlikely that rates below 50% of design would be sustained for long periods of time.

With this in mind, more companies are shifting toward fixed valves for distillation trays. As a rule of thumb, fixed valves typically have a turndown ratio of 2:1 (although proper design can push the turndown range higher). This turndown on distillation tray hydraulic capacity is close to the hydraulic turndown of other parts of the operating unit (*e.g.,* minimum flowrates of pumps and heaters, control valve sizing, etc.).

Severe fouling. The refining and chemical industries both have severe services, and operating units' run times are often limited by fouling on the distillation trays, which can eventually render some types of valve trays inoperable. Moving valves are more prone to fouling than fixed valves. Thus, when fouling is a problem, moving valves will cause downtime more often. Figure 10 compares the fouling resistance of various mass-transfer devices.

Fouling can occur in many different types of applications. Foulants can be sticky, granular, or film-like. In some processes, the foulants collect on the tops of the trays; in others, the undersides of the tray are affected. In some cases, the foulants enter from an upstream process unit; in others, they are formed inside the trayed tower.

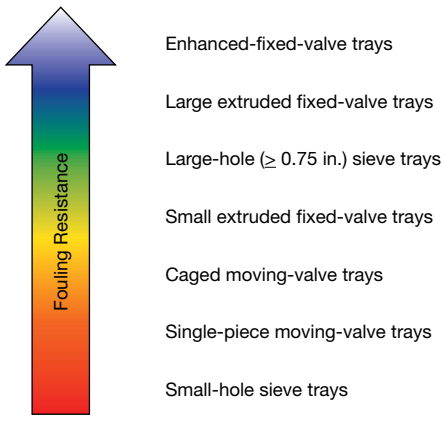

▲ **Figure 10.** Mass-transfer devices provide different levels of fouling resistance. The enhanced-fixed-valve tray provides the most resistance, sieve trays the least.

Here are a few examples of problematic fouling that commonly occurs in the CPI:

• Acrylonitrile (ACN) plants experience fouling in the recovery columns, the head columns, and the drying columns. Polymer fouling can occur from the polymerization of hydrogen cyanide (HCN) and the polymerization of ACN. The use of high-performance fixed valves with directional-flow enhancements (*e.g.*, push valves) combined with the injection of polymer inhibitors help to minimize polymerization and maximize run time.

• In bioethanol plants, the fermentation broth, which contains 10–15% solids, is fed to a beer stripper column that removes the ethanol. The trays in this tower are fouled primarily on the underside but also on the upper side of the trays. Enhanced fixed valves help to mitigate fouling in both areas by reducing the froth heights and driving the foulants across the tray decks.

• The recent substantial increase in light domestic crude oil production in the U.S. is giving oil refiners a readily available alternative feedstock. However, when some of these lighter crude oils are blended with other light crudes or with heavier crude oils, asphaltene — a foulant that will deposit on trays in crude distillation towers — can precipitate *(2)*.

• Olefins plants have several columns that are susceptible to fouling. Ethylene quench columns suffer from fouling by coke fines and by a sticky, oligomer-type foulant. Caustic wash towers can experience the build-up of foulants, typically referred to as red oil, created by aldol-condensation polymerization. Large fixed valves with a high net rise have been successfully used in these towers.

Although fixed valves do offer benefits, they are not as operationally flexible as moving valves. However, this loss of flexibility — a narrower turndown range that precludes running at significantly lower vapor flowrates — is usually a reasonable price to pay to avoid the problems associated with moving valves, such as:

• more fouling than fixed valves, because moving valves have more places for dirt, debris, polymers, and other contaminants to collect

• the potential to stick to the deck, which reduces capacity and tray efficiency

• loss of tray performance if they pop off the deck and entrainment through unrestricted orifices increases

• higher capital expenditures.

Many companies have performed a cost/benefit analysis and determined that the installation of fixed valves with a smaller operating window is adequate for their process and helps avoid some of the disadvantages inherent to moving valves. The following examples illustrate the benefits of switching to fixed valves.

Sour-water stripper

Sour-water strippers *(3)* are often difficult to operate because they process feed streams of widely varying compositions, and they experience severe foaming as well as fouling.

A refinery had two identical sour-water strippers equipped with sieve trays that had 0.5-in. orifices. The towers processed the same sour feed and suffered chronic fouling problems so severe that they required several shutdowns each year for maintenance. The parallel feed arrangement of the two identical sour-water stripper towers presented a unique opportunity to test the performance of new trays under the same conditions as the existing sieve trays.

In the first test, the refiner installed two enhanced-fixed-valve trays in one stripper at a location where the fouling was most severe. After the stripper operated for a typical run length, it was shut down for maintenance and the trays were examined. The two new trays had negligible visual evidence of fouling, while the adjacent sieve trays had considerable fouling and their flow area was reduced by about 90% (Figure 11).

Based on these results, the refiner installed new enhanced-fixed-valve trays throughout the second stripper and then restarted operation. Approximately two weeks later, the first tower was cleaned and restarted, with the existing sieve trays still in place. After a typical run length (130 days), the tower with the sieve trays had to be shut down for cleanout. After the same run time, the sour-water stripper with the new trays was processing sour-water feed at the same rate, yet with no significant increase in pressure drop (Table 1).

A process upset occurred when the sour-water feed was contaminated with caustic, which greatly increased fouling. This provided a third opportunity for testing. At the time of the upset, the sieve-tray tower had been online for 42 days since its last cleanout, while the tower with the enhanced-fixed-valve trays had been online for 191 days. On the eighth day after the upset, the pressure drop of the sieve-tray tower was so high that the feed flowrate was cut in half (Figure 12).

Thirty days after the upset, the sieve-tray tower was taken offline for cleanout. Meanwhile, the tower outfitted with new fixed-valve trays remained online, although the liquid rate was limited to 350–450 gpm. And, 350 days after the upset, the newly trayed tower was still online and processing 350 gpm of sour water. The test results clearly demonstrated the improved performance and fouling resistance of enhanced-fixed-valve trays in sour-water service. The sieve-tray tower was subsequently revamped with new fixed-valve trays.

Solvent-recovery dehydration column

A solvent-recovery dehydration column with sieve trays experienced severe fouling that limited run-length time (Figure 13). Shutdowns were required for cleanout when tower pressure drop became excessive, after approximately 120 days.

The fouling material was a flaky black polymer. To correct the problem, the company installed extruded fixed valves; unfortunately, those fixed valves were too small and the trays had less open area than the sieve trays they replaced. The tower soon became completely fouled; the most severe fouling was toward the bottom of the tower.

The company initially reverted to sieve trays throughout

Table 1. After 130 days of operation, the tower with enhanced-fixed-valve trays was processing more sour-water feed than the tower with sieve trays.

	Tower with 0.5-in. Sieve Trays	Tower with Enhanced-Fixed-Valve Trays
Sour Water Feed, Initial, gpm	480	600
Sour Water Feed after 130 days, gpm	200	550–600
Column Pressure Drop after 130 days	Flooded	No Increase

▲ **Figure 11.** After a sour-water stripper operated for a typical run length, the adjacent sieve (left) and enhanced-fixed-valve (right) trays were examined. The sieve trays had significantly more fouling than the fixed-valve trays.

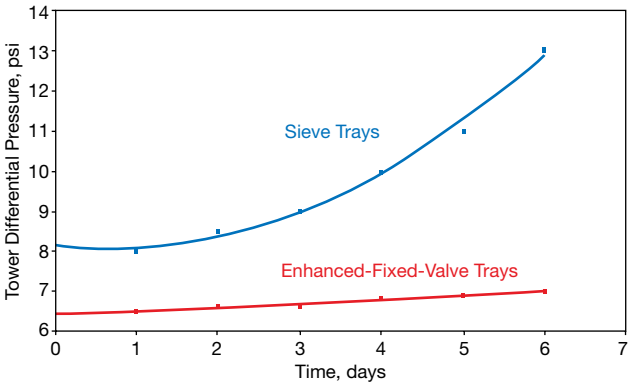

▲ **Figure 12.** After caustic contaminated the feed, the tower with the sieve trays (blue) experienced a much larger pressure drop than the tower with the enhanced fixed valves (red).

most of the column and enhanced-fixed-valve trays — with the same downcomer area, same weir height, and same downcomer clearance as the sieve trays — in the bottom section. The tower was restarted and achieved a record run length of 197 days (an increase of 65%), and was shut down only for inspection (cleaning was not needed). While the sieve trays in the top section were considerably fouled, the new fixed-valve tray orifices had no signs of fouling, with minimal polymer coating on the tray decks.

Before restarting the column, the operators carefully cleaned the trays in the top section of the column. Ninety days into the run, the tower pressure drop was lower than it was when the column had all sieve trays. The good results of these runs convinced the company to install new enhanced-fixed-valve trays in three identical towers.

Acryolnitrile production

A European acrylonitrile producer experienced a significant loss in production due to fouling in a recovery column. Fouling was occurring on the active areas of the moving-valve trays; one of the two recovery columns had to be shut down every four months for a lengthy and costly cleanout, during which plant capacity was cut in half.

The company decided to revamp the problem tower to increase the feed flowrate by 10% and to increase its run length. To do this, it replaced the existing moving-valve trays in the active areas with high-performance extruded fixed-valve trays.

After the revamp, the column was started up with no problems. About six months later, reactor problems (unrelated to the recovery column) forced the plant to shut down. The facility's staff took this opportunity to enter and inspect the recovery column — the trays were clean and required no cleanout maintenance whatsoever. After the reactor problems were corrected, the unit started up again and the recovery column operated for more than a year at a 10% higher capacity.

The success of this project prompted the company to revamp the trays in the other recovery column by replacing the moving valves with high-performance extruded fixed valves during the next downtime.

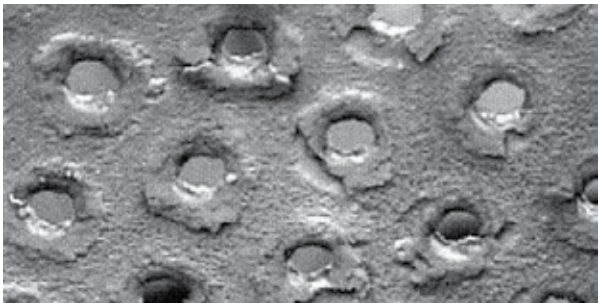

▲ **Figure 13.** Sieve trays in a solvent-recovery dehydration column experienced severe fouling after approximately 120 days in service.

Butadiene plant

A butadiene plant was revamped to increase production. Existing moving valves were replaced with high-performance extruded fixed valves to debottleneck a distillation column. The objectives were to increase column capacity by 15% and eliminate fouling on the trays caused by butadiene polymerization.

Before the revamp, the company had to filter polymer out of the column using dual-strainer filters at the top and bottom of the column. The filters required frequent cleaning, with one filter in service while the other filter was being cleaned.

After the revamp, filter cycling for cleaning was no longer necessary. During a plant shutdown for maintenance, operators inspected the column and found that the trays were clean, with no polymer on the trays. The photos in Figure 14 show the fouled moving-valve trays before the revamp (top) and the clean high-performance extruded fixed-valve trays after operation (bottom).

Tower pressure drop was reduced from about 18 psi before the revamp to about 10 psi after the revamp. In addition, the reflux ratio was reduced from 4.8 to 4.2 while the same product purities were maintained. Energy savings were achieved by a reboiler duty reduction of approximately 9%. The tower capacity was ultimately increased by 32%, which significantly exceeded the target of 15%.

▲ **Figure 14.** Conventional moving-valve trays (top) in a butadiene plant had considerable fouling. The high-performance extruded fixed-valve trays (bottom) remained clean after operation.

▲ **Figure 15.** After operating for one cycle in a coker fractionator, these moving caged valves had considerable fouling.

▲ **Figure 16.** Enhanced fixed valves had little fouling after being in service in a coker fractionator for several years.

Vinyl chloride monomer plant

A VCM producer wanted to debottleneck its ethylene dichloride (EDC) heavy-ends column to increase capacity by 25% and increase run length. The tower experienced frequent shutdowns due to tray fouling.

The company used sieve trays for the EDC heavy-ends column because moving valves were unreliable in this application. A process evaluation indicated that the existing trays were operating at their capacity limits, which was confirmed by a gamma scan. Based on this information and the type of fouling involved, high-performance extruded fixed valves were recommended for the tower revamp.

After the new trays were installed, the unit was started up and a test run was performed to evaluate the effectiveness of the new trays. The unit operated at a 10% higher capacity and the product met the target EDC purity of 99.6%. After two years, the tower was operating at a 24% higher capacity without any problems. The column did not need to be shut down to correct fouling problems. The new trays also proved to be more efficient — the tray spacing in one section of the tower was changed and the revamped tower contained three fewer trays.

Heavy oil service

Fouling is a major consideration in the design of refinery coker fractionators, which process dirty feed in harsh conditions. Figure 15 shows trays from a coker fractionator with moving caged valves after the tower completed one run cycle.

Fixed valves — either large extruded fixed valves or enhanced fixed valves — are strongly recommended for coker fractionator service. The enhanced-fixed-valve tray technology discussed previously has been installed in more than 25 coker fractionators worldwide, in towers ranging in diameter from 6.5 ft to 25 ft. Figure 16 shows trays with these valves after many years of service in a coker fractionator. Notice that while some fouling material accumulated on the valve cover, the orifice and the area around the orifice are virtually clean.

Fixed-valve trays have worked reliably for refinery and chemical plant services, where high temperature, fouling, and corrosion are significant concerns.

Wrapping up

In today's chemical processing world, companies need optimum fractionation efficiency with maximum run times and minimum operating costs. Therefore, choosing the correct distillation valve for new or revamped towers is critical. While moving valves still have their place in many distillation applications, they should generally be reserved for nonfouling services where high turndowns are absolutely necessary. Consequently, the CPI is experiencing a shift from moving valves to fixed valves. Fixed valves offer several key advantages, including higher fouling resistance, durable construction, uplift resistance, higher capacity (in some cases), reasonable turndown ranges, and lower capital costs. Enhanced-fixed-valve trays offer superior fouling resistance and capacity (in moderate to high liquid loads) compared to conventional extruded fixed valves, and are well-suited for extended operation in severe services. CEP

SCOTT HEBERT is a refining specialist at Koch-Glitsch, LP, in Houston, TX. He works with the Koch-Glitsch refining team to provide custom solutions for new and revamp mass-transfer applications. He draws on more than 15 years of previous refining industry experience, ranging from process engineering to refinery operations to economics and optimization. He received his BS in chemical engineering from Texas A&M Univ. and is a registered Professional Engineer in the state of Texas. He has been a member of AIChE for over 20 years.

NEIL SANDFORD is the Tray Product Manager at Koch-Glitsch, LP, in Wichita, KS. Previously, he worked as a process engineer and technical sales engineer in Europe and the U.S., involved with designing separation columns for the refining and petrochemical industries. He has more than 25 years of experience in distillation, absorption, liquid-liquid extraction, and heat transfer tower design and troubleshooting. He has a BS in chemical engineering from the Univ. of Salford, U.K.

Literature Cited

1. **Fair, J. R.,** "Historical Development of Distillation Equipment," AIChE Symposium Series, **80** (235), AIChE, New York, NY (1983).
2. **Wiehe, I.,** "Crude Oil Compatibility Testing," www.solublesolutions.com/?page_id=14 (accessed April 10, 2015).
3. **Hauser, R., and T. Kirkey,** "Refinery Tests Demonstrate Fixed Valve Trays Improve Performance in Sour Water Stripper," presented at the 2003 AIChE Spring National Meeting, New Orleans, LA (Mar. 31, 2003).

Leveraging Smart Valve Positioners

Janine McCormick
Steve Hagen
Emerson

Smart valve positioners offer a range of diagnostics, but the volume of information they can provide can be daunting. Establish a program to deal with alerts and analyze data to help you benefit from the information without getting overwhelmed.

Most of us interact with our personal devices — smartphones, tablets, e-readers, laptops, etc. — frequently throughout the day, everyday. We have incorporated these smart devices into our lives, but are we taking full advantage of all their functionalities? Because the power of these technologies can be overwhelming, some of us do not enable all of our devices' functions or might be totally unaware an option is available.

As more smart devices are incorporated into process equipment, this tendency to underutilize them has extended into the industrial environment. The smart valve positioner has become the standard across the chemical process industries (CPI), but are you leveraging all of the functionality of your valve positioner? Like the smartphone in your pocket, you probably are not.

Nearly every corporate or site control valve specification requires a smart positioner for all or most new valves and for replacements of existing valves. Many plants are being asked to do more on a tighter budget, and smart positioners can help meet this demand. Smart positioners offer diagnostics that can be used for predictive maintenance programs, which can save time and money.

Valve positioners

A valve positioner is the interpreter between the control valve assembly and the control system. It translates output signals from the control system and adjusts the air to the actuator, which moves the valve to the position requested by the control system (Figure 1). The positioner may also take position feedback from the valve stem/shaft and send that information back to the control system.

Valve positioners can help to overcome high valve friction, as well as reduce deadband (during which there is no valve movement) and hysteresis. The higher the friction, the more deadband associated with the control valve. Mechanical feedback from the valve assembly to the positioner enables the positioner to vary its output to overcome the friction and provide accurate control. For example, if the positioner receives a 50% input signal, it will provide whatever air output is required to move the valve to the midpoint of its range of travel. A positioner must be used with a piston actuator (with or without springs) to provide throttling control.

Smart (*i.e,* intelligent, digital) valve positioners perform the same basic functions as a traditional valve positioner,

but they have expanded functionalities. The International Society of Automation (ISA) does not differentiate between traditional and smart positioners in its standards. Like any "smart" device, a smart positioner includes a small computer that enables additional capabilities. A smart positioner is analogous to a smartphone, while a traditional positioner is like your landline — both can make calls, but one can do considerably more.

The capabilities beyond positioning are what make smart positioners unique and valuable, but also what can make them intimidating. Smart positioners make the basic positioning functionality across your plant more accurate and reliable. Every positioner can be calibrated exactly the same and that calibration can be maintained, which provides more accurate control to setpoint and thus optimum process control.

Smart positioners enable accurate calibration. Users often specify an input signal with a larger range than necessary to compensate for inaccurate positioner calibration. In the case of analog 4–20-mA inputs, users will drop the input to well below 4 mA and then adjust it to exceed 20 mA to ensure the valve shuts off and travels from 0% to 100%.

The autocalibration feature of a smart positioner eliminates the need to rely on the skill of the technician adjusting the mechanical parts. The typical calibration of a smart positioner allows a 4-mA signal to be sent to a positioner enabled for highway addressable remote transducer (HART) communication (sidebar); at that point no air would go to the actuator. If the input signal is increased to 4.12 mA, the valve would start to travel. When the signal reaches 19.92 mA, the valve would go to full 100% valve travel.

Plant Communication Protocols

Plant automation requires communication between the control system and the process equipment. The type of protocol used at a facility affects how data are transferred.

Highway addressable remote transducer (HART) protocols use the Bell 202 audio frequency-shift keying (AFSK) standard to superimpose digital communication signals on top of a 4–20-mA analog signal.

FOUNDATION Fieldbus is an all-digital, serial, two-way communication protocol used for communications among field devices and control systems.

Process Fieldbus (PROFIBUS) is an international fieldbus communication standard for linking process control and field devices.

HART is a question/response type of control communication and can only transmit a limited number of variables. FOUNDATION fieldbus and PROFIBUS allow for two-way communication, but they operate at different speeds. FOUNDATION fieldbus and PROFIBUS communications provide constant feedback of digital data.

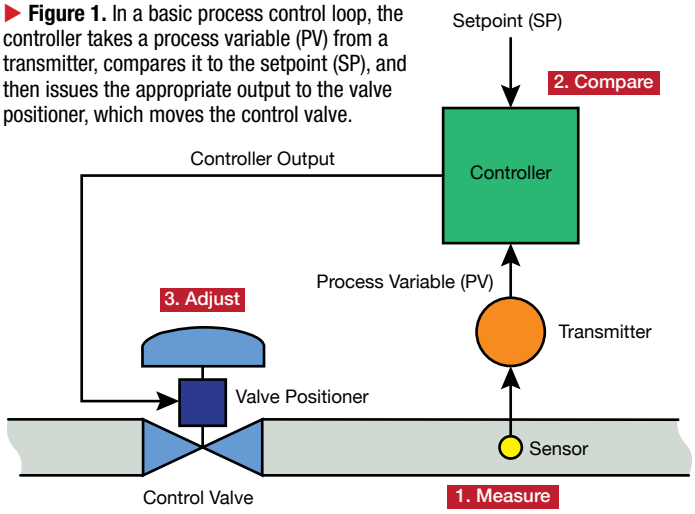

Figure 1. In a basic process control loop, the controller takes a process variable (PV) from a transmitter, compares it to the setpoint (SP), and then issues the appropriate output to the valve positioner, which moves the control valve.

Positioning functions, on average, use only about 10% of the microprocessor's capabilities, which leaves most of the electronics available for diagnostics that provide insight into the valve's performance. Most smart positioners have a range of diagnostic capabilities that include both in-service and out-of-service diagnostics.

Typical in-service diagnostics include monitoring, friction analysis, troubleshooting, and air consumption tests. Monitoring diagnostics indicate important parameters such as air pressure, input setpoint, valve travel, and other values critical to operation. A friction analysis can be done while the valve is in operation to determine the amount of friction present in the valve assembly; excessive friction can make the valve more difficult to control. Air consumption tests can be conducted to determine whether the valve assembly is using an excessive amount of air. Excessive air usage can be caused by wear or damage to the pressure-retaining portions of the actuator assembly and/or to the instrument tubing. All of these non-intrusive in-service diagnostics can highlight a failure or performance degradation and alert the operator that it is time to schedule maintenance on the assembly.

Out-of-service diagnostics include valve signatures and step-response tests. The valve signature (Figure 2) is a graphical representation of the relationship between the actuator pressure input and valve position while the valve is slowly opened and closed. The data can be used to calculate spring settings, spring rate, valve friction, and valve closure forces. Step-response tests (Figure 3) move the valve in predetermined increments and measure the actual valve travel in response to the input, which helps to evaluate valve performance, calibration accuracy, positioner tuning, and stroking speed.

Out-of-service diagnostic tests should be conducted prior to control valve installation, as well as before or at the start of a turnaround to aid planning efforts. When done in com-

bination, they can detect abnormalities in a valve assembly, which can be used to determine whether work needs to be done on the valve and, if so, what kind of work. Knowing the type and extent of work that needs to be done on the valve ahead of a turnaround can save time and money and, hopefully, eliminate any surprises or unnecessary work.

Establish a valve monitoring program

You may already be aware of your smart positioner's capabilities, but like many of your smartphone's functions, you choose not to leverage them. The typical excuses for this are lack of time, personnel, and/or procedures to deal with the many diagnostic alerts, which can be overwhelming.

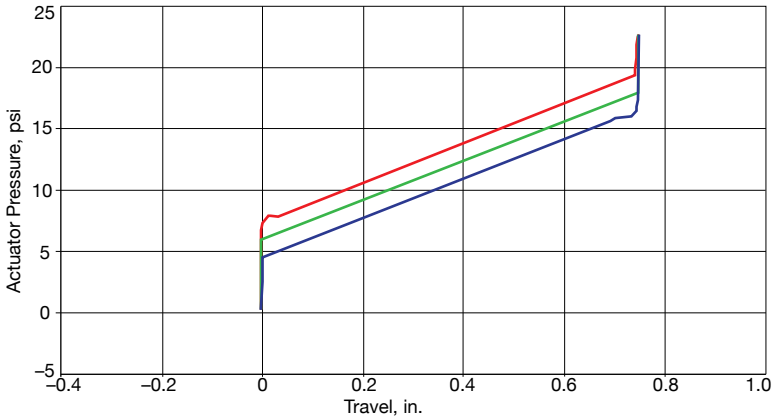

▲ **Figure 2.** A valve signature indicates the integrity of the valve body and the actuator. The red line represents the recorded travel as output pressure increases until the valve is 100% open. The blue line is the recorded travel once the positioner releases the pressure and the valve travels to the closed position. The green line is the best-fit line; the distance between the green line and red or blue lines can be used to calculate valve friction. Valve signatures should be recorded when the valve is brand new so that future valve signatures can be overlaid to check for changes

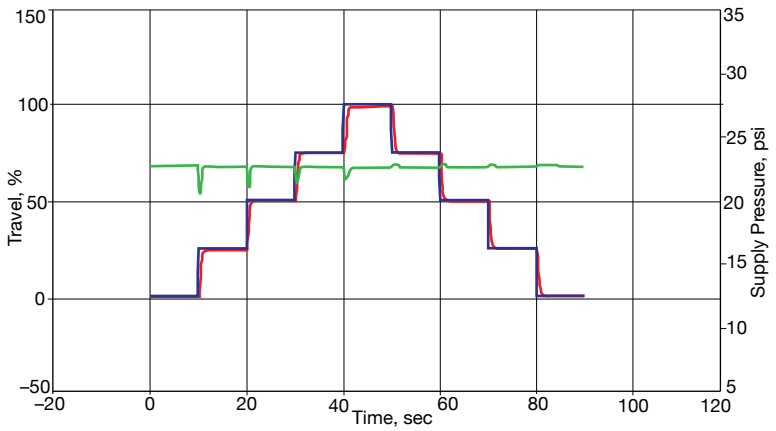

▲ **Figure 3.** A step-response test checks the response of the entire valve assembly and indicates the effectiveness of the instrumentation tuning and accessories. The blue line is the input signal to the positioner that directs the valve to move to a certain travel point. The red line is the actual valve travel as it attempts to reach the setpoint. The blue and red lines should follow a similar path to indicate good operation. The green line records supply pressure as the valve moves to the setpoints.

A process to leverage diagnostic information is essential to starting a control valve monitoring program. Follow these seven steps to get a program off the ground at your plant.

Step 1. Determine who will own the process. Great ideas without an owner stay just that — great ideas. An owner who leads the program might be from the maintenance, instrumentation and electrical, or reliability department. If you have staffing challenges or other priorities, consider outsourcing the responsibility.

The ownership plan should be for the long term. Many programs get started and have some success, then the owner moves on to another role, leaving an ownership void and the program fades.

Step 2. Establish a route for gathering data. The positioner can provide much valuable diagnostic information, but you first need to get that information from the positioner to a point where you can use and analyze the data.

The communication protocol (*e.g.,* HART, FOUNDATION Fieldbus, Process Fieldbus, etc.) that you use in your plant impacts your options. Software tools can transfer diagnostics through your control system network. These tools may already be implemented at your plant and simply need to be leveraged for this new application. If your plant does not already have such software, consider sending the information wirelessly, or use a route-based process in which an operator manually pulls diagnostic information directly from the valve positioner.

Step 3. Create a list of valves to be monitored. To get your valve monitoring program up and running, start small. Do not try to start the program with every control valve in your facility. Turning on all the alerts in all your smart positioners at once is a good way to overwhelm your operations and program teams. Instead, make a list of a handful of critical valves to be monitored. It is easier to work out the process on a few valves and then expand the program slowly.

Plant assets have varying levels of criticality. A criticality assessment will help you to identify the most important valves that should be part of the initial monitoring program.

A simple A-, B-, C-rating scheme works well. A-rated assets are the most critical and have the biggest impact on plant operations; these assets require more monitoring and receive the highest work order priority. An example of an A-rated asset is a compressor antisurge valve. B-rated assets, such as valves in applications that also have a bypass valve, are of medium criticality. C-rated

assets are of the lowest importance, and include such equipment as general service water or instrument air valves. Once you have assessed and rated your valves, start incorporating your A-rated valves into your diagnostic monitoring program.

Step 4. Identify the parameters to be monitored and the diagnostic alerts to be issued. To avoid information overload, start small with three key alerts. We suggest starting with travel deviation, drive signal (*i.e.,* how hard the positioner is working to maintain or go to its intended position), and supply pressure.

A typical A-rated asset is a throttling control valve. For this type of valve, the travel target (where it is told to be) and the actual travel (where it actually is) should be very close. The difference between these two values is the travel deviation. Travel deviation, which indicates that the valve is not following setpoint, is commonly caused by increased friction, broken components, low air supply volume, internal part galling, or calibration issues.

The travel deviation alert usually has two other components: percent of allowable deviation and time of deviation. These can be adjusted to prevent nuisance alerts, such as for very large actuators that move very slowly; typical throttling of the valve should not trigger a travel deviation alert.

The drive signal is the output current to the I/P converter, typically shown as a percentage, which provides the air output value necessary to correctly position the valve. The standard drive signal range is 55–85% when the valve is in its throttling range. An alert is triggered if the drive signal is too low or too high when the valve is not on the seat or in the wide-open position. High drive signal values can indicate sticking, internal plugging by debris from the air supply, or pneumatic leakage. Low drive signal values may indicate low supply pressure, internal blockage, damage to the positioner, or mechanical failure of the valve. Run additional diagnostic tests if this alert is active.

A low supply pressure alert indicates that the valve does not have enough force to operate correctly. If the supply pressure is lost or too low, the valve may move very slowly or not reach full travel. Low supply pressure could also trigger a travel deviation alert because the supply may not be high enough to move the valve to its set location, as well as a drive signal alert because the positioner is working as hard as it can and the supply is not adequate to move the valve. If all three alerts are active, low (or lack of) supply pressure likely triggered them.

Setting and monitoring these three critical alerts should give adequate warning of an impending issue with your control valve without triggering nuisance alarms or alerts.

Step 5. Devise a process for handling the information. Pilot the program in one area of your plant. This will allow you to work through the process details, such as who will generate a work order in response to an alert. Personnel should be trained on the process so that they can react to alerts with the proper tools and methods. Once the alert is addressed, you can use the diagnostics to decide whether the valve should be returned to service, repaired, or replaced.

After the alert has been addressed, conduct a review. The discussion should cover potential repair parts that need to be ordered and work scheduling. Major repairs are usually scheduled during shutdowns, but if a shutdown is not in the near future, personnel may need to be advised to closely monitor the equipment until the work can be done.

Step 6. Keep track of your costs. Maintaining asset reliability comes at a cost, and your management team will want to know how the extra money and time are being spent.

The monitoring program will save money in the long term. Celebrate any successes and pass that information on to management. Document efforts that prevent a shutdown or downtime to establish an argument for continuing and expanding the program.

Step 7. Give it a try. Once you have your plan, try it out. As with most new things, everything will not go as planned. Do not be discouraged. Starting small will help you to better handle any issues that might arise. Challenges are an opportunity to go back and review the program, refine it, and try again. After you get the program running smoothly, consider expanding it to other control valves.

An industrial success story

The HART Communication Foundation named Monsanto 2012 HART Plant of the Year for leveraging its smart input/output (I/O) infrastructure. Monsanto implemented an asset reliability optimization strategy to prioritize, plan, and schedule downtime. To gather data, they used both handheld and remote office-based systems (a combination of the options suggested in Step 2). They conducted an asset criticality review (Step 3), and assigned ratings to more than 14,000 pieces of equipment, including control valves, transmitters, vapor sensors, and other equipment. The monitoring program saves the plant an estimated $800,000 to $1.6 million per year in avoided costs. CEP

JANINE McCORMICK (Email: Janine.McCormick@Emerson.com) is a refining industry manager at Emerson. During her 12 years with the company, she has focused on Fisher control valves. She has a BS in chemical engineering from Iowa State Univ., and she is a member of the Society of Women Engineers (SWE). McCormick received the Leading Change award in Dec. 2016 from Iowa State Univ.'s Women in Science and Engineering (WiSE) program.

STEVE HAGEN (Email: Steve.Hagen@Emerson.com) is a senior product manager at Emerson. He has over 28 years of experience with valve, instrument, and diagnostic applications. He previously served as an instructor for Fisher Educational Services. He has a BA in industrial technology and safety from the Univ. of Northern Iowa. Hagen is an International Society of Automation (ISA) member and an ISA-certified control system technician (CCST).

Solid-Liquid Separation: A Guide to Centrifuge Selection

Tom Patnaik
HEINKEL Filtering Systems, Inc.

Centrifugation is a necessary step in many pharmaceutical and chemical production processes. These guidelines will help chemical engineers better understand the process of centrifuge selection.

Solid-liquid separation through centrifugation is often a crucial step to obtain the desired product after precipitation or crystallization. There are two types of centrifugation (also called dewatering or deliquoring): filtering and sedimenting. This guide focuses mainly on filtering centrifugation because it is the more common type of solid-liquid separation in chemical and pharmaceutical production applications.

Three steps to centrifuge selection

This three-step process for choosing the best centrifuge for a specific application evaluates the process characteristics, the product properties, and the numerous design options that should be considered to determine the optimal centrifuge to fit process requirements (Figure 1).

The selection of a centrifuge is governed by a myriad of factors. First, it is important to know whether the reaction is crystallization or precipitation, because reaction type greatly influences the morphology of the solid particles, which, in turn, has a direct bearing on the filterability of the slurry. It is also beneficial to determine the temperature, pH, and flowrates or batch sizes generated by the reaction. Some of the process and operational parameters that influence the selection criteria include: containment and washing requirements, vessel size, and batch cycle times. Particle characteristics such as size and shape, porosity, hardness, density, and concentration are also important. After the process and product parameters have been considered, centrifuges can be evaluated based on their size, automation and containment capabilities, and typical applications of a similar nature.

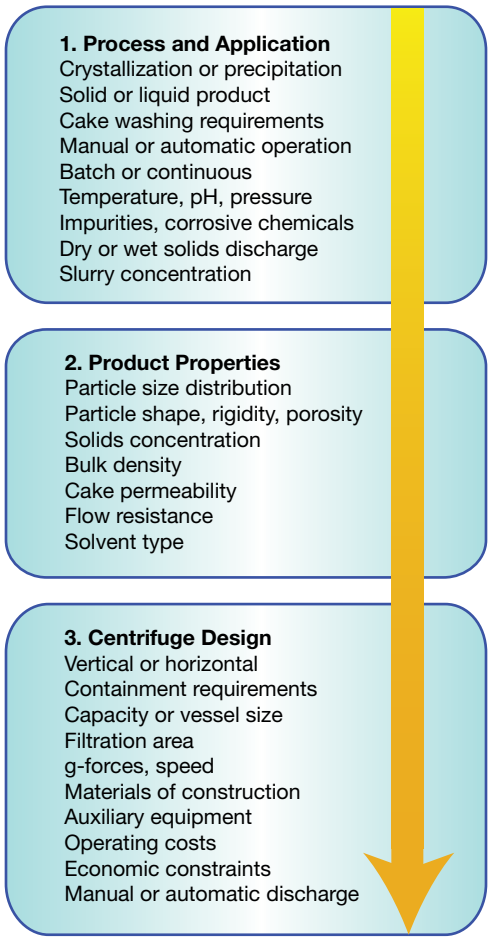

▲ **Figure 1.** The three-step process for centrifuge selection begins with an evaluation of the process and product properties, and then an assessment of centrifuge options.

Table 1. Process characteristics determine whether filtering or sedimenting centrifugation should be used.		
Process or Product Criteria	**Separation Requirement**	**Centrifugation Type**
Dry solid product	Extended spinning	Filtering
Solids washing required	Long residence time for washing	Filtering
Small mean particle size	High g-forces	Sedimenting
Low solids concentration in slurry; liquid product	Continuous operation	Sedimenting
High throughput	Continuous operation	Sedimenting

Step 1: Selection by process and application

The first step in centrifuge selection is to determine whether filtering or sedimenting centrifugation will be used. A filtering centrifuge is a batch-operated machine that uses a filter media to capture and collect a filter cake inside a rotating basket; a sedimenting centrifuge is usually continuous, and uses high rotational velocities to produce very high gravitational forces (*i.e.,* g-forces) inside a solid bowl that separates the liquid from the solid (or liquid from another liquid) based on specific gravities. Some of the criteria used to select the most appropriate type of centrifugation are listed in Table 1.

Particle size affects cake porosity and filterability, which, in turn, influence the selection of the centrifuge type. In general, larger particles are easier to filter than smaller particles, which makes slurries with large particles more suitable for filtering centrifuges. If dry solids discharge is required, mechanical drying with extended spinning may be performed inside a batch-filtering centrifuge. Continuous sedimenting centrifuges are not suitable for dry filter cake discharge.

Because filtering centrifuges can be operated with variable batch times, they can provide a longer wash-liquid residence time inside the solid cake, which may be required for effective cake washing. Therefore, filtering centrifuges, which can have a batch time as short or as long as required, are usually preferred when the solid particles must be washed and the cake is the valuable product.

When the concentration and particle size of the solids are low (*i.e.,* the slurry is thin) and the liquid volume is large, a sedimenting centrifuge is often more effective than a filtering centrifuge. Under these conditions, a filtering centrifuge would require a very large filter area to accommodate the large liquid volume.

Whether the solid or the liquid is the valuable product also impacts centrifuge selection. Filtering centrifuges are usually preferred when solids are the desired product, and sedimenting centrifuges are preferred when the liquid is the valuable product.

Table 2. A particle's shape affects the density of the cake formed during centrifugation.	
Particle Shape	**Shape Factor**
Spherical	1.0
Rounded	0.8
Irregular	0.7
Needles	0.6
Plates	0.4
Fibrous	<0.1

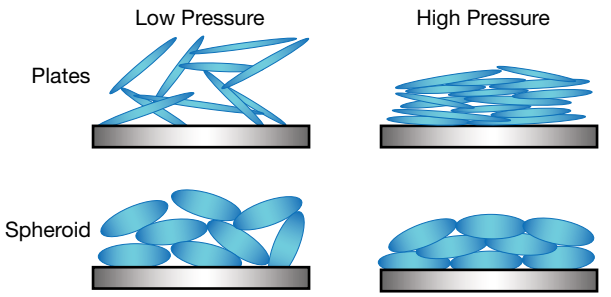

▲ **Figure 2.** Compact cakes have smaller voids between particles, which limits filterability.

Step 2: Selection by product properties

Particle shape, size, and distribution play a significant role in the filtering process. Once the type of centrifugation (filtering or sedimenting) has been determined from the process parameters, a particle size distribution (PSD) analysis and morphological examination of the solid particles may be conducted.

▲ **Figure 3.** The vertical basket bottom-discharge centrifuge may be suitable for hazardous substances, as it offers better containment.

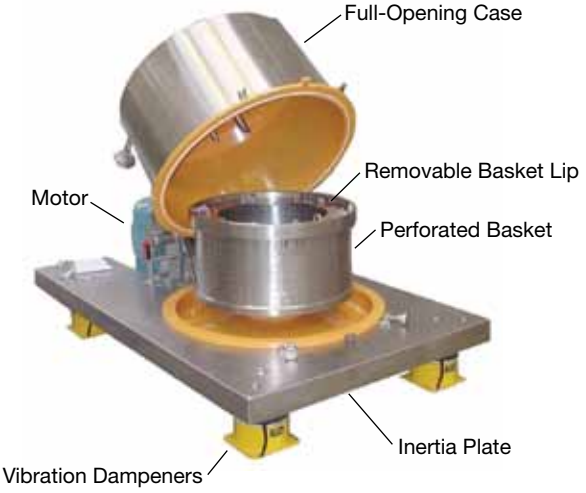

▲ **Figure 4.** This cGMP vertical basket centrifuge has a full-opening cover to allow complete sanitization of all internal surfaces.

Particle shape greatly influences filterability; spherical and rounded particles are typically the easiest to filter. Fibrous and entangled particles form denser cakes, which makes filtering more difficult and time consuming (Table 2). The shape factor is a dimensionless value that represents the degree of deviation from an ideal shape, such as a sphere. As shown in Table 2, the shape factor is normalized, so that the number varies from 0 (worst) to 1 (ideal).

While particle shape affects the cake density, particle size impacts cake porosity, residual cake moisture, and throughput rates. Bigger particles usually form cakes with larger capillaries and hence greater porosity, a factor that is critical to cake filtration. Therefore, bigger particles can be handled at higher throughput rates than smaller particles.

System pressure can also play a role in a solid's filterability. Some solids filter well at low pressures, but under high pressures they compact or collapse. Compact cakes have smaller voids and capillaries between particles, and thus fewer and narrower pathways for liquids to evacuate the cake (Figure 2). This results in lower filterability and longer filter times.

Slurry filterability is another important property-dependent factor. Filterability is a measure of how well a liquid passes through a solid cake. It is a function of particle size, shape, and structure, and is expressed in terms of flux rate in gal/min per square foot of filter basket area. To filter well, a slurry must have a flux rate anywhere from about 1 gpm/ft^2 to about 6 gpm/ft^2.

Step 3: Selection by centrifuge design

After determining the mode of separation based on the process and application, and the ease of filterability based on product properties, the specific centrifuge must be chosen.

Filtering centrifuges are known as solid-liquid separators, where the solid, or cake, is usually the valuable product. They use a perforated bowl (*i.e.,* basket) lined with a filter cloth to retain the cake. The liquid (*i.e.,* centrate) passes through and is discarded. They are typically operated in batch mode, but can be operated semi-continuously when fitted with automatic feeding and discharging equipment. Applications for the different centrifuge types often overlap, and sometimes the determining factor as to which is preferred is the degree of filterability.

Vertical basket centrifuges are used for slow- or medium-filtering slurries. This allows for an even distribution of the cake across the vertical filtering surface. Rapid-filtering slurries produce a cake that is thick at the bottom and thin at the top, which results in poor capacity utilization and low washing efficiencies.

Vertical basket centrifuges tend to be prone to vibration

due to their inability to handle process variations. They can have poor washing efficiencies, lack access to all the product contact surfaces, and require a high floor-to-ceiling clearance for proper installation.

There are three main types of vertical basket centrifuges:

• Vertical basket manual-discharge centrifuges can be used for products that filter only moderately well (*i.e.,* a flux rate of approximately 1–3 gpm/ft^2), provided that high containment and automatic operation are not required. In a vertical basket top-unloading centrifuge, the cake discharge is performed manually or with a removable rim and an overhead lifting device. When solid particles are dry enough to be siphoned off, the cake can be dilute-phase conveyed using a vacuum discharge mechanism. However, vacuum discharge is suitable only in certain applications, and has generally not found widespread use.

• Vertical basket peeler- or plow-discharge centrifuges can process toxic solvents and slurries that cannot be discharged manually due to safety requirements. The automatic plow or peeler can discharge solid cakes without the need for operator interaction with hazardous materials (Figure 3). The plow may be single-motion (*i.e.,* radial) or dual-motion (*i.e.,* radial and vertical).

• Vertical basket cGMP (current good manufacturing practices) centrifuges are completely accessible and are designed for sanitary operation in pharmaceutical applications. They have a full-opening case, polished surfaces, special features for improved containment, and an automatic clean-in-place (CIP) system of spray nozzles (Figure 4). Their vertical and sloping surfaces allow for complete draining of the CIP and other fluids.

Horizontal peeler centrifuges can be used for moderate- to well-filtering slurries (*i.e.,* flux rates in the range of 1–6 gpm/ft^2) that require high washing efficiencies and stable, high-volume production. They have high capacities (some models have baskets with volumes up to 1,500 L), and can be fully automatic and enclosed for hazardous applications.

These centrifuges can be configured so that their process components are separated from their mechanical components by a cleanroom wall, which enables quick maintenance and sanitization. Since only part of the centrifuge is within the cleanroom, the machine has a smaller footprint inside the cleanroom, which is desirable because cleanrooms are expensive to build and maintain.

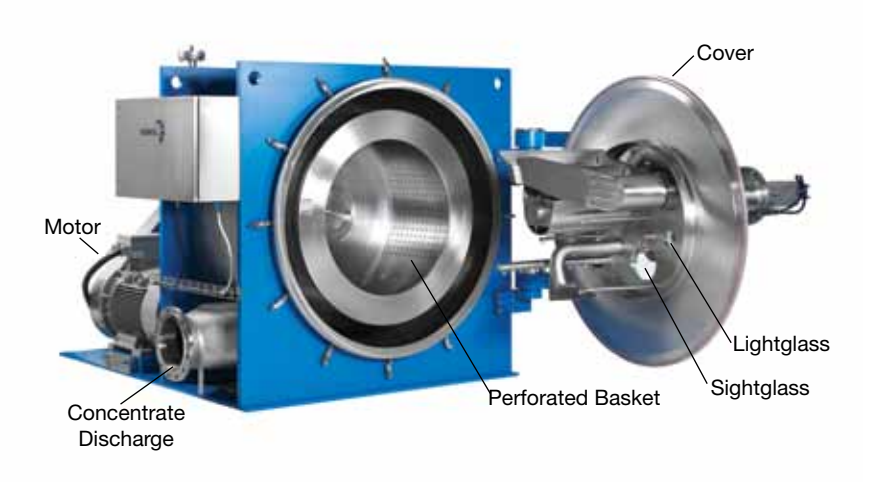

▲ **Figure 5.** A wall separates the process equipment and mechanical components of a horizontal peeler. A horizontal peeler for chemical applications uses a screw to discharge the solids.

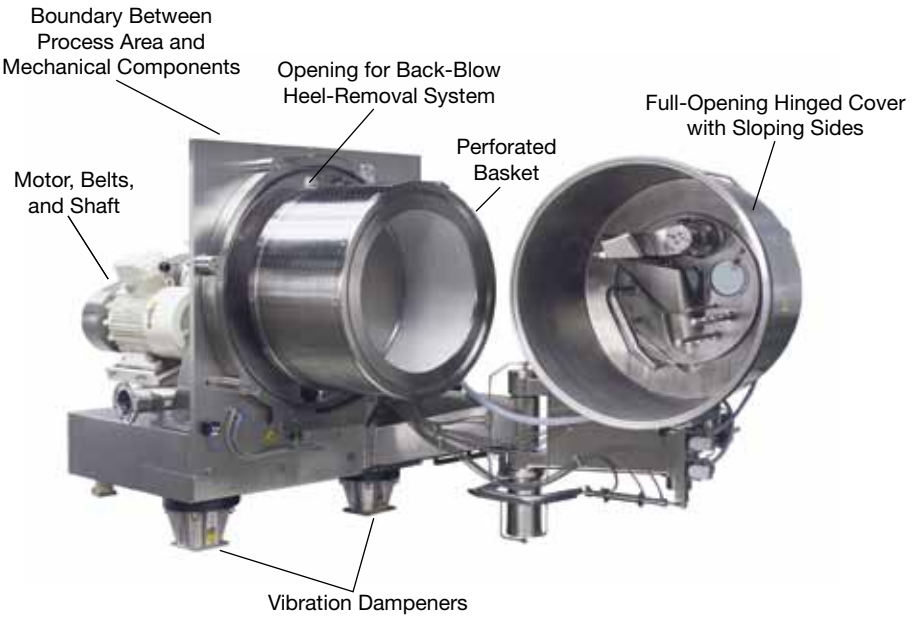

▲ **Figure 6.** A horizontal peeler for pharmaceutical applications features a CIP system and discharge chute for sanitary operation.

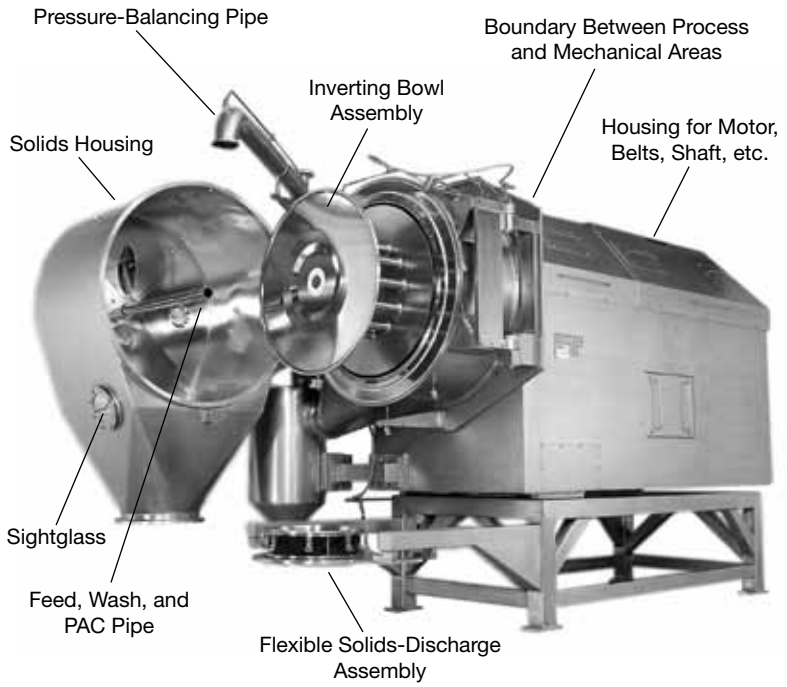

◀ **Figure 7.** An inverting filter centrifuge is the most versatile of all centrifuges and allows for cake thicknesses less than 1/2 in.

Horizontal peeler centrifuges are available in chemical and pharmaceutical designs. The chemical design (Figure 5) is optimal when internal surface sanitization is not a priority. It uses a screw to discharge the cake, and is available with baskets ranging from 250 mm to 2,000 mm in diameter. The pharmaceutical design uses a discharge chute and an integrated CIP system (Figure 6). It is available with 300-mm to 1,250-mm diameter baskets. Pharmaceutical peelers may also have options such as polished internal surfaces, a full-opening case, sloping surfaces, electric or pneumatic control devices, and a nitrogen inerting system.

Inverting filter centrifuges (Figure 7) are very versatile, and can be used for both easy- and poor-filtering slurries, with flux rates ranging from less than 1 gpm/ft^2 to 8 gpm/ft^2. They are suitable for difficult-filtering products, such as those that stop filtering when the cake thickness is less than 1/2 in. Because inverting filter centrifuges do not leave a residual heel (as centrifuges with plows or peeler devices do), they are suitable for thin-cake (*i.e.,* less than 0.1 in.) operation.

Pressure-added centrifugation (PAC) systems can be added to inverting filter centrifuges to facilitate drying without the use of heat or vacuum (Figure 8). Pressure is used to dry the cake beyond the capabilities of high g-forces alone. The overall cycle time required to produce a dry powder is lower than that of a combined centrifuge and dryer. PAC can reduce the load in a downstream dryer or eliminate the need for one entirely in many applications, which saves on both capital and operating costs.

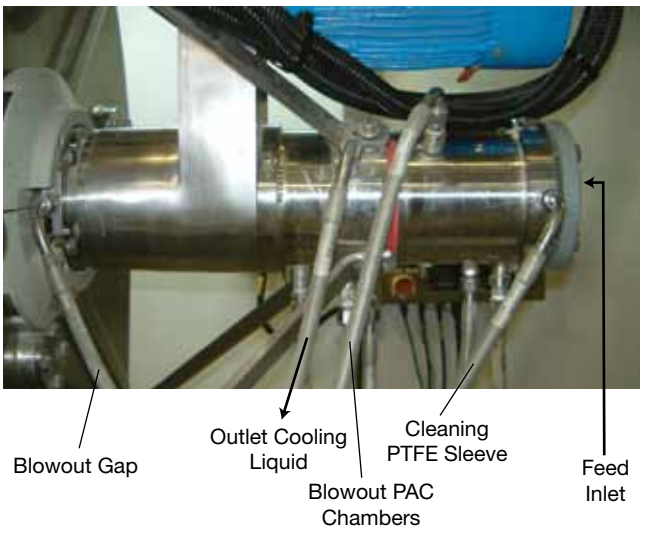

▲ **Figure 8.** Pressure-added centrifugation (PAC) uses pressure as its driving force to help dry the solid cake.

A possible limitation of horizontal peelers is the presence of a residual product heel. The heel is a 1/4-in. to 3/8-in. thick layer of product that remains inside the basket after the plow has peeled out the cake, because the plow is restricted from contacting the filter media. Any centrifuge that uses a plow or peeler mechanism for cake discharge will also have a product heel that may need to be removed.

Decanters

Although a decanter is a sedimenting centrifuge, it is included in this discussion of filtering centrifuges because it lends itself to specific bio-pharmaceutical processes in which high g-forces are required.

Decanters, like other sedimenting centrifuges, are used mainly for separations in which the liquid is the desired product. They usually handle thin slurries with low solids concentrations, in applications where the solids are typically discarded as waste.

Decanters are suitable for continuous, high-volume

Table 3. Process requirements and particle characteristics determine centrifuge choice.

	Vertical Basket			Horizontal Peeler	Inverting Filter with PAC	Decanter
	Manual Discharge	Peeler Discharge	cGMP			
Diameter, mm	200–1,600	800–1,800	Up to 1,250	250–2,000	300–1,300	~1,500
Operation	Batch	Batch	Batch	Batch	Batch	Continuous
Cake Washing	Yes	Yes	Yes	Yes	Yes	No
Discharge	Manual	Automatic	Automatic	Automatic	Automatic	Automatic
Containment	No	Yes	Yes	Yes	Yes	Yes
Solids Filterability	Low to Medium	Low to Medium	—	Medium	Medium	—
Volume Capacity	Low	Medium to High	—	High	Medium to High	High

applications in which cake washing and low residual moisture are not required. They have a nonperforated solid bowl. Instead of using a filter cloth, high gravitational force is used to separate a slurry via sedimentation based on the individual components' densities or specific gravities. The heavy solids phase settles out from the lighter liquid phase and concentrates along the wall of the bowl. The liquid phase is clarified on top of the cake and flows out one end of the decanter while a screw mechanism moves the solids along the length of the bowl and out the other end (Figure 9).

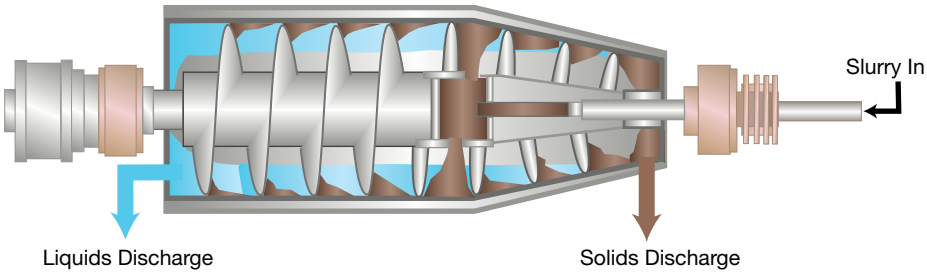

▲ **Figure 9.** A cross-sectional view of a decanter shows the movement of liquids and solids via high rotational forces.

Decanters can handle a wide range of products with different particle sizes, shapes, densities, and porosities, and are used for slurries that exhibit poor filtration characteristics. The forces generated by industrial decanters approach 3,000 g's in solid-bowl decanters, and up to 20,000 g's in tubular-bowl super-centrifuges. The latter have tall, hollow cylinders that produce high g-forces and have limited solids holding capacity. The liquids pass through, while the solid particles are retained inside the centrifuge and removed manually from time to time.

Closing thoughts

Table 3 summarizes the characteristics of the various centrifuge types described in this article. Centrifuge selection requires a thorough understanding of the process, the product characteristics, and the many types of centrifuges available. Because a centrifuge's life can span several decades, choosing the right centrifuge can result in more-efficient production and significant monetary savings.

It is best to consult a reputable manufacturer of this equipment early in the design phase. Centrifuge manufacturers have the capability to test several centrifuge options on a pilot scale, which can aid in centrifuge selection. Additionally, some of these manufacturers will readily provide separations expertise and knowledge for free. CEP

TOM PATNAIK is Director and VP of Sales and Marketing at HEINKEL Filtering Systems, Inc. (Email: tpatnaik@heinkelusa.com), a manufacturer of centrifuges, nutsche filter dryers, and conical vacuum dryers and mixers. He has nearly two decades of experience in the field of solid-liquid separation, specifically in centrifuge, nutsche filter, and vacuum dryer technology.

ACKNOWLEDGMENTS

The author would like to recognize the contributions to this article by all the centrifuge team members at HEINKEL, including Thomas Ahrens, Dave Altum, Markus Oswald, and Helge Fiedler. He would also like to acknowledge the many customers who have contributed to his understanding of the complex process occurring inside a centrifuge, and who have, in a way, participated over time in the writing of this article.

Selecting a Heat Exchanger Shell

Thomas G. Lestina, P.E.
Heat Transfer Research, Inc.

The first step in specifying a shell-and-tube heat exchanger is choosing the right shell to meet process requirements.

Most chemical processes require heat exchangers to transfer heat from a hot stream to a cold stream. This heat-transfer equipment must meet the thermal, mechanical, operational, installation, and maintenance demands of the process. The optimal heat exchanger design minimizes operating costs and maximizes product output.

The most common process heat exchanger is the shell-and-tube exchanger (Figure 1), which consists of a bundle of tubes inside a cylindrical shell. One fluid (the tubeside fluid) flows inside the tubes while the other (the shellside fluid) flows through the shell and around the tubes. Heat is transferred across the tube wall separating the hot and cold streams.

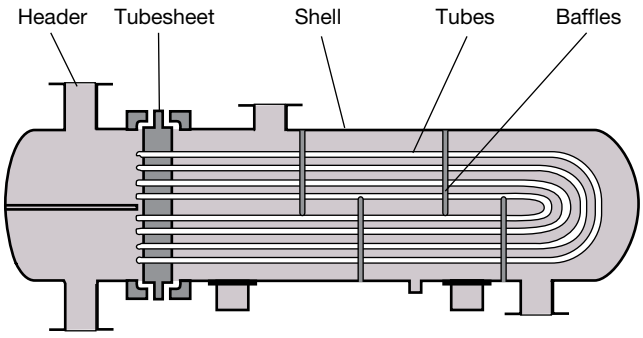

▲ **Figure 1.** In shell-and-tube heat exchangers, heat is transferred across the tube walls separating the hot and cold streams.

The shell type has a significant effect on the flow configuration and thermal performance of the heat exchanger. This article (the first in a series of three on shell-and-tube heat exchangers) provides guidance on choosing the appropriate shell type.

Table 1. Each shell type has a unique combination of flow pattern and design features.

Shell Type	Description
E	One-pass shell Counter- or co-current flow
F	Two-pass shell Longitudinal baffle
G	Split flow Longitudinal baffle Full support plate under nozzle
H	Double split flow Two longitudinal baffles Full support plate under nozzles and at shell midpoint
J	Divided flow Full support plate under center nozzle
K	Kettle reboiler or vaporizer Liquid disengages from vapor in dome Nozzle for liquid draw-off is not required for vaporizers
X	Crossflow Multiple nozzles typical for flow distribution

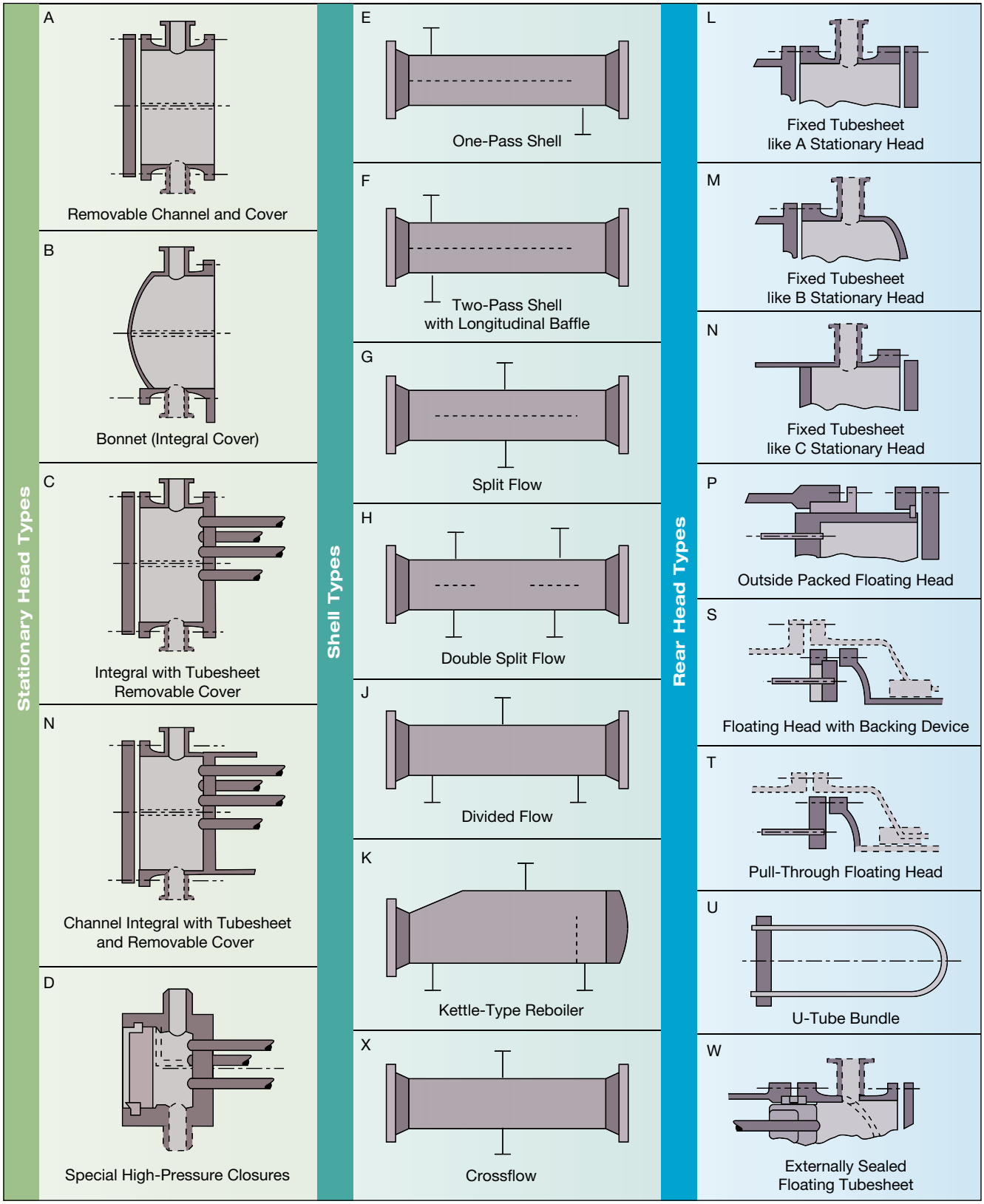

▲ **Figure 2.** TEMA's notation system designates a shell-and-tube heat exchanger's type of front head, shell, and rear head.

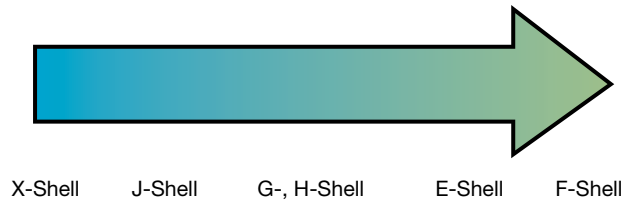

▲ **Figure 3.** Shellside pressure drop is a function of shell type (among other factors).

The Tubular Exchanger Manufacturers Association (TEMA) has developed a three-letter notation system *(1)* to describe shell-and-tube heat exchangers, where the first letter designates the type of front head, the second letter the type of shell, and the third letter the type of rear head. Table 1 summarizes the features of the different shell types, and Figure 2 illustrates the TEMA notation system.

Several factors impact shell selection:

• *Plant piping layout constraints*. When replacing existing exchangers, it is often prohibitively expensive to move nozzles and piping, which constrains designers to replacement shells of the same type. For new construction, limits on bundle length and nozzle locations may influence shell type. For example, pipe racks facilitate the use of stacked E-shells with an even number of tube passes.

• *Temperature profile of the hot and cold fluid streams.* When the terminal temperature approach (*i.e.,* the difference between the outlet temperature of the hot stream and the outlet temperature of the cold stream) is greater than 3°C, any of the shell types can be used for the application. When the temperature approach is less than 3°C, some shell types have a clear advantage. For example, multipass shells (*i.e.,* F-, G-, H-shells) can handle a low temperature approach and even some temperature cross. Among single-pass shells, E-shells with one tube pass and X-shells are the best option to accommodate a temperature cross or low approach.

• *Shellside pressure drop.* Shell type is one of many factors affecting pressure drop (along with baffle design,

Table 2. Each shell type has advantages and disadvantages that make it suitable for specific applications.

Shell Type	Advantages	Disadvantages
E	Many baffle types are available to reduce pressure drop Widely applicable in single-phase, boiling, and condensing services Temperature cross is possible without reverse heat transfer with a single tube pass	Reverse heat transfer is possible with an even number of tube passes and no fouling
F	Temperature change for fluid streams can be higher than in an E-shell Fewer shells in series are needed	Longitudinal baffle can leak if it is not welded Thermal conduction occurs across the longitudinal baffle Removable bundles are more costly to maintain
G	Split flow reduces entrance and exit velocities Lower risk of vibration due to lower velocity and better tube support under nozzle Suited for horizontal shellside reboilers	Fewer tube-pass options with removable bundle Thermal conduction occurs across the longitudinal baffle Temperature profile is not as good as with counter- or co-current flow
H	Double split flow lowers entrance and exit velocities and provides more support than in G-shells Suitable for horizontal shellside reboilers	More nozzles than G-shells Thermal conduction occurs across the longitudinal baffle Temperature profile is not as good as with counter- or co-current flow
J	Split flow lowers velocities Many baffle types are available to reduce pressure drop	More nozzles than an E-shell Temperature profile is not as good as with counter- and co-current flow
K	Low pressure drop Circulation promotes wet-wall boiling	Larger shell requires entrainment calculations Circulation is complicated, which could lead to the buildup of heavy components
X	Low pressure drop due to single cross pass Temperature cross is possible without reverse heat transfer Widely applicable to single-phase, boiling, and condensing services	Maldistribution is possible, often requiring the use of a distribution plate Multiple nozzles are common Removal of noncondensables is complicated for X-shell condensers

Table 3. Design conditions for the water-water heat exchanger in Example 1.	
Cold Fluid	Water
Hot Fluid	Water
Cold Temperature	In = 25°C, Out = 50°C
Hot Temperature	In = 115°C, Out = 53.55°C
Design Heat Load	4.39 MW

Table 4. An AFU exchanger performs better in the water-water application of Example 1.		
TEMA Type	**AEU**	**AFU**
Number of Tube Passes	2	4
Maximum Heat Load	5.03 MW	5.64 MW
Mean Temperature Difference under Clean Conditions	15.8°C	21.2°C
Shellside Pressure Drop	9.4 kPa	8.3 kPa
Shell Diameter and Length	0.508 m × 7.315 m	0.7 m × 4.877 m
Heat-Transfer Area	146 m^2	137 m^2

tube pitch, and bundle entry and exit design). Figure 3 compares the relative pressure drop of the common shell types, assuming the same shell diameter, shell length, and flowrate. K-shells are not included in this comparison because they are usually considered to have negligible pressure drop.

• *Maintenance.* When bundle removal is required, multipass shells have a disadvantage compared to single-pass shells, particularly when the longitudinal baffle must be removed. Longitudinal-baffle removal requires mechanical leaf seals, which can be damaged during the removal and installation process. Flow bypassing due to damaged seals severely reduces thermal performance. Because of this susceptibility, some processing facilities do not allow the use of F-shells.

• *Specific applications.* In some applications, one shell type has a clear advantage over other types. For pure-component boiling with 100% vaporization, K- and X-shells are most common. For tubeside thermosiphon reboilers, vertical E-shells are typically selected. For viscous liquids, horizontal E-shells with segmental horizontal baffles are the norm. For high-pressure applications where

When bundle removal is required, multipass shells have a disadvantage compared to single-pass shells.

special channel closures are used (TEMA D-type front heads), E-shells are usually chosen.

To determine the best shell type for an application, consider the advantages and disadvantages summarized in Table 2.

The following examples demonstrate the selection of shells for several common applications (using results generated by HTRI's Xist v. 6 software).

Example 1: Water-water heat exchanger

A water-water heat exchanger in service for more than 30 years experienced material degradation and needs to be replaced. Table 3 lists the current design process conditions. The design terminal temperature approach is 3.55°C, which any shell type can handle. Reverse heat transfer is observed for 25% of the surface area under clean conditions, which is attributed to the flow configuration and substantial fouling factors (60% of the thermal resistance). This situation is not desired, since heat duty should be maximized for this application.

Table 4 compares the existing TEMA AEU design (A = stationary front head with removable channel and cover; E = one-pass shell; U = U-tube bundle rear head) with an AFU design (F = two-pass shell with longitudinal baffle). Under clean conditions, the F-shell design exhibits no reverse heat transfer, the mean temperature difference and duty are larger, and the required heat-transfer area is less. In addition, the F-shell — a 4-pass U-tube design — can be removed without removing the longitudinal baffle. One surprising result is that the shellside pressure drop is lower for the F-shell, the result of a change in the baffle design and a shorter bundle length.

In this application, the shellside nozzle locations can be moved. Therefore, the F-shell is a better choice for this retrofit application.

Example 2: Once-through reboiler

A once-through vertical reboiler unit failed upon startup, and the operator plans to replace it with a horizontal shellside reboiler. Shellside reboiler designs are less

Table 5. Comparison of E-, G-, and X-shells for the reboiler in Example 2.			
TEMA Type	**E-Shell**	**G-Shell**	**X-Shell**
Shell Diameter and Length	1.55 m × 6.096 m	1.5 m × 6.096 m	1.7 m × 6.096 m
Mean Temperature Difference	11.1°C	9.5°C	10.9°C
Required Static Head	6.8 m	4.8 m	4.0 m

Thermal designers should be aware of the attributes of the TEMA shells and choose the shell type wisely.

susceptible to flow instability than once-through vertical reboilers with the cold fluid on the tubeside, which is a contributing factor to the original unit failure.

Table 5 compares E-, G-, and X-shells for this application (the tube length is held constant), because they are typical selections for horizontal shellside reboilers. The E-shell design has one tube pass because reverse heat transfer is observed with two tube passes, while the G- and X-shells have two tube passes to increase tubeside heat transfer. The G-shell has the smallest shell diameter and is a suitable selection for this application.

Example 3: Vacuum condenser for a hydrocarbon mixture

A small condenser for a hydrocarbon mixture (Table 6) was initially designed with an excessive pressure drop (1.3 kPa) and inadequate heat transfer (30% underdesign). The baffle design was not optimized (segmental baffles with 45-deg. baffle cut and 200-mm spacing), but a successful design could be attained with optimized baffles (segmental baffles with 25-deg. cut and 250-mm spacing).

Table 7 compares the thermal performance of E-, X-, and J-shells, with the shell inside diameter and bundle length held constant. In this case, an E-shell is the best option, since the J-shell has poor performance and the X-shell has the disadvantage of requiring a challenging vent design to remove noncondensables.

Table 6. Process conditions for the condenser in Example 3.

TEMA Type	BEU
Shell Diameter and Length	0.7 m × 1.829 m
Duty	90 kW
Hot Inlet Pressure	1 kPa
Hot Fluid Temperature	In = 230°C, Out = 30°C
Cooling Water Temperature	In = 25°C, Out = 30°C

In closing

Performance deficiencies of operating exchangers can often be attributed to improper shell selection. Thermal designers should be aware of the attributes of the TEMA shells and choose the shell type wisely.

Looking forward

This article is the first of a three-part series on shell-and-tube heat exchangers The next article will discuss the selection of baffle types for different applications. Baffle selection is just as important as shell selection to ensure adequate operation.

The third article will discuss tube inserts and how they can be used to augment exchanger performance. Tube inserts are underused, most likely due to the lack of understanding of how they can be applied. CEP

Literature Cited

1. **Tubular Exchanger Manufacturers Association,** "Standards of the Tubular Exchanger Manufacturers Association," 9th ed., Tarrytown, NY (2007).

Further Reading

Mukherjee, R., "Effectively Design Shell-and-Tube Heat Exchangers," *Chem. Eng. Progress,* **94** (2), pp. 21–37 (Feb. 1998).

Mukherjee, R., "Does Your Application Call for an F-Shell Heat Exchanger?," *Chem. Eng. Progress,* **100** (4), pp. 40–45 (Apr. 2004).

R.L. Shilling *et al.*, Heat Transfer Equipment, Section 11, *Perry's Chemical Engineers' Handbook,* McGraw-Hill, New York, NY (2007).

THOMAS G. LESTINA, P.E., is Vice President of Engineering Services at Heat Transfer Research Inc. (HTRI) (Email: tgl@htri.net), where he oversees contract services, training, and technical support activities. He teaches workshops and courses as part of the HTRI training program and is the instructor for the American Society of Mechanical Engineers (ASME) and AIChE short course on heat exchanger design. He has over 25 years of engineering and project management experience. Prior to joining HTRI, he worked as a lead engineer for MPR Associates. He is a member of ASME and serves on the technical committee for the ASME Performance Test Code 12.5, Single-Phase Heat Exchangers. He earned a BS in mechanical engineering from Union College and an MS in mechanical engineering from Rensselaer Polytechnic Institute. He is a licensed professional engineer in Texas.

Table 7. Comparison of E-, X-, and J-shells for the condenser in Example 3.

TEMA Type	E-Shell	X-Shell	J-Shell
Shell Diameter and Length	0.7 m × 1.829 m	0.7 m × 1.829 m	0.7 m × 1.829 m
Mean Temperature Difference	31.5°C	41.2°C	22.5°C
Overdesign/Underdesign	+9.48%	+4.76%	–41.7%
Hot Fluid Pressure Drop	0.363 kPa	0.032 kPa	0.052 kPa

Designing Hoppers, Bins, and Silos for Reliable Flow

Greg Mehos
Mike Eggleston
Shawn Grenier
Christopher Malanga
Grishma Shrestha
Tristan Trautman
Univ. of Rhode Island

Follow a guided approach to measure solids properties, choose bin shapes, and calculate hopper angles and outlet sizes for effective storage and use.

Engineers are often asked to design or recommend equipment for storing and handling bulk solid feedstocks, intermediates, and products. Unfortunately, chemical engineers' education and training on bulk solids are often insufficient for such tasks. To make the situation more difficult, critical solids flow properties are often unavailable and must be determined experimentally.

In bulk solid storage discussions, the terms hopper, bin, and silo are often used interchangeably. Hopper and bin frequently refer to small storage vessels, while silo usually refers to tall vessels that store several tons of material. Examples of hopper, bin, and silo geometries are given in Figure 1. In this article, the term bin is used to describe a storage vessel of any volume. The converging section of a storage vessel is called the hopper section.

This article presents methods for measuring fundamental bulk solids flow properties and explains how to use them to design hoppers, bins, and silos for reliable flow. It expands on previous *CEP* articles devoted to solids storage and handling and bin design by providing a step-by-step guide to the graphical analyses and calculations necessary for bin design *(1, 2)*. An example calculation section illustrates how to specify storage vessel shapes, outlet sizes, and hopper angles.

The first step in the design process is to determine the fundamental properties needed to predict the flow behavior of bulk solids: cohesive strength, internal friction, compressibility, wall friction, and permeability. Test results are used to calculate the size of the hopper section outlet and the recommended hopper angle. The properties are determined by calculations, measurements, and graphical analysis.

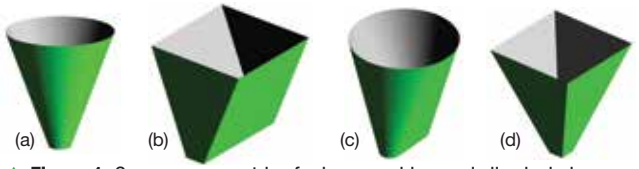

▲ **Figure 1.** Common geometries for hoppers, bins, and silos include (a) conical, (b) wedge, (c) transition, and (d) pyramidal.

Cohesive strength, internal friction, and compressibility

Shear cell testers are used to measure cohesive strength, internal friction, and compressibility.

To measure cohesive strength, place a sample in a cell and preshear the sample: Exert a normal stress (σ) and shear it until the measured shear stress (τ) is steady and the sample is consolidated. Next, conduct the shear step: Reduce the vertical compacting and shear the sample until it fails. Repeat the preshear and shear steps at the same consolidation level for a range of normal stresses. To determine the yield locus, plot the failure shear stress

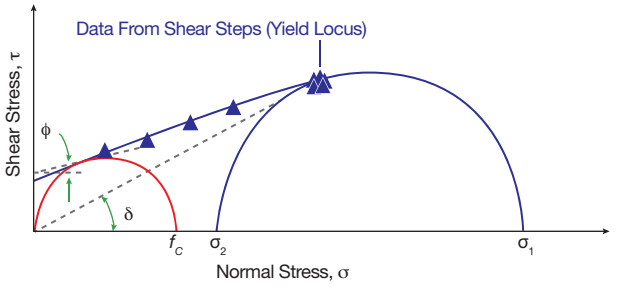

▲ **Figure 2.** The yield locus, determined by the shear cell tests, is used to calculate the major principal stress (σ_1), unconfined yield strength (f_c), effective angle of friction (δ), and kinematic angle of internal friction (ϕ).

against the normal stress (Figure 2).

The next step in the data analysis is to determine the major principal stress (σ_1), *i.e.,* the maximum normal stress exerted on the bulk solid during the test, and the unconfined yield strength (f_C), *i.e.,* the cohesive strength of the bulk solid. This is done by constructing a graphical representation of the stress transformation equations (referred to as a Mohr's circle) to determine the components of stresses acting on the bulk solid.

First draw a line through the shear step data. Next, draw a semicircle tangential to the yield locus line at the average of the steady-state results. The larger-valued intersection of the semicircle with the horizontal axis is the major principal stress (σ_1). Then draw a second semicircle tangent to the yield locus through the origin. The other point of intersection of this circle and the horizontal axis is the unconfined yield strength (f_C). Most modern automated shear cell testers assume that the yield locus is linear, which allows analytical expressions to be used to calculate σ_1 and f_C.

The volume is recorded during a shear cell test so that the material's bulk density (ρ_b) is also measured.

These shear cell tests are also used to find the effective angle of friction (δ) and the kinematic angle of internal friction (ϕ). To find the effective angle of friction, draw a line through the origin that is tangent to the larger Mohr's circle. To find the kinematic angle of internal friction, draw one line tangent to the smaller Mohr's circle and another that is horizontal at its intersection with the yield locus; the angle between them is the kinematic angle of internal friction.

The plot of the unconfined yield strength (f_C) against the major principal stress (σ_1) is the flow function of a bulk solid, and describes the relationship between a bulk material's cohesive strength and its consolidation stress. Figure 3 shows the construction of a flow function from three yield locus measurements. An envelope of the Mohr's semicircles forms the effective yield locus (Figure 4).

Wall friction angle

To measure the friction between a bulk solid and a vessel's wall material, place a sample of the bulk solid inside a retaining ring on a flat coupon of the wall material. Apply a normal load to the bulk solid so that it slides along the stationary wall material, and measure the steady shear stress. Reduce the load and continue the test.

To construct the wall yield locus, plot the shear stress against the normal stress (Figure 5). The angle of wall friction (ϕ') is the angle that is formed between the horizontal axis and a line drawn from the origin to a point on the wall yield locus. Note that the wall friction angle is constant only when the yield locus is a straight line that passes through the origin; otherwise, the wall friction angle decreases with increasing normal stress.

Some bulk materials gain cohesive strength and adhere to wall surfaces when they are stored at rest, so if a bin is not expected to operate continuously, time tests are conducted to measure the cohesive strength and static friction between the wall surface and the bulk solid after storage at rest *(3)*. The time test subjects the sample of powder to a normal load for a period of time (*e.g.*, two to three days to simulate a weekend downtime) at the start of test.

Permeability

To determine the permeability of a bulk solid, run a gas through a bed of powder contained in a cylinder. Measure the pressure and flowrate in two locations of the bed. The

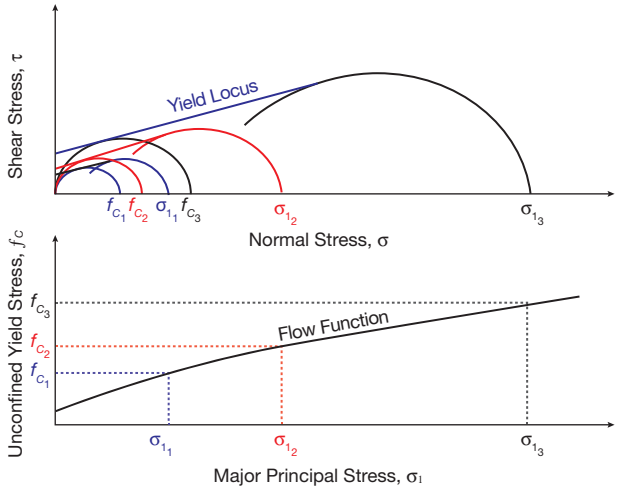

▲ **Figure 3.** The flow function is the relationship between the major stress and the unconfined yield strength. A graphical representation is constructed by connecting the points of different yield locus measurements.

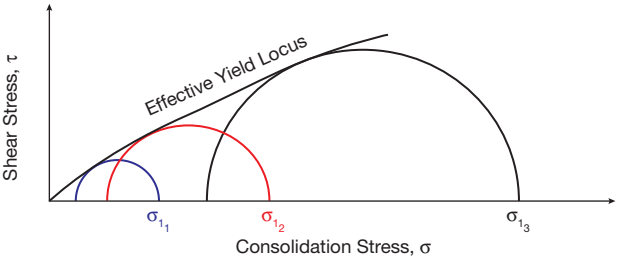

▲ **Figure 4.** The curve drawn tangent to the larger Mohr's circles is the effective yield locus.

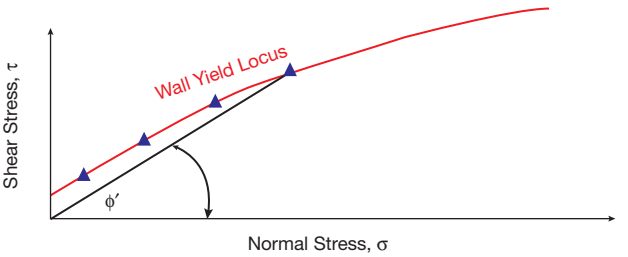

▲ **Figure 5.** The wall yield locus is constructed by plotting shear stress against normal stress.

permeability (K) is calculated from Darcy's Law:

$$u = -\frac{K\Delta P}{\rho_b g h} \quad (1)$$

where u is the superficial gas velocity, P is the gas pressure, ΔP is the difference between two pressure measurements separated by a distance of h in the bed, g is the acceleration due to gravity, and ρ_b is the bulk density.

Bin design

The design of a new bin takes into account the cohesiveness of the bulk solid, headroom or footprint constraints, segregation concerns, the likelihood of degradation over time (*e.g.*, caking or spoilage), and discharge rate requirements.

Three flow patterns can occur in a bin: mass flow, funnel flow, and expanded flow. In mass flow (Figure 6a), the entire bed of solids is in motion when material is discharged from the outlet. This behavior prevents the formation of stagnant material and ratholes, affords a first-in/first-out flow sequence, and ensures a more uniform velocity profile during operation.

In funnel flow (Figure 6b), a channel of flowing solids forms above the outlet and stagnant material remains at the periphery. Bins in which funnel flow occurs may require a very large outlet to ensure that the ratholes collapse, stagnant material does not accumulate, and the bin empties (Figure 7). Funnel flow can cause erratic flow and exacerbate segregation, and stagnant material may spoil or cake.

Designing a mass flow bin with the desired capacity for a facility that has headroom restrictions may be a challenge. In general, for a given volume, mass flow bins are taller than those designed for funnel flow. Whenever this is the case, confirm that the constraints are necessary. Alternatively, consider whether a funnel flow bin, or an expanded flow bin, which has a lower mass flow section and an upper funnel flow section (Figure 6c), will suffice.

Mass flow hopper angle

The hopper angle measured from the vertical (θ') for a mass flow bin depends on the effective angle of friction (δ), the wall friction angle (ϕ'), and the geometry of the hopper. Figures 8 and 9 plot the allowed mass flow hopper angles for conical bins and bins with flat walls and rectangular (slot) outlets. The boundaries between mass flow and funnel flow depend on the effective angle of friction. Any combination of θ' and ϕ' that falls within the mass flow region of the chart will provide mass flow *(3)*.

The actual hopper angle of a conical mass flow bin should be 2–3 deg. less than the theoretical angle obtained from Figure 8. The actual hopper angle of a bin with flat walls and a rectangular outlet can be 5–10 deg. larger than the recommended angle without risking funnel flow. For Figure 9 to apply to a planar flow bin, *i.e.,* one having a wedge-shaped or transition hopper section, the outlet must be at least twice as long as it is wide if the bin has vertical end walls and three times as long if its end walls converge.

As an alternative to the graphical technique of Figures 8 and 9, the theoretical boundary between mass flow and funnel flow can be calculated mathematically. For conical hoppers with round outlets *(4)*:

$$\theta' = 90 - \frac{1}{2}\cos^{-1}\left(\frac{1-\sin(\delta)}{2\sin(\delta)}\right) - \beta \quad (2)$$

where β is the angle between the principal plane and the plane normal to the hopper wall and is calculated from:

$$2\beta = \phi' + \sin^{-1}\left(\frac{\sin(\phi')}{\sin(\delta)}\right) \quad (3)$$

As with the graphical approach, a safety factor of 2–3 deg. should be subtracted from the value of θ' in Eq. 2.

For hoppers with rectangular outlets and $\phi' < \delta - 3$ *(5)*:

$$\theta' = \frac{\exp\left[3.75 \times 1.01^{(\delta-30)/10}\right] - \phi'}{0.725\left(\tan(\delta)\right)^{1/5}} \quad (4)$$

In all types of hoppers, the stress at the wall (σ') and the major principal stress (σ_1) are not equal. For both rectangular and circular openings, the wall friction angle is determined by superimposing the wall yield locus and effective

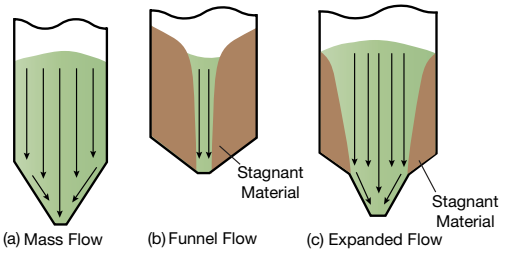

▲ **Figure 6.** Mass flow (a) ensures a more-uniform discharge of bulk solids than funnel flow (b) or expanded flow (c).

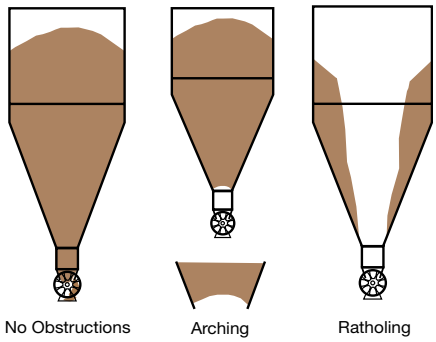

▲ **Figure 7.** Obstructions such as cohesive arches and ratholes prevent flow through a hopper.

yield locus on the same graph (Figure 10). The value of ϕ' is found at the intersection of the Mohr's circle that passes through σ_1 and the wall yield locus.

Mass flow hopper outlet size

The outlet dimension of a hopper is critical to prevent the formation of a stable cohesive arch (Figure 7), which blocks the flow of material. To ensure that a cohesive arch does not form, the external stress must be greater than the powder's unconfined yield strength (f_C). The flow factor (*ff*) is defined as the ratio of the major principal stress (σ_1) to the stress acting on the arch of material at the outlet (σ_A) *(3)*:

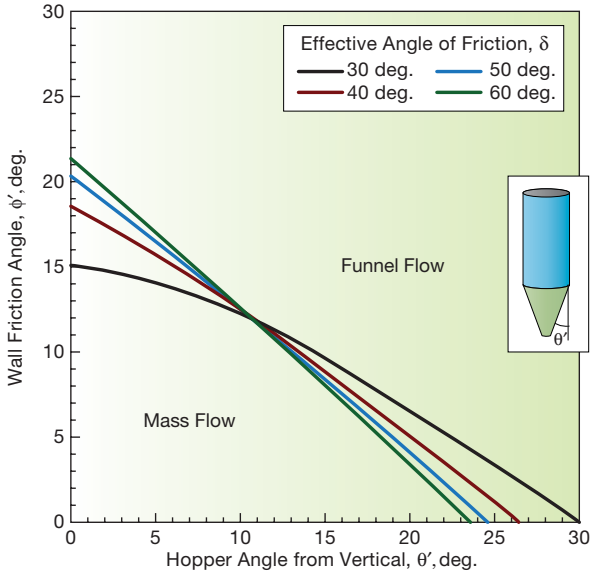

▲ **Figure 8.** When designing a hopper with round or square outlets, select a hopper angle (θ') that falls to the left of the appropriate curve.

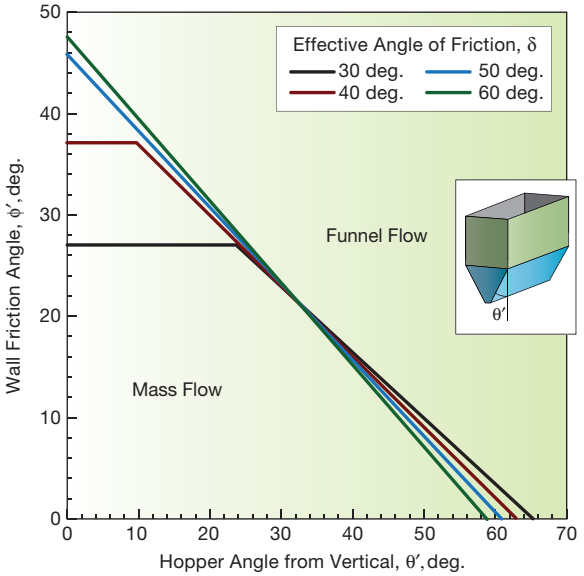

▲ **Figure 9.** Wedge-shaped outlets for mass flow have hopper angles (θ') that are typically 10 deg. less steep than those of conical hoppers.

$$ff = \frac{\sigma_1}{\sigma_A} \tag{5}$$

Charts such as Figure 11 are used to determine the flow factor based on the powder's effective angle of friction (δ), the wall friction angle (ϕ'), and the hopper angle (θ'). Typical values of the flow factor range between 1.1 and 1.7. The dotted lines in Figure 11 represent the boundary between mass flow and funnel flow.

Analytical expressions for the flow factor of a bulk solid in a bin are *(6, 7)*:

$$ff = \frac{Y\left(1+\sin\left(\delta\right)\right)H\left(\theta'\right)}{2\left(X-1\right)\left(\sin\left(\theta'\right)\right)} \tag{6}$$

$$X = \frac{2^i \sin\left(\delta\right)}{1-\sin\left(\delta\right)}\left[\frac{\sin(2\beta+\theta')}{\sin\left(\theta'\right)}+1\right] \tag{7}$$

$$Y = \frac{\left[2\left(1-\cos\left(\beta+\theta'\right)\right)\right]^i \sin\left(\theta'\right)\left(\beta+\theta'\right)^{1-i}}{\left(1-\sin\left(\delta\right)\right)\sin^{2+i}\left(\beta+\theta'\right)} + \frac{\sin\left(\beta\right)\sin^{1+i}\left(\beta+\theta'\right)}{\left(1-\sin\left(\delta\right)\right)\sin^{2+i}\left(\beta+\theta'\right)} \tag{8}$$

$$H\left(\theta'\right) = \left(\frac{130+\theta'}{65}\right)^i \left(\frac{200+\theta'}{200}\right)^{1-i} \tag{9}$$

where *i* is an outlet shape indicator equal to 0 for rectangular outlets and 1 for circular outlets.

To determine the size of the outlet required to prevent the formation of a cohesive arch in a mass flow bin, the flow factor and flow function are superimposed on the same graph (Figure 12). The flow factor is constructed as a line with a slope equal to 1/*ff* that passes through the origin. The flow function, as discussed earlier, is the plot of the major principal stress and the unconfined yield strength. Figure 12 illustrates three possible situations:

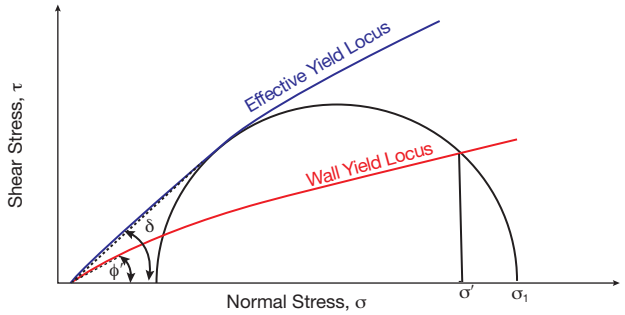

▲ **Figure 10.** The angle of wall friction and effective angle of friction are found by plotting the effective yield locus and wall yield locus.

Article continues on next page

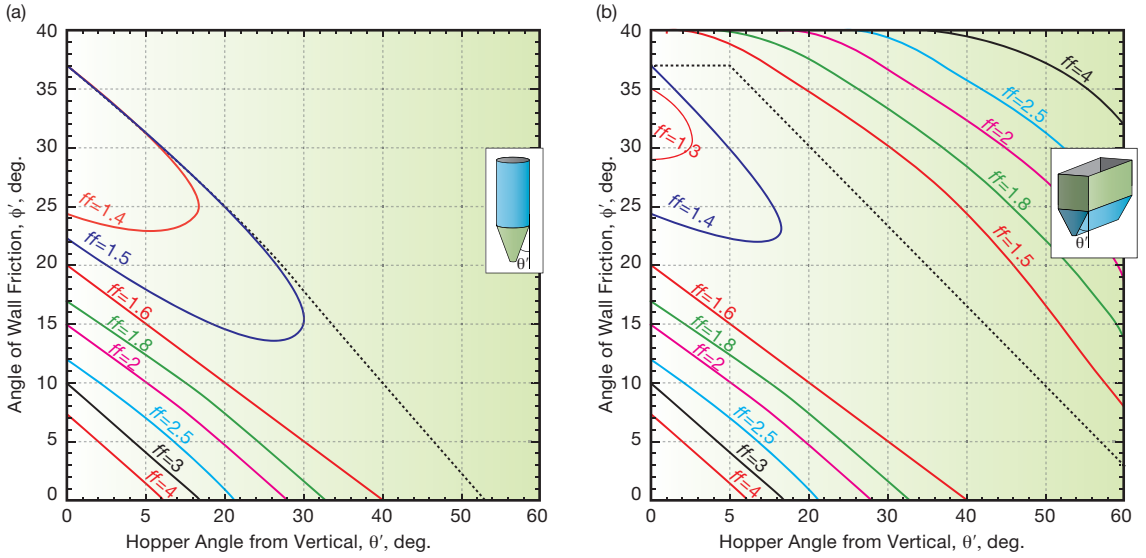

▲ **Figure 11.** The flow factor (*ff*) depends on the hopper angle from the vertical (θ′), the wall friction angle (ϕ′), and the effective angle of friction (δ). These sample charts are for (a) conical hoppers and (b) planar flow hoppers with rectangular outlets; for both, the effective angle of friction δ = 40 deg. The dotted line represents the boundary between mass flow and funnel flow. Source: Adapted from *(3).*

• *The flow function lies below the flow factor, and the two do not intersect.* In this case, the stress imparted on the abutments of the arch is always greater than the material's cohesive strength, and it is not necessary to specify a minimum outlet dimension to prevent cohesive arching. Instead, the outlet dimension B (*i.e.*, the diameter of a round outlet or the width of a rectangular outlet) is determined by other considerations, such as the required discharge rate. To calculate the hopper angle required for mass flow, the major principal stress (σ_1) at the outlet must be known. This stress is:

$$\sigma_1 = ff\,\frac{\rho_b g B}{H(\theta')} \qquad (10)$$

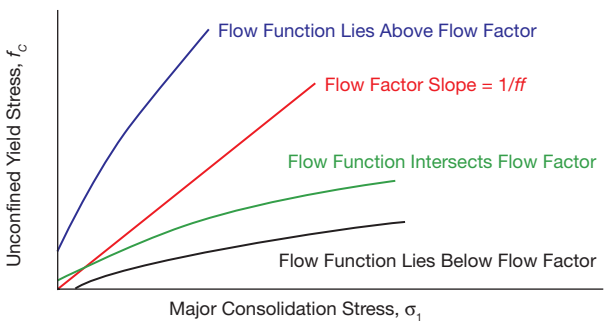

▲ **Figure 12.** To determine if a critical stress exists and a cohesive arch is likely to form, the flow function and flow factor are plotted on the same graph.

• *The flow function lies above the flow factor and the curves do not intersect.* The powder will not flow due to gravity alone. Consider changing the flow properties of the material, such as increasing its particle size, or using a flow aid or standpipe.

• *The flow function and flow factor intersect.* At the intersection of the two lines, the arch stress and the cohesive strength of the bulk solid are identical and equal to the critical stress (σ_{crit}). The hopper outlet diameter that must be exceeded to prevent arching (B_{min}) is:

$$B_{min} = \frac{H(\theta')\sigma_{crit}}{\rho_b g} \qquad (11)$$

A safety factor of 20% is sometimes added to B_{min} to obtain the outlet diameter, *i.e.,* $B = 1.2\,B_{min}$.

Because the bulk density (ρ_b), the effective angle of friction (δ), and the angle of wall friction (ϕ′) all depend on stress, calculating critical hopper angles and arching dimensions is an iterative procedure. Use the flowchart in Figure 13a to calculate the minimum hopper outlet diameter and recommended mass flow hopper angle. Figure 13b outlines the steps to determine the recommended mass flow hopper angle based on a known outlet dimension (B).

To prevent mechanical interlocking at the outlet, follow these two rules of thumb:

• for a conical hopper, the outlet diameter should be 6–8 times the size of the largest particle that will be handled

• for a planar hopper, the outlet width should be 3–4 times the largest particle size.

Discharge rate from a mass flow hopper

The discharge of the solid is driven by gravity and the discharge rate depends on the size of the outlet and the hopper angle.

For coarse, incohesive powders, the solids discharge velocity (v_o) is:

$$v_o = \sqrt{\frac{Bg}{2(i+1)\tan(\theta')}} \quad (12)$$

and the mass discharge rate ($\dot{m}_s$) is:

$$\dot{m}_s = \rho_{b,o} A_o v_o \quad (13)$$

where A_o is the cross-sectional area of the outlet and $\rho_{b,o}$ is the bulk density at the outlet.

As the powder dilates (*i.e.,* expands), an adverse gas pressure gradient develops near the outlet. For fine powders, the gradient can be severe, and the maximum discharge rate of a fine powder can be orders of magnitude less than that of a coarse powder. For fine, incohesive powders, the discharge velocity is *(8, 9)*:

$$v_o = \sqrt{\frac{Bg}{2(i+1)\tan(\theta')}\left(1+\frac{1}{\rho_b g}\left.\frac{dP}{dz}\right|_o\right)} \quad (14)$$

$$\left.\frac{dP}{dz}\right|_o = \frac{v_o \rho_{b,o}^2 g}{K_o}\left(\frac{1}{\rho_{b,mp}} - \frac{1}{\rho_{b,o}}\right) \quad (15)$$

where dP/dz is the gas pressure gradient and the subscripts o and mp denote the hopper outlet and the hopper location corresponding to the minimum gas pressure, respectively. Combining Eqs. 14 and 15 gives:

$$\left[\frac{2(i+1)\tan(\theta')}{Bg}\right]v_o^2 + \left[\frac{1}{K_o}\left(1-\frac{\rho_{b,o}}{\rho_{b,mp}}\right)\right]v_o - 1 = 0 \quad (16)$$

To be conservative, $\rho_{b,mp}$ is assumed equal to the material's bulk density at the major principal stress at the cylinder-hopper junction *(10)*. This stress is given by the Janssen formula:

$$\sigma_1 = \frac{\rho_b g R_H}{k\tan(\phi')}\left[1-\exp\left(\frac{-kh\tan(\phi')}{R_H}\right)\right] \quad (17)$$

where R_H is the hydraulic radius of the cylinder (the ratio of the perimeter to the cross-sectional area). The bulk density at the hopper outlet ($\rho_{b,o}$) is set equal to the powder's minimum bulk density because the solids' stress is zero at the limiting solids discharge rate.

Funnel flow hoppers

For applications where a shallow hopper angle is desired to enable a bin with a larger capacity, a funnel flow bin should be considered. The outlet of a funnel flow bin must be large enough to prevent the formation of both cohesive arches and stable ratholes.

The critical ratholing diameter (D_F) is the minimum diameter of a round outlet or the minimum diagonal of a rectangular outlet to ensure that ratholes collapse. It is calculated from:

$$D_F = \frac{G(\phi_t) f_C}{\rho_b g} \quad (18)$$

where $G(\phi_t)$ is a ratholing parameter that is a function of the static angle of internal friction (ϕ_t) as determined by the timed cohesive strength tests, and f_C is the unconfined yield strength of the bulk solid at the major principal stress given by the Janssen equation (Eq. 17).

An analytical approximation of $G(\phi_t)$ is given:

$$G(\phi_t) = -5.066 + 0.490\phi_t - 0.0112\phi_t^2 + 0.000108\phi_t^3 \quad (19)$$

Other considerations

For some bulk materials, an expanded flow bin design is another good option. An expanded flow bin is essentially a funnel flow hopper above a mass flow hopper. The diameter of the upper mass flow section must be larger than the critical rathole diameter (D_F), while the outlet size must be larger than the critical arching dimension (B_{min}). As the bulk material is discharged, all the material in the bottom portion of the bin will be in motion, but in the top portion, flow will occur only in a central channel. Ratholes that develop will collapse, and the bin will completely empty.

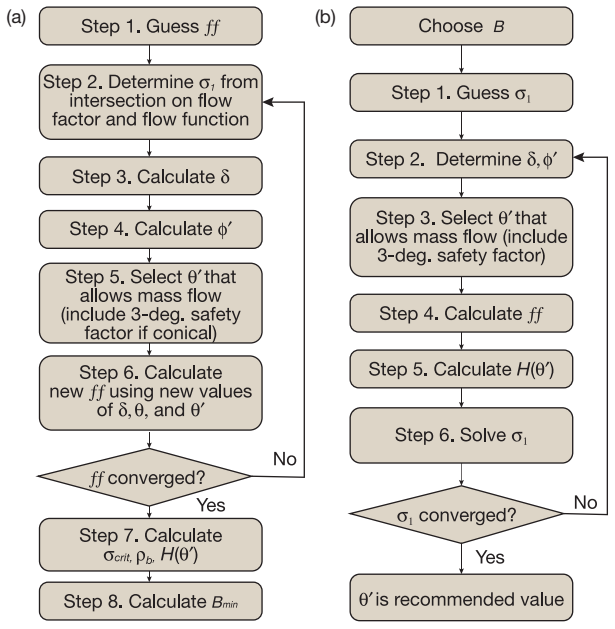

▲ **Figure 13.** (a) When the flow function and flow factor intersect, follow the steps in the flowchart on the left to determine the critical hopper outlet size and recommended mass flow hopper angle. (b) Use the flowchart on the right to find the recommended hopper angle for mass flow for a hopper with a known outlet dimension *(B)*.

Article continues on next page

A feeder or slide gate (or both) is often installed beneath a bin. If a rotary valve is used, a short cylindrical section should be placed above it to prevent preferential flow in the bin. If mass flow is required in a bin with a rectangular outlet, the capacity of the feeder should increase in the direction of discharge; otherwise, a narrow flow channel will form and problems associated with funnel flow will arise.

Sample design calculations

We want to design bins for two powders (A and B). Figure 14 summarizes their key flow properties: (a) cohesive strength, (*i.e.,* the flow function), (b) internal friction, (c) wall friction (*i.e.,*the wall yield locus), and (d) compressibility. Powder A is a coarse powder, and the permeability of Powder B is equal to 0.024 m/sec at its lowest bulk density.

Powder A. A conical hopper is generally preferable, because a round outlet with a simple feeder or valve can be used. The outlet dimensions are unknown and Figure 13a is used to calculate the size of the outlet.

Step 1. Estimate the flow factor *ff* = 1.2.

Step 2. Plot the flow factor as a line with slope 1/*ff* on the same plot as the flow function in Figure 14a. The intersection occurs at σ_1 = 0.65 kPa.

Step 3. Read Figure 14b to find that with the major principal stress σ_1 = 0.65 kPa, the effective angle of friction δ = 43 deg.

Step 4. Draw a Mohr's circle and the wall yield locus from Figure 14c. The Mohr's circle has a radius of $\sigma_1 \sin(\delta)/(1+\sin(\delta))$ = 0.26 kPa and passes through σ = 0.65 kPa. Draw a line from the intersection of the wall yield locus and the Mohr's circle to the origin. This creates Figure 15. The angle formed is ϕ' = 33 deg.

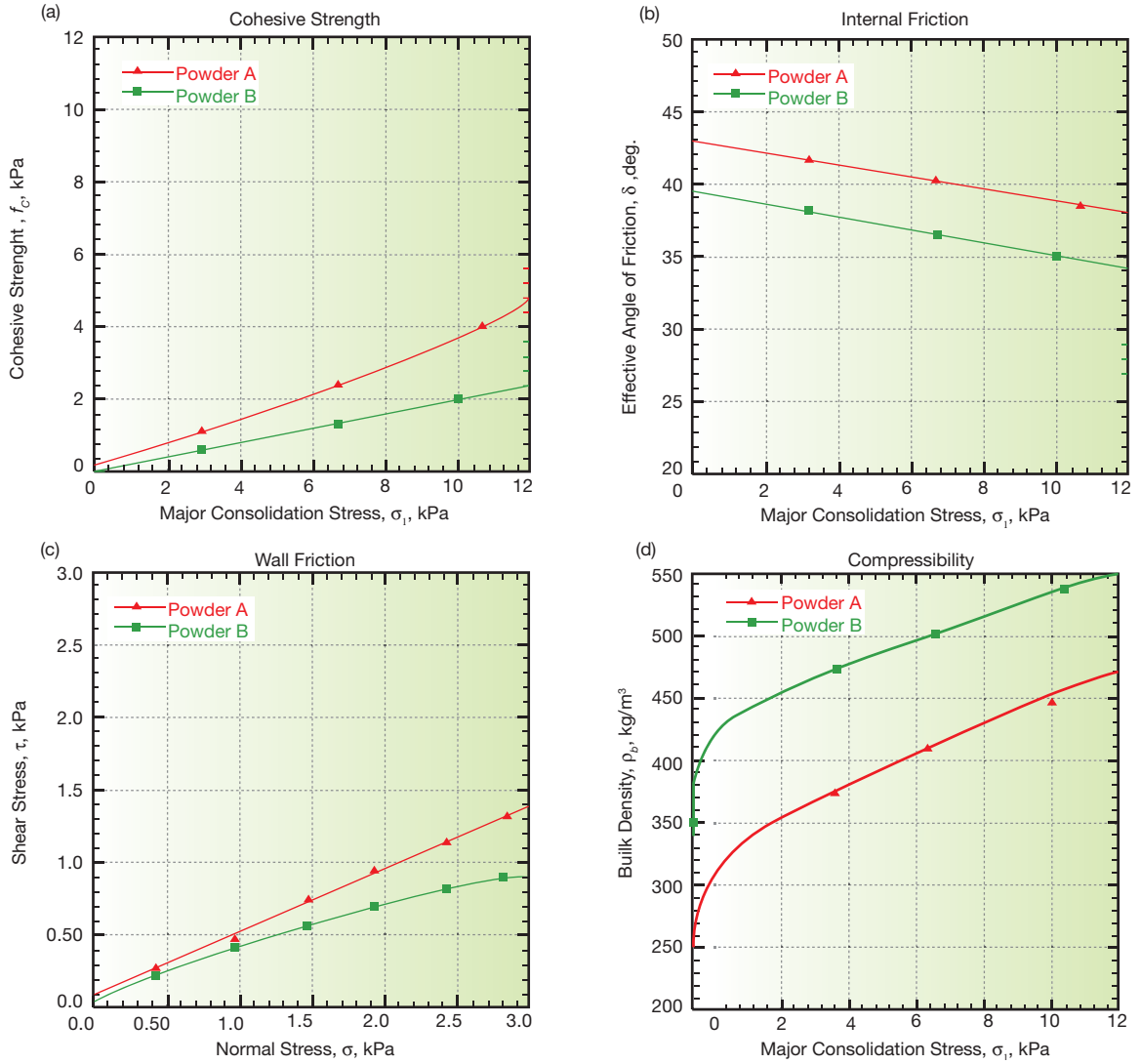

▲ **Figure 14.** Fundamental flow properties of Powders A and B for the sample design calculations.

Step 5. Use Eq. 2 to calculate the theoretical minimum hopper angle (θ'), then subtract a 3-deg. safety factor to obtain a recommended mass flow hopper angle $\theta' = 5.6$ deg.

Step 6. Use Eq. 6 to calculate a new value of $ff = 1.28$. The solution has not converged, so Steps 2 through 6 must be repeated with the new $ff = 1.28$.

Steps 2–6. The intersection of the flow function and the updated flow factor occurs at $\sigma_1 = 0.73$ kPa, so the effective angle of friction $\delta = 43$ deg. The intersection of the wall yield locus and a new Mohr's circle gives $\phi' = 32$ deg. With a 3-deg. safety factor, Eq. 2 gives $\theta' = 7.6$ deg. From Eq. 6, the new value of $ff = 1.30$. The solution still has not converged, so another iteration of Steps 2–6 is needed. With the new value of $ff = 1.3$, $\sigma_1 = 0.74$ kPa, $\delta = 43$ deg., $\phi' = 31.4$ deg., and $\theta' = 8$ deg. Equations 6–9 give $ff = 1.30$. The solution has converged.

Step 7. Find the intersection of the flow function and the flow factor on Figure 14a to determine $\sigma_{crit} = 0.57$ kPa. Solve Eq. 9 to find $H(\theta') = 2.12$. Find $\rho_b = 313$ kg/m^3 from Figure 14d.

Step 8. Use Eq.11 to calculate the critical arching diameter $B_{min} = (2.12)(0.57 \text{ kPa})/[(313 \text{ kg/m}^3)(9.8 \text{ m/s}^2)] = 0.40$ m.

A conical hopper with a 0.40-m diameter and hopper walls 8 deg. from the vertical is not practical. We could consider other wall materials that have a lower wall friction. Instead, let's repeat the design procedure for a wedge-shaped or transition hopper:

Step 1. Estimate $ff = 1.2$.

Step 2–4. The major principal stress, effective angle of friction, and angle of wall friction are the same as for a conical hopper as previously calculated: $\sigma_1 = 0.65$ kPa, $\delta = 43$ deg., $\phi' = 33$ deg.

Step 5. For a hopper with a rectangular outlet, use Eq. 4 to calculate $\theta' = 16.2$ deg.

Step 6. Use Eq. 6 to recalculate the flow factor $ff = 1.42$. The flow factor has not converged and the calculations in Steps 2–6 are repeated.

Steps 2–6. The intersection of the flow function and flow factor occurs at $\sigma_1 = 0.88$ kPa. The effective angle of friction is $\delta = 42$ deg. and the wall friction angle is $\phi' = 30$ deg. The new mass flow hopper angle is $\theta' = 20.5$ deg. The new flow factor is $ff = 1.42$. The solution has converged.

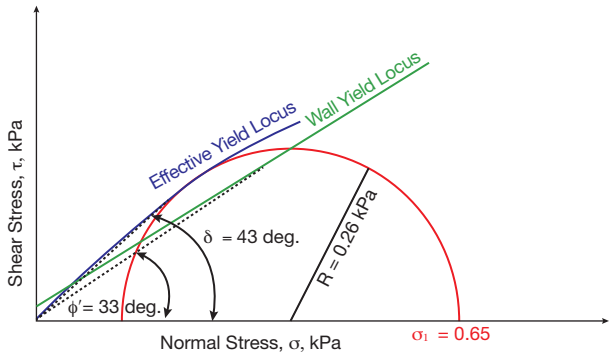

▲ **Figure 15.** A Mohr's circle is used to determine the wall friction angle from the effective yield locus and wall yield locus.

Step 7. Plot the flow function and the flow factor on the same graph to determine $\sigma_{crit} = 0.62$ kPa. Use Eq. 9 to solve for $H(\theta') = 1.10$. Figure 14d shows $\rho_b = 318$ kg/m^3.

Step 8. Use Eq. 11 to determine the width of a rectangular outlet to prevent arching $B_{min} = 0.22$ m.

Solution. The recommended bin is wedge-shaped with a 0.22-m rectangular outlet and walls sloped 20.5 deg. from vertical. All of the dimensions represent limiting conditions for flow; therefore, larger outlets and steeper hoppers are acceptable. Use Eq. 12 to determine the outlet size that provides the required solids discharge rate.

Powder B. Plot the flow factor along with the data in Figure 14a. Determine where the flow function and flow factor lie in relation to each other. For this powder, the flow factor will always lie above the flow function. Follow the steps laid out in Figure 13b to determine the mass flow hopper angle for a specified outlet diameter. Begin by choosing a conical hopper with an outlet diameter $B = 0.305$ m:

Step 1. Guess $\sigma_1 = 0.73$ kPa.

Step 2. Use Figure 14b to find that for $\sigma_1 = 0.73$ kPa, the effective angle of friction is $\delta = 39$ deg. A Mohr's circle determines $\phi' = 26$ deg.

Step 3. Use Eq. 2 and subtract a 3-deg. safety factor to find the hopper angle $\theta' = 15$ deg.

Step 4. Solve Eq. 3 and Eqs. 6–9 to find a new flow factor $ff = 1.42$.

Step 5. Use Eq. 9 to calculate $H(\theta') = 2.24$.

Step 6. Evaluate Eq. 10 to get a new $\sigma_1 = 0.85$ kPa. The system has not converged and Steps 2–6 must be reiterated with the new $\sigma_1 = 0.85$ kPa.

Steps 2–6. Graphical analysis of Figure 14b using Mohr's circles and $\sigma_1 = 0.85$ kPa gives $\delta = 39$ deg. and $\phi' = 25$ deg. Based on Eq. 2, the hopper angle $\theta' = 17$ deg. Use Eq. 3 and Eqs. 6–9 to calculate values of $ff = 1.44$ and $H(\theta') = 2.27$.

Solution. The solution to Eq. 10 is $\sigma_1 = 0.88$. The calculation converges and a conical hopper with a 0.305-m-dia. outlet and walls 17 deg. from vertical allows mass flow.

Capacity and flow calculations. The maximum steady-state discharge rate depends on the dimensions of the cylindrical section of the bin. For a 2-m-dia., 3-m-tall cylinder completely filled with Powder B, Eq. 17 yields $\sigma_1 = 11$ kPa at the hopper-cylinder junction. To be conservative, use Figure 14d to set $\rho_{b,mp} = 540$ kg/m^3, the bulk density at $\sigma_1 = 11$ kPa. From Eq. 16, the maximum steady discharge velocity $v_o = 0.068$ m/sec at the outlet. The minimum bulk density $\rho_{b,o} = 351$ kg/m^3, and based on Eq. 13, the maximum steady-state discharge rate is therefore

$[\pi (0.305\ m)^2/4](351\ kg/m^3)(0.068\ m/sec)(3600\ sec/hr) = 6{,}300\ kg/hr$.

A funnel flow bin can also be considered. The outlet diameter of a funnel flow hopper that must be exceeded to prevent the formation of ratholes depends on the cylinder dimensions. For a 2-m-dia., 3-m-tall cylinder completely filled with Powder B, Eq. 18 gives a critical rathole diameter of 1 m ($\phi_t = 30$ deg.). A conical funnel flow bin is therefore not recommended.

Final remarks

The design methods presented here (which are based on the pioneering work of Andrew Jenike) allow us to use flow property test results to design reliable hoppers, bins, and silos to store and handle bulk solids. Without exception, the materials that are handled should be tested under anticipated process conditions. Never rely on experience with reportedly similar materials, as even a small change in particle size, moisture content, or purity can result in a significant change in flow behavior. CEP

Literature Cited

1. **Maynard, E.,** "Ten Steps to an Effective Bin Design," *Chemical Engineering Progress*, **109** (11), pp. 25–32 (Nov. 2013).
2. **Mehos, G., and E. Maynard,** "Handle Bulk Solids Safely and Effectively," *Chemical Engineering Progress*, **105** (9), pp. 38–42 (Nov. 2013).
3. **Jenike, A. W.,** "Storage and Flow of Solids, Bulletin 123," *Univ. of Utah Engineering Station*, Salt Lake City, UT (1964, rev. 1976).
4. **Shamlou, P. A.,** "Handling of Bulk Solids: Theory and Practice," Butterworth & Co., Oxford, U.K. (1988).
5. **Arnold, P. C. and A. G. McLean,** "Bulk Solids: Storage, Flow and Handling," 2nd Ed., TUNRA Bulk Solids Handling Research Associates, Newcastle, Australia (1980).
6. **Arnold, P. C., and A. G. McLean,** "An Analytical Solution for the Stress Function at the Wall of a Converging Channel," *Powder Technology*, **13** (2), p. 255 (1976).
7. **Arnold, P. C., and A. G. McLean,** "Improved Analytical Flow Factors for Mass-Flow Hoppers," *Powder Technology*, **15,** p. 276 (1976).
8. **Schulze, D.,** "Powders and Bulk Solids: Behavior, Characterization, Storage and Flow," Springer-Verlag Berlin Heidelberg, Springer, Berlin (2008).
9. **Gu, Z. H., *et al.*,** "Modeling of Air Pressure Distributions in Mass Flow Bins," *Powder Technology,* **72** (2) (1992).
10. **Johanson, K.,** "Successfully Dealing with Erratic Flow Rates," *Powder Pointers*, **3** (A) (2009).

Acknowledgments

The authors acknowledge the contributions of Jenna Rider and David Bruno.

Nomenclature

A	= area
B	= outlet dimension
D_F	= critical ratholing diameter
f_C	= unconfined yield strength
ff	= flow factor
$G(\phi_t)$	= rathole parameter
g	= acceleration due to gravity
$H(\theta')$	= geometric factor for a cohesive arch
h	= height
i	= 0 for slotted outlet, 1 for round outlet
K	= permeability constant
k	= Janssen coefficient
$\dot{m}_s$	= solids discharge rate
P	= pressure
R_H	= hydraulic radius
u	= superficial gas velocity
v_o	= discharge velocity
X	= radial stress field parameter
Y	= radial stress field parameter
z	= vertical coordinate

Greek Letters

β	= angle between principal plane and plane normal to hopper wall
δ	= effective angle of friction
ϕ	= kinematic angle of internal friction
ϕ'	= angle of wall friction
ϕ_t	= static angle of internal friction
θ'	= hopper angle referenced from vertical
ρ_b	= bulk density
σ	= normal stress
σ'	= wall stress
σ_1	= major principal stress
σ_A	= stress on the abutment of an arch
τ	= shear stress

Subscripts

a	= actual
$crit$	= critical
min	= minimum
mp	= at minimum gas pressure
o	= outlet

GREG MEHOS, PhD, (4 Crusade Rd., Westford, MA 01886; Phone: 978-799-7311; Email: gmehos@uri.edu) is an adjunct professor at the Univ. of Rhode Island and a consultant specializing in the storage, handling, and processing of bulk solids. He has worked as a project engineer at Jenike & Johanson and as a process development engineer at Cabot Corp. He received a BS and PhD in chemical engineering from the Univ. of Colorado, and a master's degree from the Univ. of Delaware. He is a registered professional engineer in Massachusetts and a member of AIChE. He served on the executive board of AIChE's Particle Technology Forum and is a past chair of the Boston Local Section. He is the author of the section on powder flow and hopper design in the 9th edition of *Perry's Chemical Engineers' Handbook*.

MIKE EGGLESTON, SHAWN GRENIER , CHRISTOPHER MALANGA, GRISHMA SHRESTHA, AND TRISTAN TRAUTMAN are undergraduate chemical engineering students at the Univ. of Rhode Island.

Introduction to Pressure Measurement

Eugen Gassmann
WIKA Instruments

Pressure-measuring devices come in a wide variety of designs and sizes to suit almost any application. This article describes the basics of pressure measurement and provides guidance on instrument selection.

Fluid pressure is a critical operating parameter in chemical process industries (CPI) plants; in fact, it is the second most common parameter measured after temperature. Pressure measurement applications range from simple setpoint monitoring to ensure sufficiently high or low pressure levels, to continuous monitoring as part of a complex automation system. The breadth of applications that require pressure measurement explains the diversity of sensing products on the market. With new instruments being introduced every year, it's no wonder that selecting the correct measuring device often seems like a daunting task. The key to matching the correct instrumentation to an application is understanding how pressure is measured and calculated.

What is pressure?

Pressure is defined as force divided by the area over which that force is distributed, *i.e.,* $P = F/A$. As this equation suggests, larger force equals larger pressure when area remains constant.

What is more difficult to understand from this definition, though, is that the existence of pressure requires a medium. When we speak of pressure in industrial settings, we are talking about the force that a liquid or gas (*i.e.,* a fluid) exerts onto a fixed area. Since pressure is a force, it cannot be measured directly; instead, the effect that force has on an area is what is actually measured.

How pressure sensors work

Almost all pressure sensors work the same way — they measure the deflection or displacement of a diaphragm or membrane that is acted on by a force and convert the amount of deflection/displacement into an electronic signal. Sensors differ in the materials used to construct the diaphragm and how the deflection is measured. Virtually all industrial sensors are based on one of two principles of deflection measurement:

• *resistive pressure measurement.* In this type of sensor, the diaphragm is in direct contact with the fluid, separating the fluid from the instrument's electronics. The diaphragm's size, thickness, and material of construction determine the sensor's pressure range and media compatibility. Diaphragm deflection causes a type of resistor called a strain gage to either compress or elongate (Figure 1a). When four strain gages are connected, they form a Wheatstone bridge (*i.e.,* an electrical circuit that measures change in electrical resistance), which converts the deflection of the gages into an electrical signal. This design is shared by metal thin-film, ceramic thick-film, and micro-electrical-mechanical system (MEMS) sensors, as well as classic bonded strain gages.

• *capacitive pressure measurement*. In a capacitive pressure sensor, two membranes are mounted in parallel, one of which is in contact with the fluid under pressure (Figure 1b). They are compressed against each other in response to a change in pressure, which causes the capacitance to change. The capacitance change is picked up by an electronic circuit and converted into a pressure equivalent signal.

A variant of resistive pressure measurement is the piezo-resistive sensor (Figure 1c). Piezo-resistive microstructures are integrated onto a semiconductor chip and encapsulated in an oil-filled chamber, and this oil transmits pressure to the sensor via an external diaphragm. Due to their high complexity, these sensors are restricted to a narrow range of applications and are mainly used in specialty sensors.

Both resistive and capacitive sensing technologies have

been in use for decades and are well established, and it can be said with certainty that they work effectively.

The sensor material that forms the diaphragm in direct contact with the fluid dictates media compatibility and can impose limitations on applicability. For example, ceramic sensors require some kind of additional sealing — unlike metallic sensors, which can be welded to achieve a hermetic seal without any additional (soft) sealing material. Sometimes the process conditions (*e.g.,* temperature) or the fluid in contact with the sensor diaphragm is so aggressive or harsh that typical sensor materials would fail. In those cases, diaphragm seals must be used. Seals separate the sensor from the harsh medium with an additional membrane (which may be constructed of a highly resistant material such as titanium, or coated with polytetrafluoroethylene [PTFE] or gold) and transmit the pressure to the sensor membrane via an additional internal fill fluid.

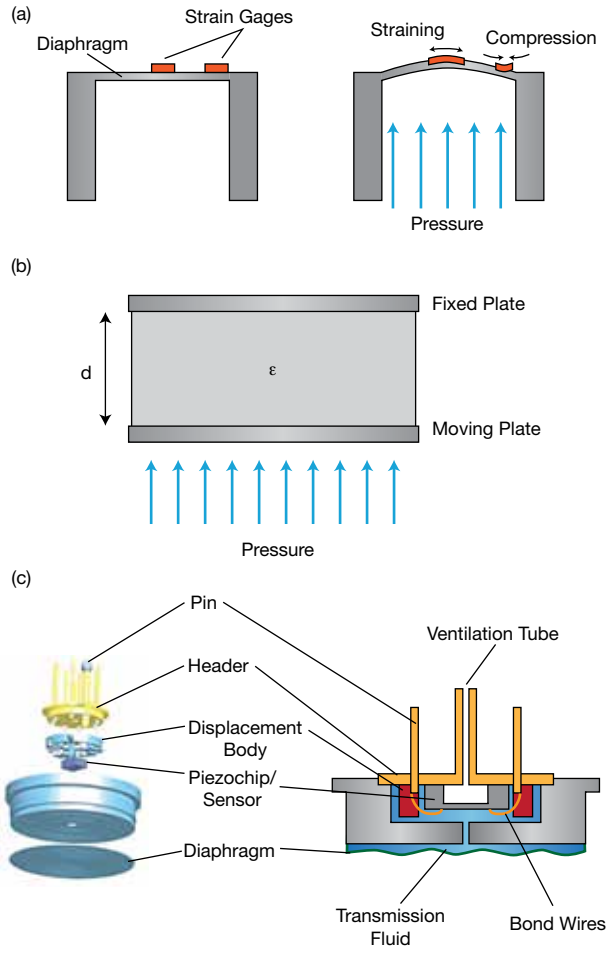

▲ **Figure 1.** Pressure sensors measure the deflection of a diaphragm or membrane that is acted on by a force and convert the amount of deflection into an electronic signal. In resistive pressure sensors (a), strain gages pick up changes in pressure by bending or compressing. In capacitive pressure measurement (b), the distance between two membranes changes with a change in fluid pressure. In piezo-resistive sensors (c), oil transmits pressure to the sensor chip via an external diaphragm.

Furthermore, pressure sensors do not have perfectly linear behavior and they can be affected by external factors such as temperature. Therefore, the manufacturer needs to accurately describe tolerances and variations in each product's datasheet.

Even seemingly comprehensive datasheets, though, can be confusing — or even misleading. For example, suppose the tolerance of a certain value is expressed as a percentage (*e.g.,* 0.25%). This can raise questions that are difficult to answer, such as: Is the value an individually adjusted parameter, or is it a maximum or typical value? Do most products center around this value, or only a small number (and if so, how many)? What is the worst-case value, and under what conditions?

Pay close attention to the format and structure of the datasheet, as these provide clues to how much data the manufacturer is willing to share in a transparent way, as well as how much knowledge and manufacturing-process know-how the company has. Any time you are in doubt, ask. If you don't get an answer, don't trust the data. Many sensors available today are marketed as "perfect" by manufacturers aiming to maximize market share. Therefore, it is very much a "buyer beware" environment.

From bare sensor to working transmitter

In most modern applications, users require a complete instrument that measures pressure in a standardized way. Typical transmitters contain a process connection and an electrical output signal; both of these interfaces are standardized, but they are connected through various proprietary designs that are determined by the sensor technology and the particular application-specific function the instrument is intended for.

The term sensor is often used as a generic term for any type of sensing element, and could refer to a bare sensing element or a complex apparatus. Most manufacturers distinguish between sensors, transducers, and transmitters, each of which has its own distinct set of features:

• *sensor* — typically a bare sensing element or simple assembly. Sensors usually require a full design process to add or integrate them into a housing, and are generally not applied directly in industrial automation systems.

• *transducer* — an assembled sensor that has defined pressure ports and defined electrical outputs in addition to generic sensing functionality.

• *transmitter* — a fully standardized instrument that includes standardized process connections, output signals, and electrical connectors. Because of their standardization, transmitters can be interfaced directly to other equipment without fundamental engineering.

• *process (or "smart") transmitter* — a high-end transmitter that features additional software with user-programmable functionality; human-machine interface (HMI) elements such as a display and keys; high accuracy; and a wide pressure range that is user-configurable. This type of transmitter offers many output and communication options, but typically has very few process connections and only a few pressure ranges. Standard industrial transmitters come with a fixed pressure range — users can generally choose from 20 to 50 (or even more) different, but predefined, ranges. Process transmitters, however, come with only five or six pressure ranges, but those can be fine-tuned by a function called turndown.

Every pressure transmitter contains a sensor; electronics that supply the sensor, amplify and condition the signal, and convert it to an output signal; a pressure connection; and an electrical connection (Figure 2).

How to select the right instrument for the job

Although selecting the best pressure-sensing instrument can involve many variables, the following five basic questions can help you get started on making the most appropriate choice.

1. What is the process connection? The process connection, also referred to as the pressure connection, channels the pressurized medium to the sensor. Many different variants are available to suit a wide range of applications and industries, so it is important to select the correct one. Some key differences to be aware of are:

• *internal vs. flush diaphragms.* The simplest connection has a passage that allows the pressurized medium to directly contact the sensor's internal diaphragm (Figure 3a). A flush-diaphragm connection (Figure 3b) has an additional diaphragm (*e.g.,* made of stainless steel) that is flush with the internal surface of the pipe or vessel and is in contact with the pressurized medium; an additional fluid transmits pressure to the sensor's internal diaphragm. Internal-diaphragm connections are less expensive, easier to handle, and are commonly used with gaseous or liquid pressurized media. Flush-diaphragm connections are recommended for viscous, adhesive, abrasive, or crystalline media applications, and for applications that require residue-free pressure connection cleaning.

• *thread.* Most pressure connections have a standard thread that allows them to be screwed in at measuring points without compatibility problems. However, different threads are standard in different regions of the world. Make sure that the instrumentation's threads match those of the applications they are intended for.

• *seal*. An important component of a thread is its seal. Some threads are self-sealing, whereas others require an additional seal. There are many seal options. Parallel threads are either sealed between the thread and the instrument's housing (behind the thread) or in front of it using a metallic spigot. Self-sealing, or conical, threads seal the process by applied torque and may require the use of additional sealing tape.

2. What is the pressure range? Pressure ranges, typi-

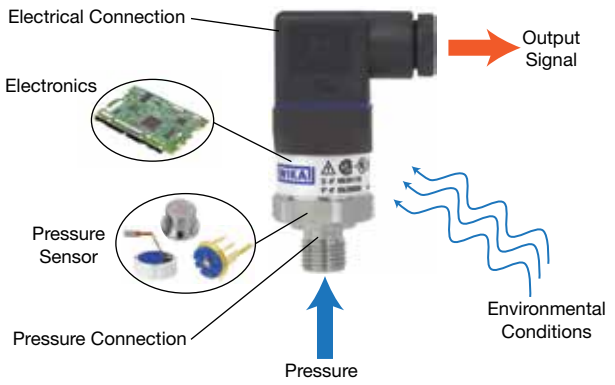

▲ **Figure 2.** A typical pressure transmitter is a fully standardized instrument that contains a pressure connection, a sensor, electronics, and an electrical connection, and outputs a standard electrical signal.

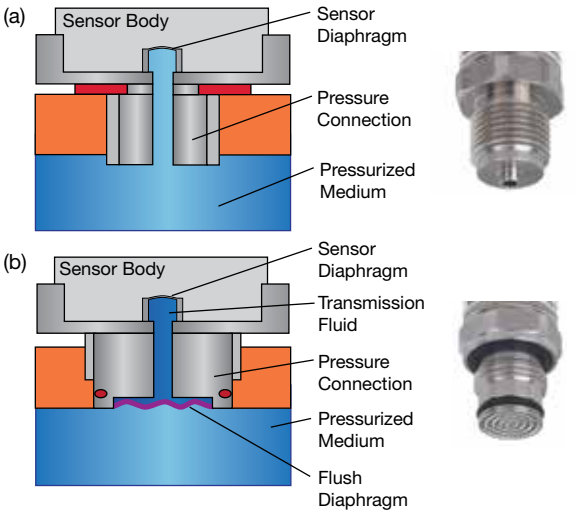

▲ **Figure 3.** In an internal-diaphragm connection (a), the process fluid comes in direct contact with the sensor diaphragm through a pressure port. In a flush-diaphragm connection (b), an additional stainless steel diaphragm is in contact with the process fluid, and a transmission fluid transmits the pressure to the internal diaphragm.

cally specified in an instrument's datasheet, define the limits within which pressure can be accurately measured or monitored (Figure 4). The most important specifications are the upper and lower limits, and whether the values are in units of absolute or gage pressure.

Overpressure limits lie outside (above and below) the pressure range. Pressure excursions into the overpressure range will not cause permanent sensor damage, but readings may be compromised (less accurate) and slightly out of specification. However, any pressure above the overpressure limit — in what is known as the destructive range — will cause irreversible damage, even if it is present for only a very short period of time (*e.g.,* pressure spikes).

The potential for pressure spikes must be considered in applications where pressure is dynamic. Dynamic pressure can be caused by switching a pump on and off, connecting or disconnecting a hydraulic system, or opening and closing a fast-acting fluid valve when fluids flow with high speed.

One well-known type of pressure spike is water hammer, which occurs in a hydraulic system when a valve is quickly turned on or off. This creates a pressure wave that propagates through the entire system, which can easily overload a sensor or even cause it to burst. Pressure spikes should be avoided by the total fluid dynamics design — the design of the system should be such that pressure spikes will not occur. The magnitude of pressure spikes can be reduced by installing either restrictors in the pressure port or a pressure port manufactured using electrical discharge machining (EDM) drillings. These drillings are used to produce extremely small holes (*e.g.,* 3-mm dia.) that provide only a small orifice for the fluid to reach the sensor, which greatly reduces the force of the pressure wave.

Both cavitation and the micro-diesel effect can also cause extremely high pressure spikes. Cavitation is generally described as the formation and implosive dissolution of hollow spaces (bubbles) in liquids due to pressure variations. The resulting short-term pressure and temperature peaks can cause erosion of metallic components.

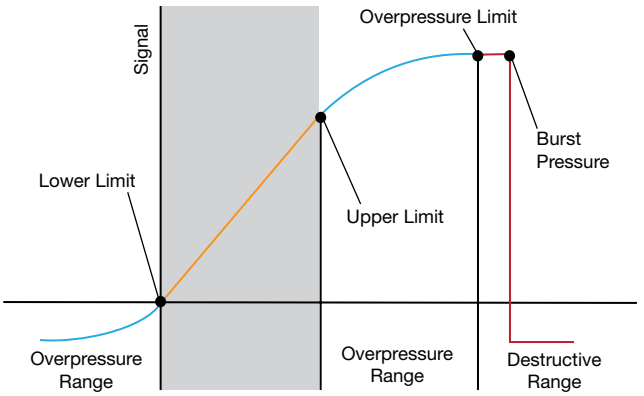

▲ **Figure 4.** A sensor's pressure range (gray region) defines the lower and upper limits of pressure measurement, as well as the overpressure range.

Bubbles forming in a combustible air-hydrocarbon mixture due to cavitation can explode by local spontaneous self-ignition during a pressure increase. This is known as the micro-diesel effect. If no special measures are taken, the pressure wave resulting from a micro-explosion can cause serious pressure spikes that can destroy a hydraulic system's components.

It is necessary to either prevent cavitation and micro-explosions, or ensure that the sensors are suitably protected from the impacts should any occur. Electronic pressure-measuring instruments designed specifically for critical applications have protective mechanisms built in, such as EDM drillings, restrictor elements, or specialized baffle and deflector plates within the pressure port.

3. What is the electrical output signal? Most electronic measuring instruments transmit an analog voltage or current signal to a downstream control unit. Instruments that output digital signals are also available. There are four main signal standards to select from:

• *standard analog.* The most common output signal, standard analog, can be a current or voltage signal. Current signals have lower sensitivity to electromagnetic interference than voltage signals and automatically compensate for loss of signal strength along the cable. The elevated zero point of the 4–20-mA current signal and 1–5-V voltage signal enables cable breaks and instrument faults to be detected. The 4–20-mA output signal is commonly transmitted using 2-wire technology, which enables the sensor to draw its power directly from the current loop. Voltage signals require a 3-wire connection that uses the third lead for the power supply.

• *ratiometric.* The most basic analog output signals are those that are proportional to the supply voltage, where the zero point and final value represent a constant percentage of the sensor supply voltage. For example, a 10–90 signal has a zero point that is 10% of the supply voltage and a final value that is 90%; if the supply voltage decreases by 5%, then the current analog signal also decreases by 5%. Thus, the ratio of the output signal to the supply voltage remains the same. Ratiometric sensors are often operated with a supply voltage of 5 V. The 10–90 signal is then specified in the datasheets as 0.5–4.5 V ratiometric.

• *digital output signal*. Pressure-measuring instruments that transmit digital output signals can communicate with other devices (*e.g.,* through a fieldbus system) to exchange operational data and parameters in addition to pressure readings. However, as industrial pressure transmitters do not require additional process data in order to function, these output signals have very few applications. Therefore, transmitters with a connection to CANbus or PROFIBUS-DP

play a relatively minor role in industrial applications at the moment.

• *digital communication modulated on an analog output signal (i.e., HART)*. This signal is employed by virtually all high-end process (smart) transmitters. Because process transmitters typically offer only a few pressure ranges (most commonly five or six), they nearly always require a change in the pressure range (referred to as turndown). The small number of ranges and styles offered by manufacturers require the user to configure each instrument for its specific application. The standardized HART signal allows the instrument to communicate via the standard 2- or 3-wire signal connection and avoids the need for proprietary terminals, software, etc.

4. What is the electrical connector? Electronic pressure sensors have a choice of either standard plug-in connectors or output cables. The type of connector and cable have a considerable influence on the instrument's ingress protection (IP) rating (a measure of how well the device is protected against dust and moisture ingress) and its resistance to aggressive media or environmental influences like ultraviolet (UV) radiation, as well as its allowable ambient temperature range. It is necessary to consider the exact installation conditions and the operating environment to determine the best electrical connection. The most important point to keep in mind when considering a plug-type connector is that the mating plug and the entire associated cable entry form an integral part of the instrument housing's sealing system; if the connector is unplugged, the seal is broken and the instrument may be susceptible to the ingress of humidity and dirt — a very common cause of premature failure of transmitters in the field. Some studies suggest that up to 50% of all sensor failures in the field are directly related to the electrical connection.

5. Are any special properties required? A list of special requirements needs to be established. This may steer the selection toward a specific model. Factors that may necessitate specialized devices include: hazardous area classifications that require specific approvals (*e.g.,* Ex-i [intrinsically safe] or Ex-d [explosionproof], etc.); harsh environmental conditions, such as excessive heat or cold, heavy vibration, or chemical attack; and large temperature gradients between the pressurized medium and the surroundings, which can cause the formation of ice or condensation. Most manufacturers offer products in different accuracy classes as well as special models suited for these conditions.

Pressure measurement applications

The tasks assigned to pressure monitoring instruments in industrial environments are diverse and run the gamut from operations like extraction of water from wells, power generation within fuel cells, and the operation of cranes and elevators. Regardless of the specific task at hand, electronic pressure measurement almost always falls into one of three categories:

- monitoring critical system pressure
- controlling pressure
- indirect measurement of process values.

Critical value monitoring

In critical-value monitoring applications, the pressure-measuring instrument reports whether a critical pressure level has been exceeded or not achieved. An example of this type of application is pressure monitoring on a supply pump. When simple monitoring of a fixed value is required, pressure switches (*i.e.,* instruments that offer a binary/digital output directly related to a fixed pressure value) are also suitable. Pressure switches can be simple mechanical devices (often with a limited lifetime and low accuracy), or they can use electronic sensor technology, such as a pressure transmitter. The use of a pressure transmitter allows continuous pressure measurement, and can be helpful in other situations, such as leak detection. System leaks cause pressure to drop, and a pressure transmitter can help to detect such situations by tracking pressure levels over time. Critical-value monitoring can also be used to measure filter clogging by measuring pressures upstream or downstream of the filter to determine whether replacement is necessary.

Pressure control

Electronic pressure-measuring instruments can be employed in two types of pressure control: constant pressure control and control of a defined pressure profile.

Constant pressure control is advisable when the pressurized medium is supplied through pumps, or when the process itself causes unwanted pressure variations. To achieve constant pressure, the instrument sends continuous pressure measurements to an electronic controller, which checks whether and to what extent the current actual pressure deviates from the setpoint pressure. This information is then sent to a pump or valve controller, which adjusts the drive power or opening of the valve. This improves efficiencies in both control of the process and in energy consumption, since the pump uses only as much energy as is demanded.

Control of a defined pressure profile is used to ensure operation corresponding to a profile of values. Some chemical or physical processes require controlled increases and decreases in pressure that are dependent on time or other process parameters to ensure safe and efficient operation.

Typical applications include high-pressure pasteurization in the food industry, controlled polymerization in reactors, and pressure control in petrochemical refineries to optimize output. All of these processes require the intentional control of the pressure profile to ensure product quality.

Indirect measurement of process values

Pressure-sensing instruments are often used to indirectly determine three parameters: force, level, and temperature.

Indirect force measurement involves the use of pressure measurements to determine the amount of force generating the pressure. This is possible only when the system's geometry is known.

For example, in Figure 5, two movable pistons with different surface areas are in contact with hydraulic oil. If the smaller piston moves down, the pressure in the liquid remains constant and the larger piston is pushed up with a greater force.

A common pressure-measurement task in hydraulic systems is overload monitoring on a lifting gear. For example, when a crane lifts a load, the pressure required to generate the counteracting force in the hydraulic liquid increases. If the maximum permitted load is exceeded, the pressure will also exceed its upper limit. By measuring the pressure of the hydraulic fluid, it is possible to calculate the load torque limit.

Since many hydraulic applications are mobile (*e.g.,* forklifts, construction machinery, and agricultural vehicles), the instruments used to measure this pressure must be capable of withstanding shock, vibration, and electromagnetic interference. Additionally, these instruments must be resistant to oil, dust, mud, and fuel, as well as extreme temperatures, and should be sealed well since they are often attached to machines that are washed with high-pressure cleaners.

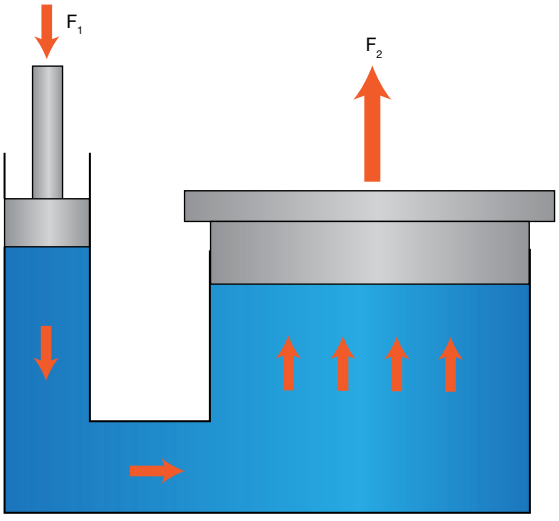

▲ **Figure 5.** In indirect force measurement, a system's known geometry can be used to calculate force based on pressure measurements. In this figure, two movable pistons are in contact with hydraulic oil. If the smaller piston moves down, the larger piston is pushed up with a greater force. Measuring the pressure exerted by the small piston allows the force to be calculated.

Indirect level measurement is possible because hydrostatic pressure under a static liquid column increases proportionately with the column's height. For example, pressure in a water tank increases 100 mbar for every meter of water depth; thus, water levels can be directly derived from pressure readings. The pressure-measuring instrument must be attached to the bottom of the tank's exterior (Figure 6) and exposed to interior pressure through an opening in the tank wall. Alternatively, submersible pressure transmitters (often referred to as level probes) can be dropped directly into the tank and provide the same functionality without drilling holes in the tank bottom.

If the tank is not vented or if it is under a pressure blanket, it is also necessary to measure the surface pressure above the liquid in the tank to determine hydrostatic pressure. This is done either by using two separate instruments and calculating the pressure differential in a downstream control unit, or by using a differential-pressure instrument that has two process connections and directly outputs the pressure difference between those as a signal.

A common application for indirect level measurement is automatic refilling of an empty (buffer) tank. An electronic pressure switch configured with both "tank is empty" and "tank is full" settings can automatically switch on and off a supply pump, and at the same time continuously indicate the current level.

Hydrostatic level-measurement devices must be resistant to the fluid and need to be sensitive to relatively small pressure changes. Submersible transmitters are submerged to depths of as much as several meters, and both the cable and the probe itself are in direct contact with the medium continuously. These instruments, particularly those installed in refineries and chemical plants, must often carry explosion-

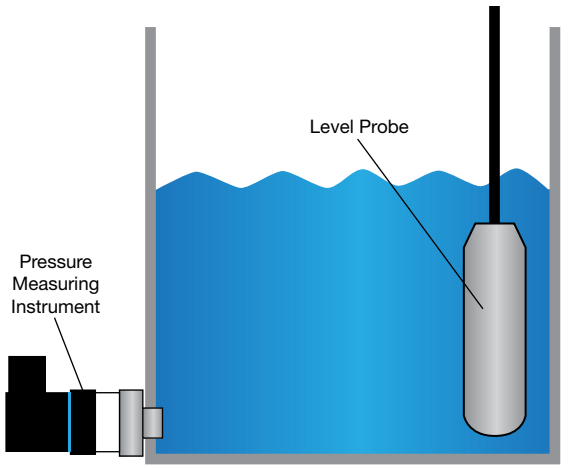

▲ **Figure 6.** The water level in a tank can be measured indirectly by a pressure sensor. Because the pressure of water increases 100 mbar for every meter of water depth, the water level can be derived based on pressure differences. Alternatively, a level probe can be used.

proof ratings and require high long-term stability. Devices designed for use in well, shaft, and bore-hole applications require slim designs and especially long, sturdy cables.

Indirect temperature measurement is typically used in refrigeration systems to monitor and control the evaporation and condensation of the refrigerant, but is also used in other chemical or physical processes.

In a typical refrigeration circuit (Figure 7), the refrigerant enters the compressor as a low-pressure gas. It is compressed, which increases its temperature, then leaves the compressor as a high-pressure gas. The hot gas flows through the condenser, where it condenses to a liquid, giving off heat. The liquid flows under high pressure to the expansion valve, which restricts the flow, lowering the fluid's pressure. The low-pressure liquid then enters the evaporator, where heat is absorbed, and the refrigerant changes from a liquid to a gas. The low-pressure refrigerant gas then moves to the compressor, and the cycle is repeated.

In a refrigeration cycle, pressure is typically measured both before and after the refrigerant passes through the compressor, which allows control of the expansion valve and the compressor, as well as the fans that dissipate heat in the condenser. In the expansion valve, targeted depressurization of the refrigerant can be used to control the cooling effect. The measured pressure can convey the state of the refrigerant, which controls the evaporation process, and can also help to prevent damage to the compressor by ensuring that the refrigerant is completely gaseous before it enters. If ventilators are used in the condenser, the power of the ventilator can be adjusted based on pressure measurements, to either speed up or slow down condensation.

Pressure-measurement instruments used in this process must be resistant to all common refrigerants and temperature extremes, as temperatures in refrigeration systems can vary between –40°C and 100°C. They must also be able to withstand condensation, the formation of ice, and vibration from the compressor.

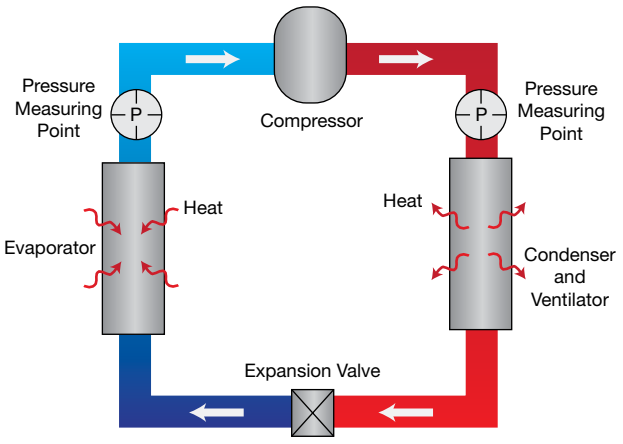

▲ **Figure 7.** In a typical refrigeration cycle, liquid absorbs heat when it changes from liquid to gas, and gas gives off heat when it condenses from gas to liquid. Pressure is typically measured both before and after the refrigerant passes through the compressor.

Closing thoughts

With hundreds — if not thousands — of different models of pressure sensors, transducers, and transmitters available, engineers are faced with a significant challenge in selecting the right instrument for the job. Picking the safe choice of a high-end, feature-rich, smart process transmitter may have been appropriate ten years ago when budgets were large and the number of measuring points small. Today's control systems are more advanced, and while the hunger for more data from more measuring points has increased, budgets have not.

Marketers may push the idea that only a certain measurement principle offers every advantage, but this tactic is often used to disguise the fact that the manufacturer has only mastered one principle and does not have products for the others. Purchasing departments sometimes try to commoditize sensors to leverage volumes and buying power, but this is far from ideal because no one instrument can be replaced by another without changes in certain specifications.

The choices are many, but the wise engineer understands the balance between price and value. You can spend $100, $1,000, or even more for basically the same function: to convert pressure into a standard output signal. The types of instruments discussed in this article, from bare sensors to smart process transmitters, span a large price range. Choosing the cheapest option may end up costing you much more in the future, but smart instruments are not always the smartest choice, either.

It pays to spend the extra time determining exactly what is required for the task at hand, discussing your options with manufacturers, and reading their literature carefully. If you are diligent in identifying the tasks and conditions for which you are selecting instruments, it will be much easier to make a financially sound choice — without overspending on something you don't need or underspending on an inferior or inappropriate device. CEP

EUGEN GASSMANN is a director of business development at WIKA Instruments (Email: eugen.gassmann@wika.com). He has more than 20 years of experience in the sales and marketing of industrial sensors, instrumentation solutions, and automation systems. He joined WIKA in 2007 to focus on pressure sensors. As the head of global product management, he restructured the company's global electronic pressure sensor portfolio. He is now applying this experience to help develop the North American market. Prior to joining WIKA, he worked for other global organizations, including Philips Electronics and Sartorius. Gassmann wrote the book *Electronic Pressure Measurement*, and he regularly speaks at industry conferences. He has a degree in electronics from the Univ. of Applied Science in Karlsruhe, Germany.

Understand the Basics of Membrane Filtration

Hua Wang
Hongyi Zhou
GE Global Research

Membrane filtration is an integral part of many industrial processes, as it is often more environmentally sustainable and cost-effective than other separation technologies.

Separation processes account for 40% to 70% of capital and operating costs in the chemicals industry *(1)*. Membrane-based separation technologies have a broad range of applications, including process water treatment, wastewater treatment and reuse, metal and catalyst recovery, solvent recovery, gas separation, and concentration of heat-sensitive biological macromolecules and proteins, among others *(2, 3)*.

This article compares some of the liquid-phase membrane technologies commonly used in the chemical process industries (CPI), and presents examples of membrane use in seawater and brackish water desalination, production of high-purity industrial process water, and protein separation.

Membrane terminology

A membrane is a semipermeable, or selectively permeable, barrier that allows some molecules or ions to cross it while hindering the passage of others. In membrane separation, a portion of fluid known as permeate (or filtrate) passes through the membrane, while other constituents are rejected by the membrane and retained in the retentate (or concentrate) stream (Figure 1).

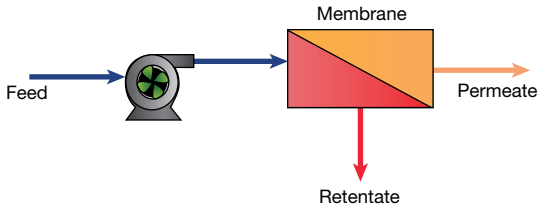

▲ **Figure 1.** In a membrane separation process, the permeate passes through the membrane while the retentate is rejected.

The transport of materials across a membrane requires a driving force. A chemical potential gradient provides the driving force for material transport from one side of a membrane to the other. The chemical potential gradient can come from a pressure difference, concentration difference, or temperature difference (Table 1). Material transport through ion exchange membranes by means of an electric potential via electrodialysis is also an important membrane separation technology but is outside the scope of this article *(4)*.

Synthetic membranes can be classified as microporous membranes or nonporous (dense) membranes according to

Table 1. The chemical potential gradient, or driving force, in membrane separation processes can arise from a pressure, concentration, or temperature difference.

Driving Force	Membrane Process
Pressure Difference	Reverse Osmosis, Nanofiltration, Ultrafiltration, Microfiltration
Concentration Difference	Pervaporation (PV)
Temperature Difference	Membrane Distillation (MD)

Table 2. Microporous and nonporous (dense) membranes employ different mechanisms of separation.

Morphology	Separation Mechanism	Membrane Process
Microporous	Size Exclusion	Ultrafiltration, Microfiltration
Nonporous (dense)	Solution-Diffusion	Reverse Osmosis, Nanofiltration, Pervaporation, Gas Separation

their structure and mechanism of separation (Table 2). Membrane separation can be further classified in terms of the size range of the permeating species.

Dead-end versus crossflow filtration. Membrane filtration can be accomplished in either dead-end flow mode or crossflow mode. In dead-end filtration, the feed stream moves perpendicular to the membrane surface, and it passes through the membrane as filtrate (Figure 2a). Particulates and aggregates rejected by the membrane form a filter cake, which reduces filtrate flux and increases feed pressure over time.

In crossflow — or tangential flow — filtration, the feed stream moves parallel to the membrane surface, and some portion of the feed stream passes through the membrane as permeate while the remainder of the feed stream becomes retentate for further processing or recirculation back to the feed (Figure 2b). The tangential (parallel) feed stream continuously sweeps across the membrane surface, which prevents the buildup of particulates and aggregates and maintains a more steady permeate flux and low transmembrane pressure.

Most large-scale industrial filtration processes operate in crossflow filtration mode.

Pressure-driven membrane separation

The most widely used membrane separation technologies are pressure-driven processes — reverse osmosis (RO), nanofiltration (NF), ultrafiltration (UF), and microfiltration (MF). Figure 3 and Table 3 compare the characteristics of these processes, and Table 4 lists some common applications.

Reverse osmosis. RO employs the tightest membranes for liquid separation. Dissolved salts, inorganic solutes, and organic solutes with a molecular weight greater than approximately 100 Dalton (Da) are rejected by RO membranes; water is able to pass through RO membranes. Rejection of dissolved salts such as sodium chloride by RO membranes is typically 95–99.8%. The operating pressures of RO processes are typically in the range of 100–1,000 psi. Examples of RO membrane applications include brackish water and seawater desalination and the production of high-purity process water for industrial applications.

Nanofiltration. NF removes multivalent ions and small molecules in the nanometer range (*e.g.,* sulfate ions, sugars). NF membranes can fractionate small compounds, such as salts and small organic molecules, and are commonly used to permeate monovalent ions while retaining divalent ions. In NF processes, salts with divalent anions (*e.g.,* sulfate) have rejection rates in the range of 90% to more than 99%, while salts with monovalent anions (*e.g.,* sodium chloride) have rejection rates of 20–80%. Solvent-resistant NF membranes are also used to separate organic compounds in an organic solvent. The operating pressures of NF processes are typically in the range of 50–225 psi.

Both RO and NF membrane processes are governed by the solution-diffusion transport mechanism, where the permeating species first dissolve into a membrane and then diffuse through it. Because of the nonporous nature of these membranes, RO and NF membranes are operated at signifi-

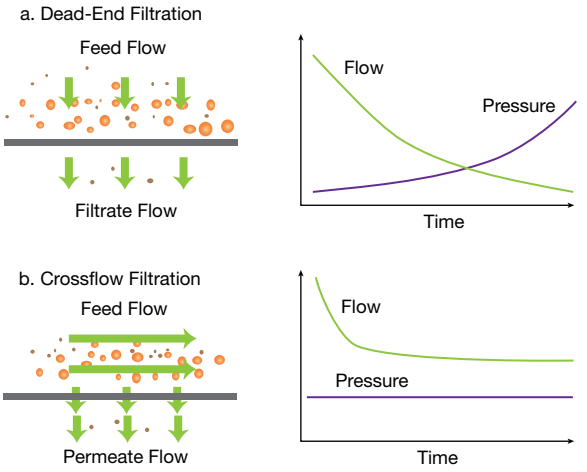

▲ **Figure 2.** In dead-end filtration, the process stream flows through the membrane, whereas in crossflow filtration, the flow is parallel (tangential) to the membrane surface.

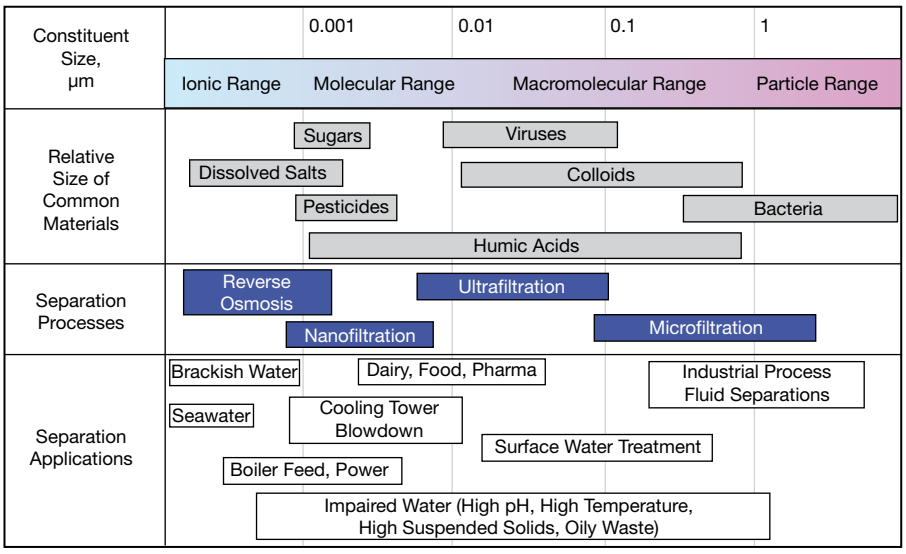

▶ **Figure 3.** The spectrum of pressure-driven membrane separation processes as a function of constituent size.

Table 3. Characteristics of commercial pressure-driven membranes *(7)*.				
	Reverse Osmosis	**Nanofiltration**	**Ultrafiltration**	**Microfiltration**
Membrane	Asymmetric, Thin-Film Composite	Asymmetric, Thin-Film Composite	Asymmetric	Symmetric, Asymmetric
Pore Size	Nonporous	Nonporous	0.002–0.1 μm	0.1–10 μm
Total Thickness	150 mm	150–250 mm	150–250 mm	10–150 mm
Thin Film	1 mm or less	1 mm or less	—	—
Rejected Components	HMWC, LMWC, Sodium Chloride, Glucose, Amino Acid	HMWC, Mono-, Di-, and Oligosaccharaides, Multivalent Ions	Macromolecules, Proteins, Virus, Polysaccharides	Particles, Clay, Bacteria
Membrane Material(s)	Polymeric (thin-film composite and integrally skinned)	Polymeric (thin-film composite and integrally skinned)	Polymeric, Ceramic	Polymeric, Ceramic
Membrane Module	Spiral-Wound, Plate-and-Frame	Spiral-Wound, Plate-and-Frame	Spiral-Wound, Hollow-Fiber, Plate-and-Frame	Hollow Fiber
Operating Pressure	5–84 bar (100–1,000 psi)	3.5–16 bar (50–225 psi)	1–7 bar (15–100 psi)	0.7–3.5 bar (10–50 psi)

HMWC: high-molecular-weight components (*e.g.,* protein molecules). LMWC: low-molecular-weight components (*e.g.,* NaCl).

Table 4. Membrane separation is used in a wide range of commercial applications *(7)*.			
	Feed	**Permeate**	**Concentrate**
Reverse Osmosis	Water	Low-salinity water	Salty water
	Whey	Low-BOD permeate	Whey concentrate
	Dyeing effluent	Clean water	BOD, salt, chemicals, waste products
Nanofiltration	Water	Softened water	Waste product
	Antibiotics	Salty waste product	Desalted, concentrated antibiotics
	Whey	Salty wastewater	Desalted whey concentrate
	Dyeing effluent	Clean, salty water	BOD/COD, color
Ultrafiltration	Water	Clarified water	Waste product
	Oil emulsion	Oil-free water (≤10 ppm)	Highly concentrated oil emulsion
	Enzymes	Waste product	High-value product
	Washing effluent	Clarified water	Dirty water (waste product)
	Bio-gas waste	Clarified liquid for discharge	Microbes to be recycled
	Milk	Lactose solution	Protein concentrate for cheese production
	Antibiotics	Clarified fermentation broth	Waste product
	Carrageenan	Waste product	Concentrated carrageenan
Microfiltration	Water	Clarified water	Waste product
	Fruit juice	Clear juice	Waste product (suspended solids, micro-organisms, and undesirable proteins)
	Wine	Clear wine	Waste product (fine fruit particles, spent yeast, bacteria, soil, debris, and fining agents)
	Therapeutic proteins	High-value product	Waste product
	Amino acid	Clarified fermentation broth	Waste product

Biological oxygen demand (BOD): a measure of the amount of oxygen that is consumed by bacteria during the decomposition of organic matter. Chemical oxygen demand (COD): a measure of the amount of oxygen that is consumed in the chemical decomposition of organic matter and oxidation of inorganic matter. Both BOD and COD are standard methods for indirect measurement of the amount of contaminants (that can be oxidized biologically or chemically) in a wastewater sample.

Article continues on next page

cantly higher pressures than the more-porous UF and MF membranes.

Ultrafiltration. UF membranes are commonly used to retain relatively large dissolved materials (*e.g.,* proteins, starches) and suspended solids (*e.g.,* colloids, viruses) while allowing salts and smaller dissolved organic compounds to permeate. UF membranes are typically classified by their ability to retain components of specific sizes dissolved in a solution. This is referred to as the molecular weight cut-off (MWCO), which is defined as the smallest molecular weight at which at least 90% of the solute is retained by the membrane. UF membranes generally have MWCO values between 1,000 and 300,000 Da and pore diameters in the range of ≤10 nm to 0.1 µm *(5, 6)*. UF membrane processes are widely used in biopharmaceutical protein separation, virus clarification, and whey protein concentration and isolation in the dairy industry. UF processes typically operate at pressures ranging from 15 to 100 psi.

Microfiltration. MF is a process by which suspended solids and large colloids are rejected, while dissolved solids and macromolecules pass through the membrane. MF membranes are suitable for the removal of total suspended solids (TSS), flocculated materials, and bacteria. Many membrane manufacturers rate their MF membranes according to nominal pore sizes, which are in the range of approximately 0.1–10 µm. MF processes operate at very low pressure, typically 10 psi or less.

Most microporous membranes tend to have highly nonuniform pores with a broad pore size distribution. Thus, MWCO and nominal pore size are only guidelines for membrane selection. Other important factors for choosing membranes include molecular shape, electrical charge, sample composition and concentration, and operating conditions. Therefore, it is important to perform pilot experiments with real feed streams to verify membrane performance.

Table 5. Commonly used polymers for membrane separation processes.

Polymer	Membrane Type
Polyamide	RO, NF, UF, MF
Cellulose acetate (CA)	RO, UF, MF
Polysulfone (PS)	UF, MF
Polyether sulfone (PES)	NF, UF, MF
Polyvinylidene fluoride (PVDF)	UF, MF
Polyimide (PI)	NF
Polyetherimide (PEI)	UF, MF, GS
Polyethylene (PE)	UF, MF
Polypropylene (PP)	UF, MF
Polyacrylonitrile (PAN)	UF, MF, PV
Polyethylene terephthalate (PET)	MF
Polydimethylsiloxane (PDMS)	NF, PV, GS

GS: gas separation. PV: pervaporation.

Membrane materials, structure, and morphology

Synthetic membranes are fabricated from a variety of materials, including both organic and inorganic materials such as metals, polymers, and ceramics. Ceramic and metal membranes can be employed in separations where aggressive media (*e.g.,* acids, strong solvents) are present. They also have excellent thermal stability, which makes them suitable for high-temperature operations *(7, 8)*.

Polymeric membranes dominate the market because they are less expensive and more versatile than inorganic membranes. They are typically formed by coating a thin polymer layer on a porous backing or support to create a combination that provides high permeability, selectivity, mechanical strength, and chemical stability. Table 5 provides a list of the most commonly used polymers for commercial membranes. Desired membrane properties include high porosity (MF/UF), narrow pore size distribution (MF/UF), sharp MWCO (UF), high mechanical strength and flexibility, high pH and chemical stability, desired surface properties (*e.g.,* surface charge and hydrophilicity/hydrophobicity balance), low fouling tendency, and low cost.

Membranes can be classified according to structure, morphology, and application. The principal structures and morphologies of commercial pressure-driven membranes are shown in Figure 4.

Symmetric membranes. Only a few commercially available membranes are symmetric throughout their thickness.

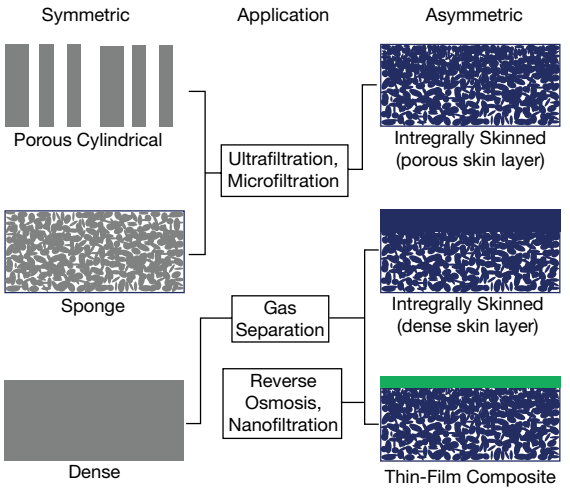

▲ **Figure 4.** Membrane structures may be symmetric or asymmetric. Membrane morphologies include porous cylindrical, sponge, and dense (symmetric); and integrally skinned and thin-film composite (asymmetric) *(10)*.

Expanded polytetrafluoroethylene (ePTFE), polyethylene (PE), and polypropylene (PP) are examples of microporous symmetric membranes.

Asymmetric membranes. Most commercially available membranes are asymmetric. An asymmetric membrane has either a thin microporous or dense permselective layer supported by a more-open porous substrate. The skin layer and its substrate may be formed in a single operation (*e.g.,* integrally skinned) or separate steps.

Composite membranes, a subset of asymmetric membranes, are comprised of a permselective skin layer and a microporous support layer made from different polymers. The skin layer determines the membrane separation performance while the open support layer provides mechanical support.

A cellulose acetate RO membrane is an example of an integrally skinned asymmetric membrane where both the dense permselective layer and microporous support layer are formed of cellulose acetate in a single-phase inversion operation *(5, 7)*. A polyamide RO membrane is an example of a thin-film composite membrane where a thin (100–200 nm) crosslinked polyamide permselective skin layer is formed on a microporous polysulfone UF support *(5, 9)*. The vast majority of commercial RO and NF processes use composite membranes because they allow high water fluxes.

Membrane format and module design

Membrane filtration employs several different membrane formats (*e.g.,* flat sheets and hollow fibers) and a wide variety of module designs (*e.g.,* cassette, cartridge, and spiral-wound). Membrane format and module design are closely related. For example, flat-sheet membranes are suitable for cassette and spiral-wound modules, whereas hollow-fiber membranes are ideal for cartridge modules. Each module design has specific hydrodynamics and is suitable for certain commercial applications based on factors such as process flux, rejection, specific surface area, and operating costs. Table 6 compares the cassette, cartridge, and spiral-wound module designs *(6, 9, 13)*, and the following paragraphs discuss these crossflow modules in more detail. Additional discussion on these modules can be found in Refs. 10–13.

Cassette modules. Membrane cassettes, which are used for MF and UF, have a complex plate-and-frame assembly of flat sheets of membranes, gaskets, spacers, and flow manifolds (Figure 5). The membrane performs the actual filtration and the gaskets provide a tight seal to separate the feed, permeate, and retentate streams. The presence of the spacers introduces turbulence in the feed stream, which would otherwise be laminar flow due to long (6–60 cm) and narrow flow channels. The flow turbulence promotes local mixing and effective mass transport, which disrupts concentration polarization (*i.e.,* formation of a gel layer) and improves process flux. However, membrane cassettes with spacers are prone to particulate plugging and are difficult to clean.

Cartridge modules. Membrane cartridges for MF, UF, or

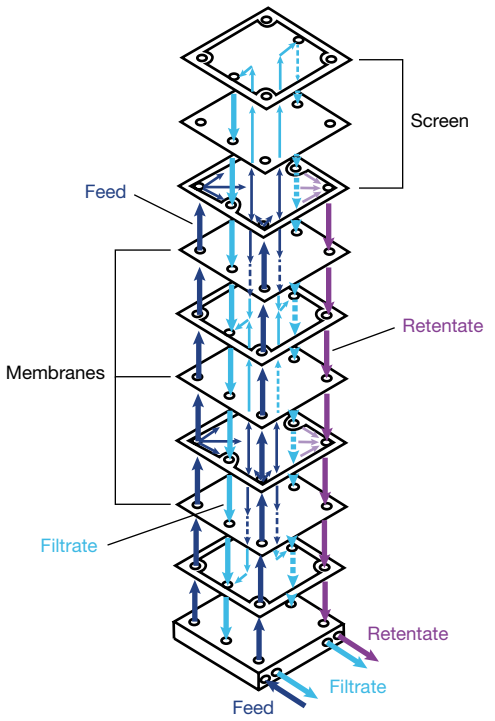

▲ **Figure 5.** Membrane cassettes have a complex plate-and-frame assembly of flat sheets of membranes, gaskets, spacers, and flow manifolds *(11)*.

Table 6. Crossflow filtration module configurations include flat-sheet cassettes, hollow-fiber cartridges, and spiral-wound modules.

	Flat-Sheet Cassette	Hollow-Fiber Cartridge	Spiral-Wound Module
Flow Channel	Narrow (0.03–0.5 cm)	Narrow (0.02–0.25 cm)	Narrow (0.03–0.1 cm)
Crossflow Velocity	2–3 m/s	0.5–2.5 m/s	0.5–1.5 m/s
Reynolds Number	>10,000	500–3,000	500–1,000
Packing Density	Low (300 m^2/m^3)	High (1,200 m^2/m^3)	High (600 m^2/m^3)
Energy Cost	Moderate	Low	Low
Ease of Cleaning	Good	Fair	Poor to Fair
Holdup Volume	Moderate	Low	Low
Particulate Plugging	Moderate	Fair	Very High

NF are produced by potting a large number of hollow-fiber membranes in a cylindrical housing with permeate ports and end caps (Figure 6). Since hollow-fiber membranes are self-supporting, the cartridge has very high packing density, and therefore has a high surface-area-to-volume ratio. For example, a cartridge with a 3-in.-dia. housing could contain more than 3,000 hollow fibers. Such a cartridge also has very little dead volume, making it ideal for product recovery. The fibers (or lumens) in a hollow-fiber membrane typically have a small diameter (0.2–2 mm) and a length between 10 and 60 cm, which creates laminar flow during the filtration process. It is possible (but not typical) to promote flow disturbance to improve local mixing for effective mass transport inside the lumen. Cartridges have flexible surface areas; the surface area can be changed by varying the fiber length and the number of fibers. Hollow-fiber cartridges can be operated either with feed flow through the lumen (inside the hollow fiber) and permeate collection from the shell (inside-out), or with feed flow from the shellside and permeate collection from the lumen (outside-in). Inside-out filtration is preferred based on fluid hydrodynamics, while outside-in filtration is used when back flushing is needed to clean the membrane.

Spiral-wound modules. Spiral-wound membrane modules are used predominantly for RO. They are composed of a multilayer assembly of flat sheet membranes and spacer screens, and are constructed by rolling the assembly around a perforated tube and sealing the membrane/spacer layers on three sides (Figure 7). Spiral-wound modules may have additional reinforcement (*e.g.,* they can be wrapped with fiberglass) to ensure safety during high-pressure filtration. The spacer screens are thin, usually between 0.3 and 1.0 mm, to ensure high packing density. Most industrial RO systems are large-scale continuous operations involving many RO modules connected in parallel.

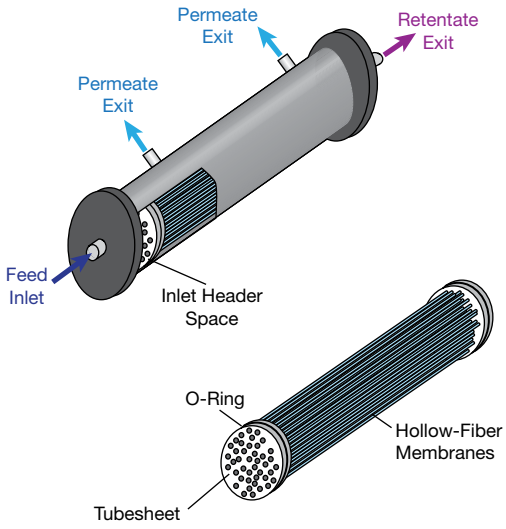

▲ **Figure 6.** Membrane cartridges contain a large number of hollow fibers in a cylindrical housing with permeate ports and end caps *(12).*

Common membrane applications

Seawater desalination by reverse osmosis. In regions with limited freshwater resources, membrane desalination has increasingly become a cost-effective option to turn seawater into potable and process water for residential, commercial, and industrial use. Impurities that need to be removed from seawater include salts, organic substances, algae, bacteria, and suspended particles.

Figure 8 shows a typical RO membrane seawater-desalination process. A pretreatment system comprised of flocculation, sedimentation, and media filtration cleans up the seawater by removing TSS and dissolved organic carbon (DOC) prior to RO membrane desalination. The RO desalination unit removes total dissolved solids (TDS) and salts (*e.g.,* NaCl, $MgSO_4$). The RO-purified water then goes through post-treatment steps, including pH adjustment, remineralization, and disinfection, to meet potable water standards before it is used by industrial, commercial, or residential customers.

Industrial water treatment. High-purity water is required for boiler feedwater and cooling tower water, as well as for process water in the electronic, medical, and pharmaceutical industries, among others. Impurities in process water can jeopardize critical and expensive equipment as well as the operational efficiency of an entire plant. For example, total organic carbon (TOC) in make-up water breaks down to lower-molecular-weight, corrosive organic acids at the high temperatures and pressures experienced in steam generators in power plants.

Figure 9a shows an example of a conventional boiler

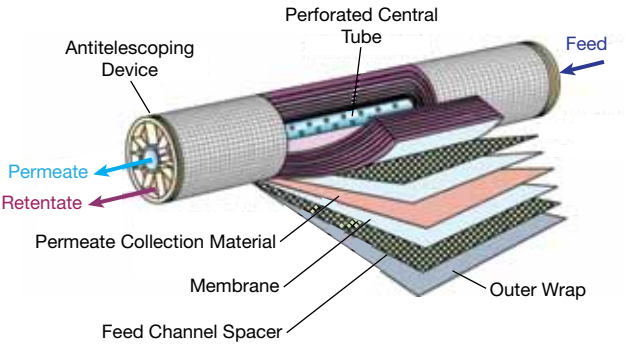

▲ **Figure 7.** Spiral-wound membrane modules are constructed by rolling a multilayer assembly of flat-sheet membranes and spacer screens around a perforated tube and sealing the membrane/spacer layers on three sides.

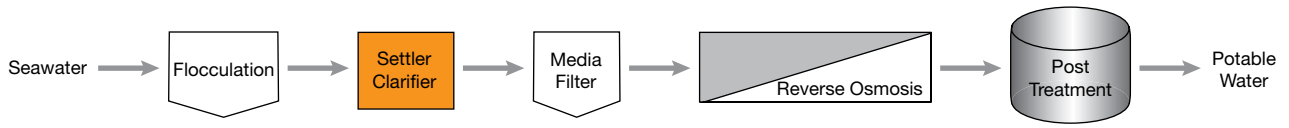

▲ **Figure 8.** Reverse osmosis is a common seawater desalination technology.

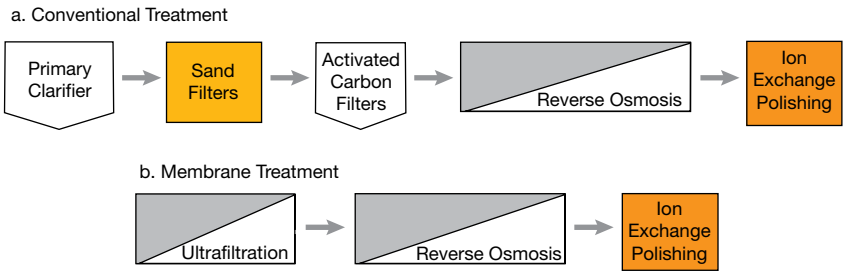

▲ **Figure 9.** Conventional boiler feedwater treatment (a) involves more steps than the hollow-fiber UF and RO water treatment process (b).

water treatment process that includes clarification and sand filtration to remove TSS, carbon adsorption to remove TOC, RO membrane filtration to remove TDS, and ion exchange to remove any remaining contaminants. In Figure 9b, a simplified UF and RO membrane process treats the boiler water. A hollow-fiber UF pretreatment step reduces the concentrations of suspended solids and organics, and is followed by an RO membrane filtration step. After a final ion exchange polishing step, the purified water is suitable for use as boiler feedwater. The integrated UF/RO membrane process is a compact design that can minimize land costs, construction costs, and operating costs.

Biopharmaceutical manufacturing. Biopharmaceutical processing includes upstream (cell culturing in a bioreactor or fermenter) and downstream (recovery, purification, and concentration of biological products) operations, as shown in Figure 10. After upstream processing, the desired product is typically in a complex mixture of unwanted cellular debris and remnants of the cell culture medium, and it is necessary to both concentrate the product and remove the impurities, while maintaining the potency of the delicate therapeutic product. The impurities that need to be removed vary widely in their physicochemical properties, and include host-derived impurities (*e.g.,* host proteins, DNA), product-related substances (*e.g.,* degraded, misfolded, cleaved, or oxidized product), and process-related impurities (*e.g.,* dye chromatography ligands, acetonitrile), as well as any adventitious agents (*e.g.,* bacteria, mycoplasmas, viruses) that may be present. Membranes are very attractive in downstream processing for purification, sterile filtration, concentration, and final formulation *(14, 15)*.

Sterile microfiltration has widespread use in bioprocessing, for streams ranging from cell cultures to buffers to final products. Microfiltration membranes typically have pore size ratings of 0.45 µm, 0.2 µm, and 0.1 µm, with the larger pore sizes providing higher flux rates or requiring a smaller membrane area. The performance of a sterile filter is rated by its log reduction value (LRV), which is defined as the logarithm of the ratio of bacteria concentration in the feed to the bacteria concentration in the filtrate ($LRV = \log[C_{feed}/C_{filtrate}]$). An LRV greater than 10^7 is usually required to ensure sterility. There is a strong correlation between membrane pore size and LRV — the smaller the pore size, the higher the LRV. Membranes are commonly used in a pleated format in dead-end filtration mode to maximize membrane capacity.

Ultrafiltration is often used for intermediate buffer exchange and final product concentration. These membranes typically have pore sizes in the range of 1 kDa to 300 kDa. Ultrafiltration membranes are highly asymmetric; they have tight surfaces with small pores to provide the separation capability, and large pores through the rest of the membrane thickness to maximize flux. Crossflow filtration with flat-sheet cassettes dominates this application, although hollow-fiber cartridges are sometimes used. Membrane performance is typically characterized by the product retention coefficient, which is defined as one minus the ratio of product concentration in the filtrate to product concentration in the feed ($1 - C_{filtrate}/C_{feed}$). Low process flux and membrane area are the tradeoffs for high retention — to achieve high flux, a

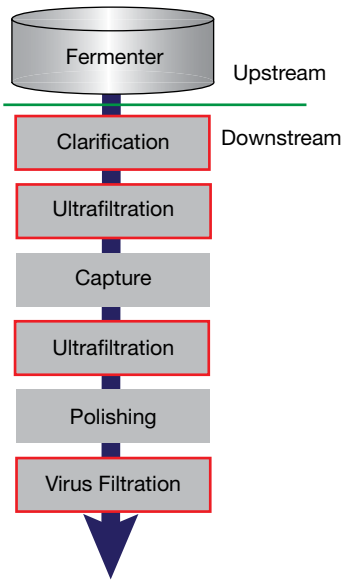

▶ **Figure 10.** A typical bioprocess consists of an upstream fermenter followed by multiple downstream separation steps. Membrane processes may be used for the operations outlined in red — clarification (often a combination of centrifugation and microfiltration), ultrafiltration, and virus filtration.

Article continues on next page

large membrane is necessary, which reduces retention.

Virus filtration is a special case of ultrafiltration, where the goal is to remove any viral contaminants from the final products. Although virus filtration operates in the ultrafiltration range based on membrane pore size, it has special requirements for pore size distribution. A virus filtration membrane must have a narrow pore size distribution for maximum virus removal and minimum product loss — this is challenging due to the small difference between the product size and the size of viruses. Another unique characteristic of virus filtration is that, unlike most UF processes, it is typically operated in dead-end filtration mode to maximize membrane capacity.

Final thoughts

Membrane technology is an established part of many industrial separation processes. Membrane processes typically do not involve phase changes or chemical additives, and are often more environmentally sustainable and have lower energy costs than other separation technologies, such as distillation and crystallization. They are modular, easy to scale up, and simple in concept and operation.

In the design of an effective membrane separation process, the first steps are to determine the separation goal (*e.g.,* clarification, concentration, fractionation, and/or purification) and to characterize the composition of the feed streams (*e.g.,* nature and loading of suspended solids, and molecular composition and concentration of the dissolved species). Next, work closely with membrane suppliers to select the appropriate membrane type (RO, NF, UF, or MF), membrane format (flat-sheet or hollow-fiber), and module design (cassette, cartridge, or spiral wound) for the specific application to achieve the highest yield of the desired product(s). Ensure the chemical compatibility between the feed liquid and membrane, and assess the membrane-fouling propensity. The chemical and thermal stability and fouling resistance are especially important for membranes deployed in more-challenging separation applications and in harsh environments (*e.g.,* oily water, nonaqueous organic solvents, high temperature, and extreme pH).

In addition, it is important to perform pilot experiments with real feed streams and the selected membrane material and module design to establish the optimum operating parameters (*e.g.,* dead-end or crossflow filtration, batch or continuous operation, membrane flux, and pressure drop) and to ensure process reproducibility with the desired product quality. Pilot studies also help quantify the degree of membrane fouling, effectiveness of a membrane cleaning regimen, and membrane lifetime under repeated cycles of usage and cleaning. Finally, it is important to perform engineering and economic analyses to determine the capital investment and operating costs. CEP

HUA WANG is a senior chemical engineer at GE Global Research (Niskayuna, NY; Phone: 518-387-4147; Email: wanghua@ge.com). He has over 20 years of industrial and academic experience in the areas of membranes and separation, polymer materials and processing, and transport of complex fluid systems. He received his PhD in chemical engineering from the Univ. of Colorado at Boulder, and did his postdoctoral work at Massachusetts Institute of Technology. At GE Global Research, he has worked on a variety of R&D projects for GE's water, energy, healthcare, and plastics businesses.

HONGYI ZHOU is a principal scientist in the Engineered Materials Chemistry and Physics Technology Organization at GE Global Research (Niskayuna, NY; Phone: 518-387-5143; Email: zhouh@ge.com). He has more than 20 years of industrial and academic experience in the design and development of complex materials and systems. He received his PhD in polymer engineering and science from Virginia Polytechnic Institute. At GE Global Research, he has worked on a wide variety of R&D projects for GE Healthcare, GE Power & Water, and GE Plastics.

Literature Cited

1. **Humphrey, J. L., and G. E. Keller,** "Separation Process Technology," McGraw-Hill, New York, NY (1997).
2. **Nunes, S. P., and K. V. Peinemann, eds.,** "Membrane Technology in the Chemical Industry," Wiley-VCH, Weinheim, Germany (2001).
3. **Pebby A. K., *et al.*, eds.,** "Handbook of Membrane Separations. Chemical, Pharmaceutical, Food, and Biotechnology Applications," CRC Press, Boca Raton, FL (2009).
4. **Strathmann, H.,** "Electrodialysis, a Mature Technology with a Multitude of New Applications," *Desalination,* **264**, pp. 268–288 (2010).
5. **Baker, R. W.,** "Membrane Technology and Applications," 2nd ed., Wiley, Hoboken, NJ (2004).
6. **Zeman, L. J., and A. L. Zydney,** "Microfiltration and Ultrafiltration — Principles and Applications," Marcel Dekker, Inc., New York, NY (1996).
7. **GE Osmonics,** "Membrane Filtration Handbook — Practical Tips and Hints," 2nd ed., www.gewater.com/pdf/1229223-%20Lit-%20Membrane%20Filtration%20Handbook.pdf (2001).
8. **Mallada, R., and M. Menéndez,** "Inorganic Membranes: Synthesis, Characterization and Applications," *Membrane Science and Technology,* Vol. 13, Elsevier Science, Amsterdam, The Netherlands (2008).
9. **Li, N., *et al.*, eds.,** "Advanced Membrane Technology and Applications," Wiley, Hoboken, NJ (2008).
10. **Pinnau, I., and B. D. Freeman, eds.,** "Membrane Formation and Modification," ACS Symposium Series 744, Washington, DC (2000).
11. **Mohanty, K., and M. K. Purkait, eds.,** "Membrane Technologies and Applications," CRC Press, Boca Raton, FL (2011).
12. **Friedman, D. R.,** "Ultrafiltration Apparatus," U.S. Patent 4,715,955 (1987).
13. **Purchas, D. B., and K. Sutherland,** "Handbook of Filter Media," 2nd ed., Elsevier, New York, NY (2002).
14. **Peinemann, K. V., and S. Pereira-Nunes, eds.,** "Membranes for Life Sciences," Vol. 1, Wiley-VCH Verlag GmbH & Co., Weinheim, Germany (2008).
15. **Lee, T., and T. D'Amore,** "Membrane Separation Theoretical and Applicable Considerations for Optimum Industrial Bioprocessing," *Journal of Bioprocessing and Biotechniques,* **1** (2), pp. 1–8 (2011).

Flame Arresters
The Last Line of Defense

Matthew B. Barfield, P.E.
Fike Corp.

Flame arresters are designed to prevent catastrophe. How do they work, and which type is right for your application?

The unassuming process-safety devices installed in flare lines, on flammable-liquid storage tanks, in vapor-control systems, and on processing vessels at your plant are called flame arresters. They may even be hiding in plain sight every day on your commute. At your local gas station, for example, the small threaded components at the ends of the underground gas tank-venting lines are likely end-of-line atmospheric deflagration flame arresters rated for National Fire Protection Agency (NFPA) Group D vapors.

Flame arresters comprise a diverse array of safety devices, ranging from small, end-of-line units with threaded connections to massive, custom-built flanged behemoths weighing several tons. They are available with different element designs, housing shapes, and materials of construction to handle various deflagration and detonation explosions, vapor (or explosion) groups, installation positions, operating pressures and temperatures, and allowable burn times. The sheer magnitude of options and configurations can be daunting to the novice user or rookie engineer. However, all flame arresters have the same purpose: to protect people and property from the impact of a safety event that is already in progress, and to serve as the last line of defense against a tragic accident.

Regular maintenance, including frequent inspections, cleaning, and occasional part replacement, is critical to ensure the long-term functionality of flame arresters. Despite their rugged appearance, the guts of flame arresters can be quite fragile. Maintenance staff must be especially careful to avoid damaging internal elements. A dropped wrench or hammer can irrevocably damage a flame arrester.

While many engineers are exposed to the basics of relief valve sizing, combustion, explosions, and other process safety fundamentals, flame arrester theory and application criteria are not typically included in courses or training. To novice engineers, flame arrester functionality and application principles can seem like a mysterious black box.

Because engineers and other personnel are often unfamiliar with flame arrester fundamentals, misapplication is quite common. This article covers the basics of flame arresters to help prevent misapplications, which can have catastrophic results.

What is a flame arrester?

Flame arrester is an umbrella term that covers numerous subdivisions of devices that are used in various applications (Figure 1). Simply using the general term when procuring or specifying a flame arrester may not provide enough detail to define the necessary unit. Several definitions have been proposed to describe a flame arrester, including:

- a device that prevents the transmission of a flame through a flammable gas/air mixture by quenching the flame on the surfaces of an array of small passages through which the flame must pass *(1)*
- a passive device designed to prevent propagation of gas flames through a pipeline *(2)*
- a device fitted to the opening of an enclosure or to the connecting piping of a system of enclosures and whose intended function is to allow flow but prevent the transmission of flame from either a deflagration or detonation *(3)*.

In general, a flame arrester is comprised of an outlet housing or weather hood, an inlet housing, and a center section, which contains the flame-extinguishing elements

(Figure 2). Design and construction of these elements includes an effective quenching diameter, typically expressed as the hydraulic diameter, as well as a quenching distance, or length that a flame would travel within the element matrix. Quenching diameter and quenching distance influence the arrester's flame quenching ability and resistance to flow.

The flame arrester element (Figure 3) can be manufactured using various methods, depending on the element structure. The most common element structure is a repeating pattern of spiral-wound, crimped metal ribbons made by weaving alternating layers of corrugated metal ribbon and flat metal ribbon around a mandrel to form a cylindrical assembly of regularly spaced triangular gaps of uniform size. The height and width of the triangular cells can be varied to provide the required quenching diameter, and the assembly can be manufactured to tight dimensional tolerances.

Other element types include metal mesh, gauze, and shot; ceramic balls; stacked parallel plates; and perforated plates; as well as packed beds that can contain metal pebbles, Raschig and Pall rings (named for their manufacturers), or other packings. Each of these element types has its own advantages, disadvantages, and application limitations, but all arresters containing these element structures can be loosely categorized as static dry flame arresters, which are the focus of this article.

The article does not cover hydraulic (liquid) seal arresters, high-velocity vent valves (or dynamic flame arresters), and flame arresters that are combined with breather valves. These types have unique purposes, applications, and functioning principles, and their application in industry is much less common than static dry flame arresters.

How do flame arresters work?

Flame arresters are a simple and elegant process safety solution that prevents flame propagation within pipes or into tanks. The passive devices have no moving parts and do not require external power, sensors, logic controllers, wiring, or manual operation to function.

Combustion reactions require fuel, oxygen, and an

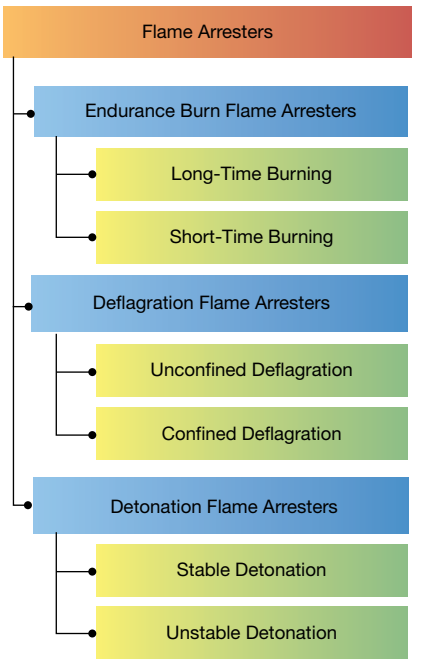

◀ **Figure 1.** When specifying a flame arrester, use the appropriate terminology to ensure you purchase the correct arrester type.

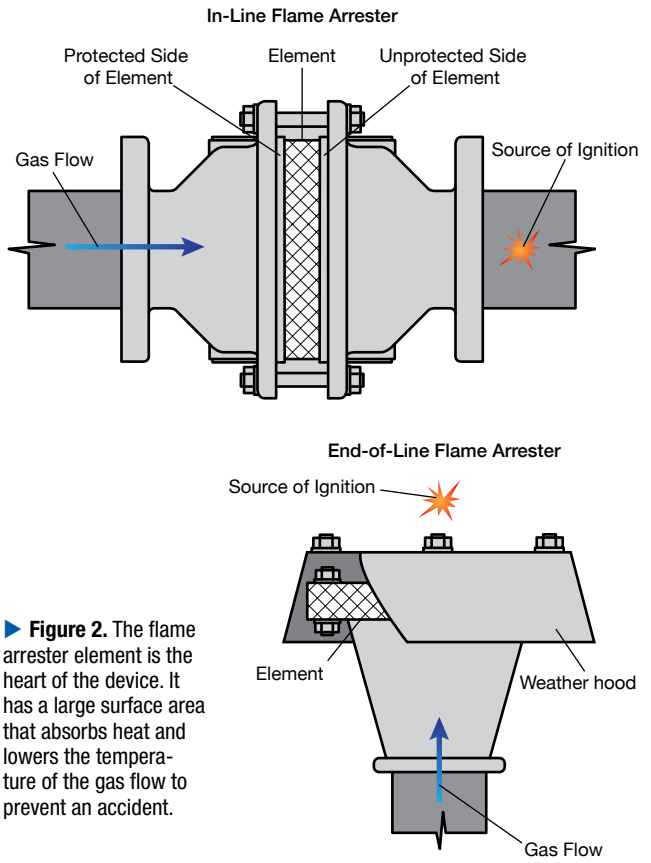

▶ **Figure 2.** The flame arrester element is the heart of the device. It has a large surface area that absorbs heat and lowers the temperature of the gas flow to prevent an accident.

▶ **Figure 3.** The large surface area of the element helps to absorb and distribute heat. Image courtesy of PROTEGO.

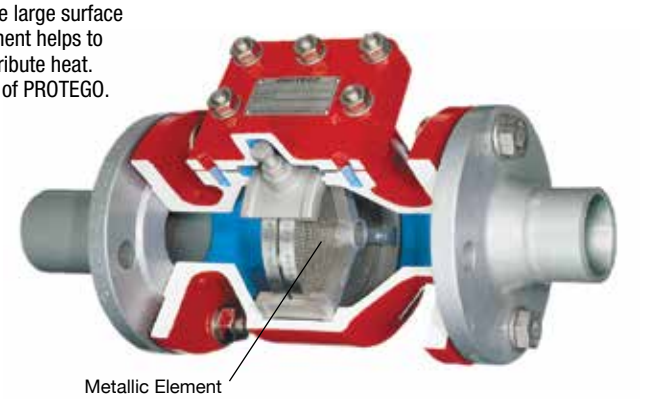

ignition source (Figure 4). If a rapid, self-propagating, exothermic combustion reaction occurs, a flame arrester can terminate the reaction by removing one side of the flammability triangle *(4)*. When a flame front flows through a flame arrester, the internal element removes the heat component, which terminates the reaction. Enough heat is removed to both extinguish the flame and prevent reignition of the hot gas on the protected side of the arrester.

The arrester works like a massive heat sink or a very swift heat exchanger. By forcing the flame to pass through an array of small passageways, it divides the frontal area of the flame into small flamelets. Within the array, heat is efficiently extracted from the sides of the flamelets. The surface-area-to-volume ratio within the element section is enormous, which encourages rapid heat transfer.

The metallic surfaces within the apertures of the element matrix absorb the heat of the reaction and the free radicals, creating an exponentially expanding boundary layer as the flame propagates through the element. As the flame front and hot gases pass through the element, the large thermal mass and specific heat of the element materials help to keep surface temperatures relatively steady. If the arrester element has a small enough quenching diameter and a long enough quenching distance, the boundary layer will expand to a point where it extracts heat to the element surfaces faster than the rate at which heat is produced by the combustion reaction. The flame front is starved of the activation energy necessary for further ignition, and therefore, self-propagation, which extinguishes the flame.

A small quenching gap is not sufficient to terminate the combustion reaction, particularly for high-velocity detonation flames. After the flame is extinguished, the gases are still hot and must be cooled further to avoid reignition on the outlet side. The quenching distance has a secondary cooling effect that lowers the gas temperature below the autoignition temperature of the fuel.

Momentum dispersion effects provided by the element or by carefully designed housing features also help to prevent reignition by slowing the gas stream and reducing the dynamic pressure, which allows for more cooling time. This is an area of interest for optimization in the research and development of flame arrester technology. By using thoughtfully designed shock absorbers or momentum attenuators to slow the flame front, the same flame extinguishing functionality can be achieved with less quenching distance and/or larger quenching diameters, both of which reduce the overall pressure drop during normal operations.

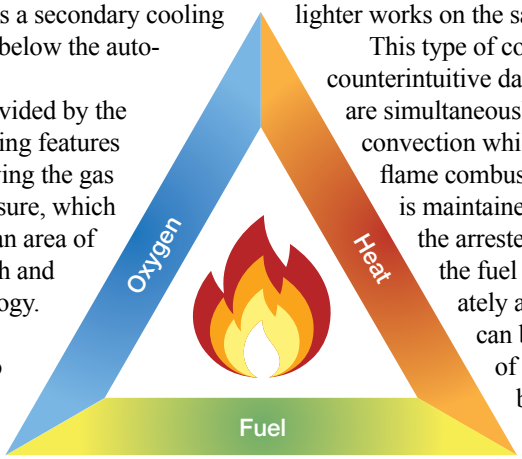

▲ **Figure 4.** A self-sustaining combustion reaction requires an oxidant source (typically oxygen in the air), an ignition source (or heat), and a fuel source. At normal pressure and temperature conditions, removing one side of the fire triangle prevents a combustion reaction from occurring.

When all of these effects combine, the stream exiting the flame arrester is simply a high-pressure jet. It no longer contains an actively combusting flame front and has been cooled enough to avoid reignition.

The theoretical underpinnings of flame arrester operation are elusive and mind-numbingly complex. Researchers have attempted to develop flame-arrester design and performance models from fundamental physical principles with varying degrees of success. However, a general, universally applicable design methodology has not yet been derived.

More than one type of combustion

Combustion can be divided into several types (Figure 5), each of which requires a specific type of flame arrester.

Unconfined deflagration is the simplest form of propagating combustion reaction, in which the combustion products freely expand into the surroundings, accumulating little to no pressure and velocity at the arrester element (Figure 6a). This type of event typically occurs when an ignition source, such as a flying spark, contacts the fuel-air cloud from a flammable liquid storage tank or vessel that is being filled.

The arresters at your local gas station are designed to quench this type of explosion. Larger units for industrial storage tanks function on the same principle. Usually, a small or single arrester element is sufficient to extinguish this type of explosion.

Stabilized burning combustion can occur when a tank or vessel is being filled at a sufficiently fast rate (Figure 6b). If the vapor-air mixture is ignited while the tank is venting, a flame can "rest" on the external surface of the arrester element. This occurs because the burning velocity of the atmospheric deflagration is less than the flowing velocity of the vapors exiting the device. A typical butane cigarette lighter works on the same principle.

This type of condition presents a unique and counterintuitive danger. The vapors exiting the tanks are simultaneously cooling the arrester element via convection while providing additional fuel for the flame combusting on the element surface. If a flame is maintained in this configuration for some time, the arrester element can become red-hot. Once the fuel flow is shut off, the vapors immediately adjacent to the red-hot arrester element can be heated via conduction to the point of autoignition, which can cause a flashback and destroy the tank being filled.

Special arrester designs are available to handle stabilized burning combustion scenarios, both for long-time and short-time burning. Short-time burning units typically incorporate a temperature sensor

to alert the operator of a standing flame so that the flow can be stopped before the element reaches red-hot temperatures. These solutions are available for end-of-line and in-line arresters. Long-time-burning units have unique features, such as thicker arrester elements and spring-loaded weather hood assemblies that open during a standing flame to release heat to the surroundings. Spring-loaded weather hoods are only available for end-of-line applications *(5)*.

Confined explosions are intrinsically dynamic events that can be difficult to describe. Upon ignition, a combustion wave and a pressure wave propagate spherically in all directions away from the ignition source. Combustion waves transform reactants into products, releasing the potential energy stored in the chemical bonds of the reactant molecules, which is then converted into internal (thermal) and kinetic energy of the combustion products *(6)*. The energy release triggers large changes in the thermodynamic and gas-dynamic states across the combustion wave. This entire process occurs rapidly — on the order of millionths of a second. If the conditions are right, the gradient fields across the wave cause physical and chemical processes to occur that produce a self-sustained propagating combustion wave.

The creation of a pressure wave, pressure pulse, or shock wave is a defining feature of a confined explosion. The propagating disturbance spreads outward from the point of ignition at a sonic velocity, traveling at the speed of sound for the medium in which it travels.

The surrounding pipe walls restrict the natural expansion of the two waves (*i.e.,* the combustion wave and the pressure wave), which forces them to travel along the path of least resistance, *i.e.,* in the axial direction of the pipe, toward additional fuel, oxidant, and space. The confining pipe material absorbs the mechanical forces exerted by the expanding gases and applies reactionary forces on the gases, causing pressure inside the pipe to increase to as high as eight times the initial pressure at the time of ignition. The flow conditions, heat-transfer effects, and piping configuration significantly influence the behavior of the explosion. For simplicity, this discussion is limited to straight pipe runs.

During the early phases of the event, the shock wave travels ahead of the flame front where the combustion reaction occurs. The propagating impulse acts like an accelerant, precompressing the unburned reactant mixture just before it encounters the flame front. The flame front propagates at a subsonic velocity, and at this condition the explosion is considered a confined deflagration.

Self-propagating deflagrations are intrinsically unstable. The boundary conditions of the event determine whether the deflagration will accelerate or deccelerate because of a deficit in the energy necessary for maintaining self-propagation.

If the conditions are suitable, the velocity of the deflagration flame front will increase as it propagates forward, aided by precompression of the shock wave and the pressure increase due to confinement. Similar to a snowball rolling down a hill, the phenomenon begins slowly but accelerates.

Given enough pipe length, the explosion will transform from a deflagration to a detonation. The point at which this conversion occurs is called the deflagration-detonation-transition (DDT). The DDT occurs when the accelerating combustion wave reaches and combines with the shock

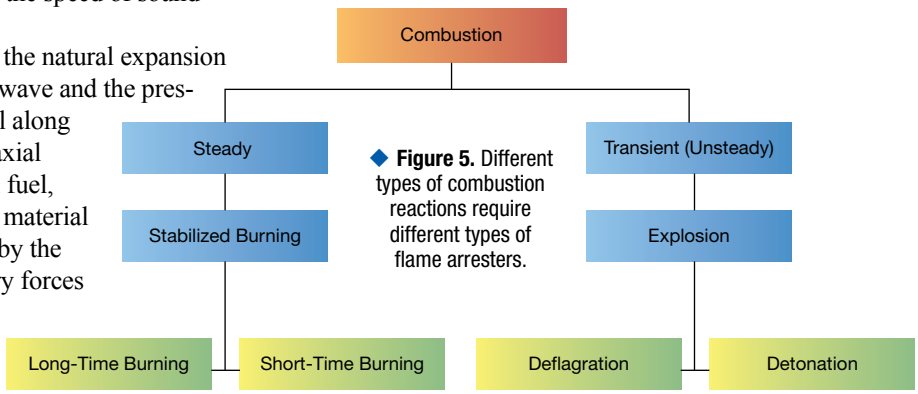

◆ **Figure 5.** Different types of combustion reactions require different types of flame arresters.

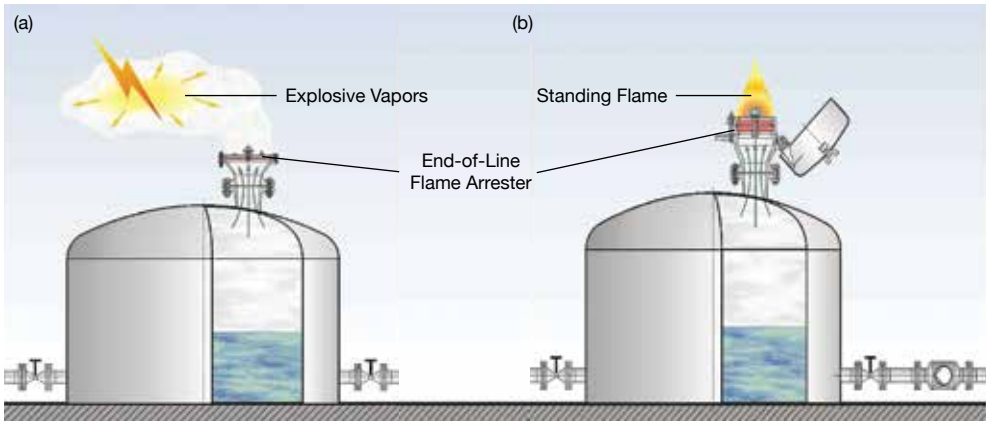

▶ **Figure 6.** (a) Short-time-burning, end-of-line flame arresters are suitable for atmospheric deflagrations, which can occur as tanks are being filled. The flammable fuel vapors mix with air to form a flammable cloud that can be ignited by an ambient ignition source. (b) Long-time-burning flame arresters extend the safe burning time without risking flashback to tank internals. A spring-loaded mechanism on the flame arrester element helps to dissipate the heat to the surroundings. Image courtesy of PROTEGO.

wave that had propagated ahead of it (Figure 7).

The joining of the combustion wave and the shock wave can be thought of as a secondary explosion. High-speed video footage of a DDT shows a flash of light and a second expanding disturbance propagating away in all directions, like the combustion wave and shock wave at the initiation of the explosion event.

When the two fronts combine, pressure and velocity spike within the system. Pressures at the pipe wall can soar to 50–100 times the initial ignition pressure, and propagation velocities can be on the order of 2,000 m/sec. However, this phase of the event lasts for only a brief moment. Complete transition occurs over the length of a few pipe diameters. At this condition, the explosion is characterized as an unstable or overdriven detonation.

After the DDT, the explosion settles into a more predictable pressure and velocity profile. The combustion wave and shock wave are now united, and they travel together as a single detonation wave at supersonic velocities. Pipe wall pressures fall to about 20 times the initial ignition pressure and remain steady.

The explosion's behavior in this final phase satisfies the definition of a stable detonation. In the absence of any external influences, upon reaching stable detonation, the explosion will continue to propagate indefinitely at that condition.

Flame arrester design and selection

Flame arrester design employs largely heuristic methods. Designs are confirmed through rigorous field testing according to international test standards under known operating conditions.

Flame arrester selection requires a thorough analysis of the application. When selecting an arrester, at a minimum, consider the following criteria:

Pressure and temperature. Flame arresters are rated for a maximum operating pressure and temperature. Typical pressure limits are only a few psig, and typical temperature limits are around 140°F (60°C). Special designs for higher pressures and temperatures are available. Process conditions during normal operation, upsets, startup/shutdown, and other scenarios should be evaluated.

Stream composition and chemical properties. Oxygen concentrations above that of air require special flame arrester designs and testing.

Stream maximum experimental safe gap (MESG) or minimum ignition current (MIC) ratio. Class I, Div. combustible materials are classified into Group A, B, C, or D via the MESG or MIC ratio according to NFPA 497 *(7)*. The MESG is an apparatus-dependent parameter used only for fuel gas classification. You may find differences between published MESG values for the same fuel, which depend on the MESG apparatus used. Flame arresters are tested and approved to function for a particular vapor or explosion group.

Stream flowrate and arrester pressure drop limitations. The pressure drop through an arrester is a function of the element's aperture size and the flowrate of the stream. Excessive pressure drop at the arrester can cause process problems downstream. Equipment vendors often provide pressure drop charts or curves that are typically calibrated for air at standard or normal conditions. To accurately estimate field performance, conversion from the actual process conditions may be required.

Installation location and orientation. Consider where the arrester will be located and the assumed location of the ignition point. Designs are available for in-line and end-of-line installations. Location and orientation also need to provide accessibility for maintenance. Some flame arresters are unidirectional to handle upstream or downstream events, while others are bidirectional to quench disturbances on both sides.

Distance from the assumed ignition point. The length-to-diameter (L/D) ratio of the arrester to the assumed ignition source helps determine whether a deflagration or detonation should be expected by the time the propagating explosion reaches the flame arrester. For typical alkane hydrocarbon fuels in straight pipes, at distances less than 30 L/D, the explosion will be a deflagration, and for distances greater than 80 L/D, the explosion will be a stable detonation. Consider the worst-case scenario if multiple assumed points of ignition exist.

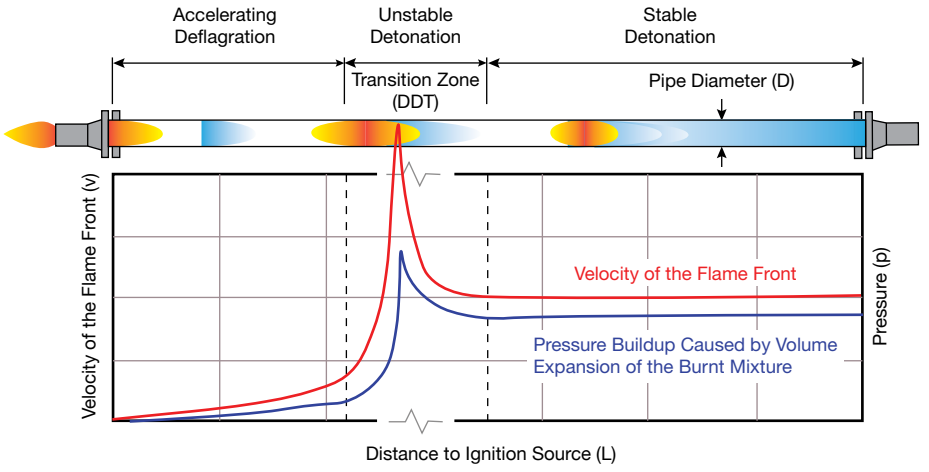

▲ **Figure 7.** As explosions propagate within a piping system, they transition from an accelerating deflagration to an unstable detonation and, finally, to a stable detonation.

Pipeline layout. The connections to the flame arrester should be the same size as, or larger than, the surrounding inlet piping (within 120 pipe diameters). If the outlet piping from the flame arrester is smaller than the flame arrester connection, the flame arrester must be tested with an outlet restriction.

Standing flame risk. If the flowrate is high enough to allow a standing flame at the arrester, consider end-of-line arrester designs rated for endurance burning or in-line arresters with temperature sensors.

Material and chemical compatibility. Chemical corrosion of the arrester housing or elements can create propagation pathways for an explosion to pass through.

Third-party certification. NFPA 69 requires flame arresters to be third-party-certified according to an international flame arrester test standard.

Special applications. Certain applications have specific needs. Consult with manufacturers for special designs. Polymerizing vapors (*e.g.,* styrene), condensing vapors, and self-decomposing vapors (*e.g.,* acetylene and ethylene oxide) may present special circumstances.

Going forward

Since Sir Michael Davy invented the miner's safety lamp in 1815, flame arresters have existed in one form or another. However, significant advances in design and testing have greatly increased the reliability and suitability of flame arresters for broader ranges of operating conditions and gases. When properly applied, used, and maintained, flame arresters are a safe and reliable explosion-protection solution.

This article is not a comprehensive guide on flame-arrester specification or a rigorous examination of the subject. It is, however, an introduction that positions you to communicate more effectively with experts and delve deeper into standards. When in doubt, seek expertise and insight from flame-arrester manufacturers.

Engineers responsible for specifying flame arresters must understand the requirements and unique needs of each application, and insist on regular inspections and maintenance after the devices have been installed. The safety of your plant and the lives of your colleagues could depend on it. CEP

MATTHEW B. BARFIELD, P.E., is an explosion-protection test engineer at Fike Corp. (Blue Springs, MO). He regularly performs explosion, fire, and pressure relief tests to aid research and development of explosion-suppression systems, rupture discs, fire-suppression systems, and other process safety products. He previously worked as a junior consulting process engineer for PROTEGO USA (Charleston, SC), a conservation vent and flame arrester manufacturer. Barfield holds a BSE in chemical engineering from the Univ. of South Carolina. He is a licensed professional engineer in South Carolina and an active member of AIChE and the Design Institute for Emergency Relief Systems (DIERS).

Literature Cited

1. **National Fire Protection Agency,** "NFPA 69: Standard on Explosion Prevention Systems," NFPA, Quincy, MA, p. 48 (2014).
2. **Perry, R. H., and D. W. Green, Eds.,** "Flame Arresters," *Perry's Chemical Engineers' Handbook, 7th Ed.,* McGraw-Hill, New York, NY, pp. 38–43 (1999).
3. **Grossel, S. S.,** "Deflagration and Detonation Flame Arresters," Wiley-CCPS, Hoboken, NJ (2002).
4. **El-Mahallawy, F., and S. El-Din Habik,** "Fundamentals and Technology of Combustion," Elsevier Science, Oxford, U.K. (2002).
5. **PROTEGO,** "Technical Fundamentals: Flame Arresters," *PROTEGO Catalogue 2012/2013,* Charleston, SC, pp. 14–18 (2013).
6. **Lee, J. H. S.,** "The Detonation Phenomenon," Cambridge Univ. Press, New York, NY (2008).
7. **National Fire Protection Agency,** "NFPA 497: Recommended Practice for the Classification of Flammable Liquids, Gases, or Vapors and of Hazardous (Classified) Locations for Electrical Installations in Chemical Process Areas," NFPA, Quincy, MA (2017).

Additional Resources

American Petroleum Institute, "API 2028: Flame Arresters in Piping Systems," API, Washington, DC (2010).

American Petroleum Institute, "API 2210: Flame Arresters for Vents of Tanks Storing Petroleum Products," API, Washington, DC (2000).

ASTM International, "ASTM F-1273-91: Standard Specification for Tank Vent Flame Arresters," ASTM, West Conshohocken, PA (2013).

British Standards Institute, "BS 7244: Flame Arresters for General Use," BSI Group, London, U.K. (1990).

CSA Group, "CSA-Z343: Test Methods for In-Line and Firebox Flame Arresters," CSA Group, Mississauga, Canada (1998).

The European Committee for Standarization, "EN 12874: Flame Arresters — Performance Requirements, Test Methods, and Limits for Use," CEN, Brussels, Belgium (2001).

FM Global, "FMRC Class 6061: Approval Standard for Flame Arresters, FM Global, Johnston, RI (2013).

International Maritime Organization, "MSC/Circ. 677: Revised Standards for the Design, Testing, and Locating of Devices to Prevent the Passage of Flame into Cargo Tanks in Tankers," IMO, London, U.K. (1994, 2001, 2009).

International Organization of Standardization, "ISO 16852 Flame Arresters — Performance Requirements, Test Methods, and Limits for Use," ISO, Geneva, Switzerland (2016).

National Fire Protection Agency, "NFPA 67: Guide on Explosion Protection for Gaseous Mixtures in Pipe Systems," NFPA, Quincy, MA (2016).

National Fire Protection Agency, "NFPA 68: Standard on Explosion Protection by Deflagration Venting," NFPA, Quincy, MA (2018).

Underwriters Laboratories, "UL 525: Standards for Flame Arresters," UL, Northbrook, IL (2008).

U.S. Coast Guard, "33 CFR Part 154, Subpart P — Marine Vapor Control Systems, Appendix A," USCG, Washington, DC (2015).

Don't forget these excellent AIChE resources for First Year Professionals:

Online Leadership Training

YP Article Bundles and Webinars

The Young Professionals Committee

The ChEnected Blog

Conferences

AIChE young PROFESSIONALS

Visit www.aiche.org/yp for more information.